SIMMER-Ⅲ Heat-and Mass-Transfer Model
- Model and Method Description -

August 2001

O-arai Engineering Center
Japan Nuclear Cycle Development Institute

〒319-1184　茨城県那珂郡東海村村松4番地49
核燃料サイクル開発機構
技術展開部　技術協力課

Ⓝ

JNC TN9400 2001-074
August, 2 0 0 1

SIMMER–III Heat- and Mass-Transfer Model – Model and Method Description –

K. Morita **, Y. Tobita *, H. Yamano *, Sa. Kondo *

Abstract

The present report gives the SIMMER-III heat- and mass-transfer model describing melting/freezing and vaporization/condensation processes in multiphase, multicomponent systems. The heat- and mass-transfer processes are modeled in consideration of their importance in and effects on the behavior of reactor-core materials in the fast reactor safety analysis. Applying equilibrium and non-equilibrium transfers generalizes the phase-transition processes except for the structure breakup transfer. The non-equilibrium transfers occurring at interfaces were formulated on the basis of the heat-transfer-limited model. The implicit solution algorithm for basic vaporization/condensation equations is tightly coupled with the analytic equation-of-state (EOS) model. The use of this approach successfully solves numerical problems encountered in the previous codes, which were mainly introduced by thermodynamic inconsistencies in EOS.

* Advanced Technology Division, O-arai Engineering Center, JNC

** Present affiliation: Institute of Environmental Systems, Kyushu University

JNC TN9400 2001-074
2 0 0 1 年 8 月

SIMMER–III 熱および質量移行モデル
ー モデルおよび手法の記述 ー

守田 幸路**, 飛田 吉春*, 山野 秀将*, 近藤 悟*

要 旨

本報告書は、SIMMER-III コードにおける多相・多成分系における溶融／固化および蒸発／凝縮過程を表す熱および質量移行モデルを記述したものである。熱および質量移行過程は、高速炉安全解析における炉心物質挙動上の重要性を考慮してモデル化されている。相変化過程は、構造材破損による移行を除き、平衡および非平衡移行を適用することで一般化している。界面で生ずる非平衡移行は、熱伝達律速モデルに基づいて定式化している。蒸発／凝縮の基礎方程式の解法アルゴリズムは、解析的状態方程式（EOS）モデルと強く結合されている。このアプローチを用いることで、先行コードに見られた主として EOS の熱力学的な不整合性よる数値的な問題を解決することに成功した。

---

* 大洗工学センター 要素技術開発部

** 現所属：九州大学大学院工学研究院 附属環境システム科学研究センター

List of contents

List of tables and figures

Chapter 1. Introduction

The purpose of the present model development was to alleviate some of the limitations in the previous SIMMER-II code [1, 2], and thereby to provide a generalized modeling of heat- and mass-transfer phenomena in a multiphase, multicomponent system for more reliable analysis of core disruptive accidents (CDAs). The scope of the model development effort was determined primarily from the needs of the accident-analysis point of view. The outcome and experience gained in course of the AFDM development [3] were used to maximum extent. The advanced features of the model must resolve many of the problems associated with SIMMER-II. The present model development was intended to provide a generalized model that is useful for analyzing relatively short-time-scale multiphase, multicomponent hydraulic problems on the basis of phenomenological consideration of flow regimes and interfacial areas, and heat- and mass-transfer processes. Although the original objective of the present model was primarily to resolve some of the key CDA issues in liquid-metal cooled fast reactors (LMFRs), its flexible framework enables us to apply the model to various areas of interest which are consistent with the modeling framework. Therefore, the model application could include: accident analyses of any types of future or advanced liquid-metal cooled reactors, steam-explosion problems in current- and future-generation light water reactors, and general types of multiphase flow problems.

The development of SIMMER-III has reached a stage, where all the models originally intended are made available [4, 5] and integral calculations with the code can be made. In parallel to the code development, an extensive program has been performed for systematic and comprehensive code assessment under the collaboration with Forschungszentrum Karlsruhe (FZK), Germany, and Commissariat à l'Energie Atomique (CEA), France [6].

The present report describes the models and methods employed in the heat- and mass-transfer model of Version 2. J of SIMMER-III released in October 2001. The following reviews of previous models and methods on the heat- and mass-transfer processes in multiphase, multicomponent flows provide background in selection of an appropriate approach for the SIMMER-III model.

A. SIMMER-II model

In the SIMMER-II heat- and mass-transfer model [2], several methods were applied to transfer mass and energy between reactor-core material components. The first was through phase-transition processes occurring at interfaces. These are called non-equilibrium

transfers because the interior component (bulk) conditions are generally not at the transition temperature. The second method of mass and energy transfer was through equilibrium melting/freezing (M/F) processes, occurring when the bulk temperatures of structure or particles exceed the solidus temperature or when liquid bulk temperatures drop below the liquidus temperature. Equilibrium melting can occur as a consequence of nuclear heating as well as heat transfer. A third method of mass and energy transfer was through models representing structure breakup and/or transfers into the particle, liquid, and vapor components. SIMMER-II represented both pin and crust breakup under some circumstances, and possessed a user option to allow particle transfer to be associated with melting.

The initial SIMMER-II code calculated heat transfers between liquid and liquid, and liquid and structure implicitly by solving 11 equations simultaneously for the end-of-time-step component (bulk) temperatures. The vaporization/condensation (V/C) processes occurring at interfaces between vapor and liquid, and vapor and structure were then determined as non-equilibrium transfers. Finally, heat and mass transfers through equilibrium M/F processes were calculated. Non-equilibrium M/F processes were treated to contribute the fuel crusts formation on structure.

The SIMMER-II code has played a pioneering role especially in studying the CDA phenomenology, but at the same time extensive code application revealed several limitations due to the code framework as well as needs for model improvement. The extensive use of the SIMMER-II code indicated several problem areas in the heat- and mass-transfer modeling. The greatest difficulties with SIMMER-II framework of multifield, multicomponent fluid dynamics arose from the heat- and mass-transfer treatments, particularly from the V/C modeling. Thermodynamic inconsistencies in the simple analytic equation of state (EOS) introduced difficulty in determining vapor temperature at high pressure, resulting in numerical problems. In addition, numerical instability upon single/two phase transition due to EOS inconsistency could lead to the nonphysical motion of fluid. Since the saturation temperature of a vapor component and the vapor mixture temperature were coupled tightly, the SIMMER-II numerical scheme resulted in slow convergence. No condensation process of fuel or steel vapor on other colder liquids caused a problem of nonphysical presence of supersaturated vapor. The V/C operation removed energy from a bulk component undergoing phase transition at the interface value, or saturation value. This could lead to artificial heating or cooling of the bulk fluid.

B. AFDM model

In the AFDM code, a heat- and mass-transfer model similar to SIMMER-II was formulated and implemented [7], but many modifications to the SIMMER-II approach were made based on the difficulties that had been encountered. Two ways of specifying EOS were tried in AFDM: simplified analytic expressions and a tabular EOS model [8]. Both the EOS models attempted to resolve the problems present in the SIMMER-II EOS. A new implicit solution algorithm was also developed to solve multicomponent V/C mass-transfer rates simultaneously with liquid and vapor heat-transfer rates. A homogeneous vapor condensation term was included in the V/C to remove supersaturated vapor. The basic V/C equations were changed such that energy associated with mass transfer was removed from a component at the bulk value, not the saturation value, with an effective latent heat to conserve energy. This eliminated spurious bulk temperature changes when coolant was vaporizing rapidly.

The use of new approaches in the AFDM heat- and mass-transfer algorithm solved some SIMMER-II problems successfully. However, it was found that further model improvement was necessary. The tabular EOS model was not successful due to the combined effects of time–consuming table search/interpolation and intended iterations to obtain mechanical equilibrium. The homogeneous condensation term proved insufficient/inappropriate to treat supersaturated fuel vapor upon significant exposure to cold sodium. Numerous special case treatments were required to solve numerical difficulties in the V/C algorithm, especially when the simplified analytic EOS model was used.

Chapter 2. Basis for heat- and mass-transfer modeling

2.1. Basic assumptions

The SIMMER-III heat- and mass-transfer model is based on the technologies developed and experience gained in the former SIMMER-II and AFDM. The followings are the basic assumptions used in the SIMMER-III model:

1. Each energy component interfaces with the other energy components simultaneously, and each interface has a uniquely defined interfacial area. Energy transfers between components are based on the interfacial area and heat-transfer coefficients determined from engineering correlations. Mass-transfer effects on vapor-side heat-transfer coefficients are not included at this level of approximation. Non-equilibrium M/F and V/C models are applied to treat the phase transitions occurring at the interfaces. The former non-equilibrium M/F model is used especially for proper calculation of insulating fuel crusts on can walls.

2. Each possible interface is assigned a specified temperature to calculate heat flows from/to each interface into/from the respective bulk materials. These heat flows are summed to give the net interfacial energy loss or gain. An interfacial energy loss is defined as positive and means condensation or freezing must occur to conserve (provide) energy. An interfacial energy gain is defined as negative and means the energy is going into vaporization/melting.

3. Equilibrium M/F transfer is modeled to eliminate subcooled liquid or metastable solid as the result of heat transfer or nuclear heating. The equilibrium melting of solid component occurs when its bulk energy exceeds the solidus energy, and the equilibrium freezing of liquid component occurs when its bulk energy falls below the liquidus energy. The equilibrium mass-transfer rate is determined from the bulk energy level exceeding the phase-transition energy.

4. In a single-phase cell, a small vapor volume fraction is assumed to always exist for numerical purpose, and hence its density and energy must be calculated reasonably to avoid numerical difficulties. In AFDM, initialization of this so-called α_0 volume was performed with an "equilibrium" approach. However, this formalism was not necessarily satisfactory because it did not allow vapor to function as a heat-transport medium (for example, it ignored vapor/structure contact). Thus, different from AFDM, an approach more consistent with the two-phase V/C treatment is adopted in SIMMER-

III. The V/C mass transfer associated with energy transfer in single-phase cells is required only to initialize the fictitious vapor volume for numerical convenience.

5. The film-boiling heat transfer is considered through a special heat-transfer coefficient. In a case of film boiling predicted by a criterion for minimum film boiling temperature, the heat-transfer coefficient is evaluated to represent conduction and radiation heat transfer across a vapor film surrounding a hot droplet or particle in a continuous-phase coolant liquid. In the heat- and mass-transfer model, energy transfers are based on this heat-transfer coefficient determined from a semi-empirical correlation.

6. The numerical solution procedure treats the vapor and the liquid coolant implicitly, but the other liquids and structures are solved explicitly. In particular, in the V/C heat- and mass-transfer calculation, the energy- and mass-conservation equations are tightly coupled with EOSs [9] and are solved iteratively. This is because of strong non-linearity in V/C processes and a probable large change in the vapor thermodynamic state. Numerical limits on the interfacial areas or heat-transfer coefficients are also imposed in the formation of an algorithm to avoid numerical difficulties. These are defined based on suitable physical justification to the extent possible.

7. A diffusion-limited V/C model seems to require further model development in the future. To treat condensation on colder liquid and structure reasonably without this model, the vapor/liquid and vapor/structure interfaces are further divided based on partial pressures. Possible vaporization is assumed to occur over an entire liquid/vapor interface except for the areas where another species is condensing.

2.2. Mass-transfer paths

Two steps are applied to transfer mass and energy between reactor material components except for the step representing structure breakup. The first step calculates the phase-transition processes occurring at interfaces, described by a non-equilibrium heat-transfer-limited model. This is a non-equilibrium process because the bulk temperature does not generally satisfy the phase-transition condition when the mass transfer occurs at the interface. The second step of mass and energy transfer is through an equilibrium process occurring when the bulk energy satisfies the phase-transition condition.

There are 42 binary contact interfaces among seven fluid energy components (liquid fuel, steel, sodium; fuel, steel and control particles; and vapor mixture) and three structure surfaces (a fuel pin, and left and right can walls). The seven fluid energy components have 21 binary

contact modes, and each fluid component can interact with the three structures. As shown in Table 2-1, there are possible 43 mass-transfer paths for V/C and 61 paths for M/F at these 42 interfaces. These include less important mass-transfer paths, which have only minor or negligible effects on key phenomena directly relevant to the accident sequences of a CDA. The key phenomena include boiling pool dynamics, fuel relocation and freezing, material expansion (through a channel and into a pool), and fuel-coolant interactions (FCIs). Therefore, the number of mass-transfer paths can be limited by eliminating some non-equilibrium mass transfers in less important situations. The basic assumptions used for this limitation are as follows:

1. Eliminate non-equilibrium vaporization and melting caused by solid particles or structures. Sodium, which is the most volatile liquid, has a high thermal conductivity, and hence the film boiling on solid surfaces could be expected to be minimal. Other cases appear either to produce second-order effects or to be seldom needed.
2. Eliminate non-equilibrium M/F caused by vapor. SIMMER-III does not model the boundary layer, in which heat production appears resulting from kinetic energy dissipation. In addition, SIMMER-III has no component that is assigned to fuel crusts on liquid droplets.
3. Eliminate non-equilibrium freezing of a liquid by a more volatile (but colder) liquid. To represent FCIs in LMFR, the sodium interface should be at the sodium saturation temperature.
4. Eliminate non-equilibrium M/F at a fuel pellet surface. It can be assumed generally that the fuel pellet might be molten by internal energy generation. Non-equilibrium freezing should be limited because of the low thermal conductivity of ceramic fuel.
5. Eliminate non-equilibrium transfers at liquid-steel/solid-fuel surfaces. These simply appear to be second-order effects even if steel could freeze/vaporize or fuel could melt under such contacts.
6. Eliminate non-equilibrium melting caused by liquid sodium. Although sodium could become hot enough to heat up cladding, the resultant melting of cladding due to the heat transfer from sodium can be treated as an equilibrium transfer to avoid the metastable solid state.
7. Eliminate non-equilibrium freezing caused by control particles. Control particles are usually less in the flow field, and hence computations involving their effects should be

minimized.

Using these simplifications, the total number of non-equilibrium processes results in 30 for V/C and 20 for M/F, as shown in Table 2-2. These include the mass-transfer paths required to represent essential phenomena. Typical mass-transfer paths are illustrated in Fig. 2-1 among a vapor mixture and three liquid components. The liquid vaporization can occur at the liquid/liquid interfaces as well as at the vapor/liquid interfaces. Note that in the V/C transfers condensation processes of fuel or steel vapor on other colder liquids are included to avoid a problem of nonphysical presence of supersaturated vapor. The vapor condensation on particles and structures are also treated in the V/C transfers. Typical mass-transfer paths are illustrated in Fig. 2-2 for binary contacts with fuel and steel droplets. The non-equilibrium M/F transfers include the crust formation on a can wall that furnishes thermal resistance, and steel ablation and particle formation that contribute to fluid quenching and bulk freezing. The M/F transfers at the liquid/particle interfaces are also included which is analogous to the liquid/structure M/F transfers for consistency.

In addition, eight (and three optional) equilibrium M/F transfers are performed to eliminate subcooled liquids or metastable solids as the result of heat transfer or nuclear heating. These include:

- Left and right fuel crust melting into liquid fuel,
- Left and right can-wall surface melting into liquid steel,
- Fuel and steel particle melting into liquid,
- Liquid fuel and steel freezing into particles, and
- Liquid steel film freezing into cladding, and left and right can walls (optional).

It is noted that the liquid transfers to structure components are not modeled by equilibrium transfers but treated as non-equilibrium processes, except for the equilibrium freezing of liquid steel film to be treated optionally. This latter option has been added recently. Other possible equilibrium transfers such as pin-fuel melting into liquid fuel, cladding melting into liquid steel, and bulk can-wall melting into liquid steel are treated by the structure breakup model.

2.3. Non-equilibrium transfers

2.3.1. Basic interface equations

The basic concept of the non-equilibrium mass-transfer model is described using Fig. 2-3, in which a binary contact interface of the energy components A and B is shown. This is a heat-transfer-limited process where the phase-transition rate is determined from energy balance at the interface. For example, Fig. 2-3 (a) shows interface (A, B) where the interface is undergoing a net loss energy to component B. This energy is either coming from condensation or freezing of component A. The resulting product will be either more of component B, or component C depending on the process involved. Fig. 2-3 (b) shows interface (A, B) where the interface is gaining energy from component A. The melted/vaporized component B will either be more of component A, or component D, again depending on the process. The heat transfer rates from the interface are:

$$q_{A,B} = R_{A,B} a_{A,B} h_{A,B} (T^{I}_{A,B} - T_A) \text{ into component A, and} \tag{2-1}$$

$$q_{B,A} = R_{A,B} a_{A,B} h_{A,B} (T^{I}_{A,B} - T_B) \text{ into component B,} \tag{2-2}$$

where a fraction of interface, $R_{A,B}$, is introduced to treat condensation of fuel or steel vapor on other colder liquids and vapor on solid surfaces. The net energy transfer rate from the interface is defined as:

$$q^{I}_{A,B} = q_{A,B} + q_{B,A}. \tag{2-3}$$

If the net heat flow, $q^{I}_{A,B}$, is zero, sensible heat is exchanged without phase transition. If $q^{I}_{A,B}$ is positive, namely the energy is lost at the interface, either a liquid component freezes or a vapor component condenses. Then the mass-transfer rate for this case is determined from:

$$\Gamma^{I}_{A,B} = \frac{q^{I}_{A,B}}{i_A - i^{I}_B} \text{ if the component formed by the phase transition is B, or} \tag{2-4}$$

$$\Gamma^{I}_{A,C} = \frac{q^{I}_{A,B}}{i_A - i^{I}_C} \text{ if component C formed by the phase transition is not B.} \tag{2-5}$$

If $q^{I}_{A,B}$ is negative, on the other hand, namely the energy is gained at the interface, either a solid component melts or a liquid component vaporizes. Then the mass-transfer rate for this case is determined from:

$$\Gamma^{I}_{B,A} = -\frac{q^{I}_{A,B}}{i^{I}_A - i_B} \text{ if the component formed by the phase transition is A, or} \tag{2-6}$$

$$\Gamma^{I}_{B,D} = -\frac{q^{I}_{A,B}}{i^{I}_{D} - i_{B}} \quad \text{if component D formed by the phase transition is not A.} \tag{2-7}$$

In the above four equations, the latent heat of phase transition is defined as the difference between the enthalpy at the interface and the bulk enthalpy of a component undergoing a phase-transition process. More correctly, the bulk enthalpy should be replaced by the interfacial. However, SIMMER-III does not calculate temperature gradients in liquid and vapors. Beside, the experience from the previous codes suggests that better results are obtained with this definition of effective latent heat. When the phase transition is predicted, the interface temperature, $T^{I}_{A,B}$, is defined as a phase-transition temperature such as melting point and saturation temperature. For the case of no mass transfer, the interface energy transfer is zero and hence the equivalent interface temperature is defined as

$$T^{I}_{A,B} = \frac{h_{A,B}T_{A} + h_{B,A}T_{B}}{h_{A,B} + h_{B,A}}. \tag{2-8}$$

2.3.2. Detailed interfacial treatments

To complete the equations in Section 2.2 for allowed/excluded interfacial processes, expressions are needed for R, a, h and T^{I}. The interfacial area and heat-transfer coefficient models define a and h, respectively, and are discussed in other documents. Detailed expression for the non-equilibrium mass-transfer paths at each of the 42 interfaces are presented as follows:

Vapor/Liquid-fuel interface: At the interface between vapor and liquid fuel, only fuel is allowed to condense or vaporize. Here the interface is divided into two parts. One part is introduced to treat the obstructive effect of non-condensable gas on the V/C phase transition. The remaining part is available for V/C of fuel. The fractions of the interface devoted to each process are defined based on partial pressures:

$$R_{G4,L1} = \min\left[\frac{f_{G4,L}p_{G4}}{p^{*}_{G}}, R_{GL,max}\right], \text{ and} \tag{2-9}$$

$$R_{GI,L1} = 1 - R_{G4,L1}, \tag{2-10}$$

where $R_{GL,max}$ is the maximum fraction of vapor/liquid contact area that is not available for vaporization, $f_{G4,L}$ is the fractional effect of non-condensable gas on the V/C phase transition, and p^{*}_{G} is given by

$$p_G^* = \sum_{m=1}^{3} p_{Gm} + f_{G4,L} p_{G4}. \tag{2-11}$$

The parameters $R_{GL,max}$ and $f_{G4,L}$ are specified by the inputs RGLMAX and FPG4L in the Namelist /XHMT/, respectively. When the fuel vaporizes or condensates, the interface temperature is defined as the saturation temperature of fuel vapor. Otherwise, in the case of no mass transfer, Eq. (2-8) is applied to the interface temperature. Therefore, the interface temperatures can be expressed by

$$T^{I}_{Gl,L1} = T_{Sat,Gl}, \text{ and} \tag{2-12}$$

$$T^{I}_{G4,L1} = T_{GL1}, \tag{2-13}$$

where the interface temperature, T_{GL1}, with no mass transfer is given by

$$T_{GL1} = \frac{h_{L1,G} T_{L1} + h_{G,L1} T_G}{h_{L1,G} + h_{G,L1}}. \tag{2-14}$$

Then, the interfacial energy transfer rate can be evaluated:

$$q^{I}_{Gl,L1} = R_{Gl,L1} a_{G,L1} [h_{L1,G}(T^{I}_{Gl,L1} - T_{L1}) + h_{G,L1}(T^{I}_{Gl,L1} - T_G)]. \tag{2-15}$$

The mass-transfer rates at the vapor/liquid-fuel interface are expressed by

$$\Gamma^{II}_{G,L1} = \frac{q^{I}_{Gl,L1}}{i_{Gl} - i_{Con,Gl}}, \qquad q^{I}_{Gl,L1} > 0, \text{ and} \tag{2-16}$$

$$\Gamma^{II}_{L1,G} = -\frac{q^{I}_{Gl,L3}}{i_{Vap,Gl} - i_{L1}}, \qquad q^{I}_{Gl,L1} < 0. \tag{2-17}$$

Vapor/Liquid-steel interface: At the interface between vapor and liquid steel, fuel vapor can condense on liquid steel and steel can either condense or vaporize. Here the interface is divided into three parts. The first part is introduced to treat condensation of fuel vapor on liquid steel. The second part is used to include the obstructive effect of non-condensable gas on the V/C phase transition. The remaining part is available for steel V/C. The fractions of the interface devoted to each process are defined based on partial pressures:

$$R_{Gl,L2} = \min\left[\frac{p_{Gl}}{p_G^*}, R_{GL,max} \frac{p_{Gl}}{p_{Gl} + f_{G4,L} p_{G4}}\right], \tag{2-18}$$

$$R_{G4,L2} = \min\left[\frac{f_{G4,L} p_{G4}}{p_G^*}, R_{GL,max} \frac{f_{G4,L} p_{G4}}{p_{Gl} + f_{G4,L} p_{G4}}\right], \text{ and} \tag{2-19}$$

$$R_{G2,L2} = 1 - R_{G1,L2} - R_{G4,L2}. \tag{2-20}$$

When the phase transition occurs, the interface temperature is defined as the vapor saturation temperature of a phase-transition species. Otherwise, in the case of no mass transfer, Eq. (2-8) is applied to the interface temperature. Therefore, the interface temperatures can be expressed by

$$T^{I}_{G1,L2} = \max[T_{Sat,G1}, T_{GL2}], \tag{2-21}$$

$$T^{I}_{G2,L2} = T_{Sat,G2}, \text{ and} \tag{2-22}$$

$$T^{I}_{G4,L2} = T_{GL2}, \tag{2-23}$$

where the interface temperature, T_{GL2}, with no mass transfer is given by

$$T_{GL2} = \frac{h_{L2,G}T_{L2} + h_{G,L2}T_{G}}{h_{L2,G} + h_{G,L2}}. \tag{2-24}$$

Then, the interfacial energy transfer rates can be evaluated:

$$q^{I}_{Gm,L2} = R_{Gm,L2}a_{G,L2}[h_{L2,G}(T^{I}_{Gm,L2} - T_{Lm}) + h_{G,L2}(T^{I}_{Gm,L2} - T_{G})], \text{ m} = 1 \text{ and } 2. \tag{2-25}$$

The mass-transfer rates at the vapor/liquid-steel interface are expressed by

$$\Gamma^{I2}_{G,Lm} = \frac{q^{I}_{Gm,L2}}{i_{Gm} - i_{Con,Gm}}, \qquad q^{I}_{Gm,L3} > 0, \text{ and} \tag{2-26}$$

$$\Gamma^{I2}_{L2,G} = -\frac{q^{I}_{G2,L2}}{i_{Vap,G2} - i_{L2}}, \qquad q^{I}_{G2,L3} < 0. \tag{2-27}$$

Equation (2-26) for m = 1 and 2 is used for fuel and steel condensation, respectively, and Eq. (2-27) is used for steel vaporization.

Vapor/Liquid-sodium interface: At the interface between vapor and liquid sodium, fuel and steel vapor can condense on liquid sodium and sodium can either condense or vaporize. Here the interface is divided into four parts. The first two parts are introduced to treat condensation of fuel/steel vapor on liquid sodium. The third part is used to include the obstructive effect of non-condensable gas on the V/C phase transition. The remaining part is available for V/C of sodium. The fractions of the interface devoted to each process are defined based on partial pressures:

$$R_{Gm,L3} = \min\left[\frac{p_{Gm}}{p^{*}_{G}}, R_{GL,max}\frac{p_{Gm}}{p_{G1} + p_{G2} + f_{G4,L}p_{G4}}\right], \text{ m} = 1 \text{ and } 2, \tag{2-28}$$

$$R_{G4,L3} = \min\left[\frac{f_{G4,L}p_{G4}}{p_G^*}, R_{GL,max}\frac{f_{G4,L}p_{G4}}{p_{G1}+p_{G2}+f_{G4,L}p_{G4}}\right], \text{ and} \tag{2-29}$$

$$R_{G3,L3} = 1 - R_{G1,L3} - R_{G2,L3} - R_{G4,L3}. \tag{2-30}$$

Similar to the vapor/liquid-steel interface, the interface temperatures can be expressed by

$$T^I_{Gm,L3} = \max[T_{Sat,Gm}, T_{GL3}], \text{ m} = 1 \text{ and } 2, \tag{2-31}$$

$$T^I_{G3,L3} = T_{Sat,G3}, \text{ and} \tag{2-32}$$

$$T^I_{G4,L3} = T_{GL3}, \tag{2-33}$$

where the interface temperature, T_{GL3}, with no mass transfer is given by

$$T_{GL3} = \frac{h_{L3,G}T_{L3} + h_{G,L3}T_G}{h_{L3,G} + h_{G,L3}}. \tag{2-34}$$

Then, the interfacial energy transfer rates can be evaluated:

$$q^I_{Gm,L3} = R_{Gm,L3}a_{G,L3}[h_{L3,G}(T^I_{Gm,L3} - T_{Lm}) + h_{G,L3}(T^I_{Gm,L3} - T_G)], \text{ m} = 1, 2 \text{ and } 3. \tag{2-35}$$

The mass-transfer rates at the vapor/liquid-sodium interface are expressed by

$$\Gamma^{I3}_{G,Lm} = \frac{q^I_{Gm,L3}}{i_{Gm} - i_{Con,Gm}}, \qquad q^I_{Gm,L3} > 0, \text{ and} \tag{2-36}$$

$$\Gamma^{I3}_{L3,G} = -\frac{q^I_{G3,L3}}{i_{Vap,G3} - i_{L3}}, \qquad q^I_{G3,L3} < 0. \tag{2-37}$$

Equation (2-36) for m = 1, 2 and 3 is used for fuel, steel and sodium condensation, respectively, and Eq. (2-37) is used for sodium vaporization.

Vapor/Particle and Vapor/Structure interfaces: At the interfaces between vapor and solid components such as particles and structures, fuel, steel and sodium vapor can condense on their surfaces. Here the interface is divided into four parts. The three parts are introduced to treat condensation of fuel, steel and sodium vapor. The remaining part is used to include the obstructive effect of non-condensable gas on the condensation. The fractions of the interface devoted to each process are defined based on partial pressures:

$$R_{Gm,K(k)} = \frac{p_{Gm}}{p_G^*}, \text{ m} = 1, 2 \text{ and } 3, \text{ and} \tag{2-38}$$

$$R_{G4,K(k)} = \frac{f_{G4,L} p_{G4}}{p_G^*}, \tag{2-39}$$

where K(k) for k = 1 – 6 represents L4, L5 and L6 for particles, and k1, k2 and k3 for structure surfaces, respectively. When the condensation occurs, the interface temperature is defined as the vapor saturation temperature of a condensate species. Otherwise, in the case of no mass transfer, Eq. (2-8) is applied to the interface temperature. Therefore, the interface temperatures can be expressed by

$$T^I_{Gm,K(k)} = \max[T_{Sat,Gm}, T_{GK(k)}], \text{ m = 1, 2 and 3, and} \tag{2-40}$$

$$T^I_{G4,K(k)} = T_{GK(k)}, \tag{2-41}$$

where the interface temperatures, $T_{GK(k)}$, with no mass transfer are given by

$$T_{GK(k)} = \frac{h_{K(k)} T_{K(k)} + h_{G,K(k)} T_G}{h_{K(k)} + h_{G,K(k)}}. \tag{2-42}$$

Then, the interfacial energy transfer rates can be evaluated:

$$q^I_{Gm,K(k)} = R_{Gm,K(k)} a_{G,K(k)} [h_{K(k)} (T^I_{Gm,K(k)} - T_{K(k)}) + h_{G,K(k)} (T^I_{Gm,K(k)} - T_G)], \text{ m = 1, 2 and 3.} \tag{2-43}$$

The mass-transfer rates at the vapor/solid-component interface are expressed by

$$\Gamma^{I(k)}_{G,Lm} = \frac{q^I_{Gm,K(k)}}{i_{Gm} - i_{Con,Gm}}, \tag{2-44}$$

where I(k) for k = 1 – 6 represents I4, I5, I6, I22, I29, respectively. Equation (2-44) for m = 1, 2 and 3 is used for fuel, steel and sodium condensation, respectively.

Liquid-fuel/Liquid-steel interface: At the interface between liquid fuel and liquid steel, steel vaporization should occur if the net heat flow is negative at the interface. In this case, the interface temperature is defined as the saturation temperature of steel vapor. Otherwise, in the case of no mass transfer, Eq. (2-8) is applied to the interface temperature. Therefore, the interface temperatures can be expressed by

$$T^I_{L1,L2} = \max[T_{Sat,G2}, T_{L1L2}], \tag{2-45}$$

where the interface temperature, T_{L1L2}, with no mass transfer is given by

$$T_{L1L2} = \frac{h_{L1,L2} T_{L1} + h_{L2,L1} T_{L2}}{h_{L1,L2} + h_{L2,L1}}. \tag{2-46}$$

Then, the interfacial energy transfer rate can be evaluated:

$$q^{I}_{L1,L2} = a_{L1,L2}[h_{L1,L2}(T^{I}_{L1,L2} - T_{L1}) + h_{L2,L1}(T^{I}_{L1,L2} - T_{L2})]. \quad (2\text{-}47)$$

The steel vaporization rate at the liquid-fuel/liquid-steel interface is expressed by

$$\Gamma^{17}_{L2,G} = -\frac{q^{I}_{L1,L2}}{i_{Vap,G2} - i_{L2}}. \quad (2\text{-}48)$$

Liquid-fuel/Liquid-sodium interface: At the interface between liquid fuel and liquid sodium, sodium vaporization can occur if the net heat flow is negative at the interface. Similar to the liquid-fuel/liquid-steel interface, the interface temperatures can be expressed by

$$T^{I}_{L1,L3} = \max[T_{Sat,G3}, T_{L1L3}], \quad (2\text{-}49)$$

where the interface temperature, T_{L1L3}, with no mass transfer is given by

$$T_{L1L3} = \frac{h_{L1,L3}T_{L1} + h_{L3,L1}T_{L3}}{h_{L1,L3} + h_{L3,L1}}. \quad (2\text{-}50)$$

Then, the interfacial energy transfer rate can be evaluated:

$$q^{I}_{L1,L3} = a_{L1,L3}[h_{L1,L3}(T^{I}_{L1,L3} - T_{L1}) + h_{L3,L1}(T^{I}_{L1,L3} - T_{L3})]. \quad (2\text{-}51)$$

The sodium vaporization rate at the liquid-fuel/liquid-sodium interface is expressed by

$$\Gamma^{18}_{L3,G} = -\frac{q^{I}_{L1,L3}}{i_{Vap,G3} - i_{L3}}. \quad (2\text{-}52)$$

Liquid-steel/Liquid-sodium interface: At the interface between liquid steel and liquid sodium, sodium vaporization can occur if the net heat flow is negative at the interface. Similar to the liquid-fuel/liquid-steel interface, the interface temperatures can be expressed by

$$T^{I}_{L2,L3} = \max[T_{Sat,G3}, T_{L2L3}], \quad (2\text{-}53)$$

where the interface temperature, T_{L2L3}, with no mass transfer is given by

$$T_{L2L3} = \frac{h_{L2,L3}T_{L1} + h_{L3,L2}T_{L3}}{h_{L2,L3} + h_{L3,L2}}. \quad (2\text{-}54)$$

Then, the interfacial energy transfer rate can be evaluated:

$$q^{I}_{L2,L3} = a_{L2,L3}[h_{L2,L3}(T^{I}_{L2,L3} - T_{L2}) + h_{L3,L2}(T^{I}_{L2,L3} - T_{L3})]. \quad (2\text{-}55)$$

The sodium vaporization rate at the liquid-fuel/liquid-sodium interface is expressed by

$$\Gamma^{II2}_{L3,G} = -\frac{q^{I}_{L2,L3}}{i_{Vap,G3} - i_{L3}}. \quad (2\text{-}56)$$

Liquid-fuel/Fuel-particle interface: At the interface between liquid fuel and fuel particles, melting of fuel particles should occur if the interfacial heat flow is still negative at the fuel liquidus temperature. Freezing of liquid fuel is the preferred path if the interfacial heat flow is still positive at the fuel solidus temperature. Otherwise, if neither of these conditions is satisfied, Eq. (2-8) is applied to the interface temperature. Therefore, the interface temperatures can be expressed by

$$T^{I}_{L1,L4} = \min[T_{Liq,1}, \max(T_{L1L4}, T_{Sol,1})], \tag{2-57}$$

where the interface temperature, T_{L1L4}, with no mass transfer is given by

$$T_{L1L4} = \frac{h_{L1,L4}T_{L1} + h_{L4}T_{L4}}{h_{L1,L4} + h_{L4}}. \tag{2-58}$$

Then, the interfacial energy transfer rate is given by

$$q^{I}_{L1,L4} = a_{L1,L4}[h_{L1,L4}(T^{I}_{L1,L4} - T_{L1}) + h_{L4}(T^{I}_{L1,L4} - T_{L4})]. \tag{2-59}$$

The mass-transfer rates at the liquid-fuel/fuel-particle interface are expressed by

$$\Gamma^{19}_{L1,L4} = \frac{q^{I}_{L1,L4}}{i_{L1} - i_{Sol,1}}, \qquad q^{I}_{L1,L4} > 0, \qquad \text{for fuel freezing, and} \tag{2-60}$$

$$\Gamma^{19}_{L4,L1} = -\frac{q^{I}_{L1,L4}}{i_{Liq,1} - i_{L4}}, \qquad q^{I}_{L1,L4} < 0, \qquad \text{for fuel melting.} \tag{2-61}$$

Liquid-steel/Steel-particle interface: At the interface between liquid steel and steel particles, melting of steel particles should occur if the interfacial heat flow is still negative at the steel liquidus temperature. Freezing of liquid steel is the preferred path if the interfacial heat flow is still positive at the steel solidus temperature. Similar to the liquid-fuel/fuel-particle interface, the interface temperatures can be expressed by

$$T^{I}_{L2,L5} = \min[T_{Liq,2}, \max(T_{L2L5}, T_{Sol,2})], \tag{2-62}$$

where the interface temperature, T_{L2L5}, with no mass transfer is given by

$$T_{L2L5} = \frac{h_{L2,L5}T_{L2} + h_{L5}T_{L5}}{h_{L2,L5} + h_{L5}}. \tag{2-63}$$

Then, the interfacial energy transfer rate is given by

$$q^{I}_{L2,L5} = a_{L2,L5}[h_{L2,L5}(T^{I}_{L2,L5} - T_{L2}) + h_{L5}(T^{I}_{L2,L5} - T_{L5})]. \tag{2-64}$$

The mass-transfer rates at the liquid-steel/steel-particle interface are expressed by

$$\Gamma^{\mathrm{II}4}_{\mathrm{L2,L5}} = \frac{q^{\mathrm{I}}_{\mathrm{L2,L5}}}{i_{\mathrm{L2}} - i_{\mathrm{Sol,2}}}, \qquad q^{\mathrm{I}}_{\mathrm{L2,L5}} > 0, \qquad \text{for steel freezing, and} \tag{2-65}$$

$$\Gamma^{\mathrm{II}4}_{\mathrm{L5,L2}} = -\frac{q^{\mathrm{I}}_{\mathrm{L2,L5}}}{i_{\mathrm{Liq,2}} - i_{\mathrm{L5}}}, \qquad q^{\mathrm{I}}_{\mathrm{L2,L5}} < 0, \qquad \text{for steel melting.} \tag{2-66}$$

Liquid-fuel/Steel-particle interface: At the interface between liquid fuel and steel particles, steel particles can be melted or fuel particles can be formed. In reality, simultaneous fuel freezing and steel melting might be expected upon contact in many situations. The interfacial energy transfer rate gives insufficient information to furnish the rates for both phenomena. The current model defines the interfacial temperature by an instantaneous contact value that ignores phase transitions:

$$T^{\mathrm{I}}_{\mathrm{L1,L5}} = \frac{(\sqrt{\kappa\rho c})_{\mathrm{L1}} T_{\mathrm{L1}} + (\sqrt{\kappa\rho c})_{\mathrm{L5}} T_{\mathrm{L5}}}{(\sqrt{\kappa\rho c})_{\mathrm{L1}} + (\sqrt{\kappa\rho c})_{\mathrm{L5}}}. \tag{2-67}$$

Then, the interfacial energy transfer rate is given by

$$q^{\mathrm{I}}_{\mathrm{L1,L5}} = a_{\mathrm{L1,L5}}[h_{\mathrm{L1,L5}}(T^{\mathrm{I}}_{\mathrm{L1,L5}} - T_{\mathrm{L1}}) + h_{\mathrm{L5}}(T^{\mathrm{I}}_{\mathrm{L1,L5}} - T_{\mathrm{L5}})]. \tag{2-68}$$

The mass-transfer rates at the liquid-fuel/steel-particle interface are expressed by

$$\Gamma^{\mathrm{II}0}_{\mathrm{L1,L4}} = \frac{q^{\mathrm{I}}_{\mathrm{L1,L5}}}{i_{\mathrm{L1}} - i_{\mathrm{Sol,1}}}, \qquad q^{\mathrm{I}}_{\mathrm{L1,L5}} > 0, \qquad \text{for fuel-particle formation, and} \tag{2-69}$$

$$\Gamma^{\mathrm{II}0}_{\mathrm{L5,L2}} = -\frac{q^{\mathrm{I}}_{\mathrm{L1,L5}}}{i_{\mathrm{Liql,2}} - i_{\mathrm{L5}}}, \qquad q^{\mathrm{I}}_{\mathrm{L1,L5}} < 0, \qquad \text{for steel-particle melting.} \tag{2-70}$$

Liquid-fuel/Pin structure interface: For a cladding surface, cladding can be ablated or fuel particles can be formed. This process is treated similarly to the liquid-fuel/steel-particle interface, and hence the interface temperatures can be expressed by

$$T^{\mathrm{I}}_{\mathrm{L1,k1}} = \frac{(\sqrt{\kappa\rho c})_{\mathrm{L1}} T_{\mathrm{L1}} + (\sqrt{\kappa\rho c})_{\mathrm{k1}} T_{\mathrm{k1}}}{(\sqrt{\kappa\rho c})_{\mathrm{L1}} + (\sqrt{\kappa\rho c})_{\mathrm{k1}}}, \tag{2-71}$$

where k1 is active for the cladding surface, SK(1) = S4. Then, the interfacial energy transfer rate is given by

$$q^{\mathrm{I}}_{\mathrm{L1,k1}} = a_{\mathrm{L1,k1}}[h_{\mathrm{L1S}}(T^{\mathrm{I}}_{\mathrm{L1,k1}} - T_{\mathrm{k1}}) + h_{\mathrm{k1}}(T^{\mathrm{I}}_{\mathrm{L1,k1}} - T_{\mathrm{L1}})]. \tag{2-72}$$

The mass-transfer rates at the liquid-fuel/cladding interface are expressed by

$$\Gamma^{I23}_{L1,L4} = \frac{q^{I}_{L1k1}}{i_{L1} - i_{Sol,1}}, \qquad q^{I}_{L1,k1} > 0, \qquad \text{for fuel-particle formation, and} \tag{2-73}$$

$$\Gamma^{I23}_{k1,L2} = -\frac{q^{I}_{L1,k1}}{i_{Liql,2} - i_{k1}}, \qquad q^{I}_{L1,k1} < 0, \qquad \text{for cladding ablation.} \tag{2-74}$$

For a pin-fuel surface, the case of no mass transfer is applied to the interface between liquid fuel and pin structure. Therefore, the interface temperature is given by

$$T^{I}_{L1,k1} = \frac{h_{L1S}T_{L1} + h_{k1}T_{k1}}{h_{L1,S} + h_{k1}}, \tag{2-75}$$

where k1 is active for the pin-fuel surface, SK(1) =S1.

Liquid-steel/Pin-structure interface: For a cladding surface, non-equilibrium M/F of steel can occur. This process is treated similarly to the liquid-steel/steel-particle interface, and hence the interface temperature can be expressed by

$$T^{I}_{L2,k1} = \min[T_{Liq,2}, \max(T_{L2k1}, T_{Sol,2})], \tag{2-76}$$

where k1 is active for the cladding surface, SK(1) = S4. The interface temperature, T_{L2k1}, with no mass transfer is

$$T_{L2k1} = \frac{h_{L2S}T_{L2} + h_{k1}T_{k1}}{h_{L2S} + h_{k1}}. \tag{2-77}$$

Then, the interfacial energy transfer rate is given by

$$q^{I}_{L2,k1} = a_{L2,k1}[h_{L2S}(T^{I}_{L2,k1} - T_{L2}) + h_{k1}(T^{I}_{L2,k1} - T_{k1})]. \tag{2-78}$$

Once the interfacial energy transfer rate is known, the mass-transfer rates are

$$\Gamma^{I24}_{L2,k1} = \frac{q^{I}_{L2,k1}}{i_{L2} - i_{Sol,2}}, \qquad q^{I}_{L2,k1} > 0, \qquad \text{for steel freezing, and} \tag{2-79}$$

$$\Gamma^{I24}_{k1,L2} = -\frac{q^{I}_{L2,k1}}{i_{Liq,2} - i_{k1}}, \qquad q^{I}_{L2,k1} < 0, \qquad \text{for cladding melting.} \tag{2-80}$$

For a pin-fuel surface, the case of no mass transfer is applied to the interface between liquid steel and pin structure. Therefore, the interface temperature is given by

$$T^{I}_{L2,k1} = \frac{h_{L2S}T_{L2} + h_{k1}T_{k1}}{h_{L2S} + h_{k1}}, \tag{2-81}$$

where k1 is active for the pin-fuel surface, SK(1) = S1.

Liquid-fuel/Can-wall (or fuel crust) interface: For a crust surface, non-equilibrium M/F of crust can occur. This process is treated similarly to the liquid-fuel/fuel-particle interface, and hence the interface temperatures can be expressed by

$$T^{I}_{L1,km} = \min[T_{Liq,l}, \max(T_{L1km}, T_{Sol,1})], \tag{2-82}$$

where km for m = 2 and 3 is active for the left crust surface, SK(2) = S2, and the right crust surface, SK(3) = S3, respectively. The interface temperatures, T_{L1km}, with no mass transfer are given by

$$T_{L1km} = \frac{h_{L1,S}T_{L1} + h_{km}T_{km}}{h_{L1,S} + h_{km}}. \tag{2-83}$$

Then, the interfacial energy transfer rates are given by

$$q^{I}_{L1,km} = a_{L1,km}[h_{L1,S}(T^{I}_{L1,km} - T_{L1}) + h_{km}(T^{I}_{L1,km} - T_{km})]. \tag{2-84}$$

Once the interfacial energy transfer rate is known, the mass-transfer rates are

$$\Gamma^{I(k)}_{L1,km} = \frac{q^{I}_{L1,km}}{i_{L1} - i_{Sol,l}}, \qquad q^{I}_{L1,km} > 0, \quad \text{for fuel freezing, and} \tag{2-85}$$

$$\Gamma^{I(k)}_{km,L1} = -\frac{q^{I}_{L1,km}}{i_{Liq,l} - i_{km}}, \qquad q^{I}_{L1,S2} < 0, \quad \text{for crust melting,} \tag{2-86}$$

where I(k) for k = 2 and 3 represents I31 and I32, respectively.

For a can-wall surface, a can wall can be ablated or a crust can be formed. This process is treated similarly to the liquid-fuel/steel-particle interface, and hence the interface temperatures can be expressed by

$$T^{I}_{L1,km} = \frac{(\sqrt{\kappa\rho c})_{L1}T_{L1} + (\sqrt{\kappa\rho c})_{km}T_{km}}{(\sqrt{\kappa\rho c})_{L1} + (\sqrt{\kappa\rho c})_{km}}, \tag{2-87}$$

where km for m = 2 and 3 is active for the left can-wall surface, SK(2) = S5 or S6, and the right can-wall surface, SK(3) = S7 or S8, respectively. Then, the interfacial energy transfer rates are given by

$$q^{I}_{L1,km} = a_{L1,km}[h_{L1,S}(T^{I}_{L1,km} - T_{L1}) + h_{km}(T^{I}_{L1,km} - T_{km})]. \tag{2-88}$$

Once the interfacial energy transfer rate is known, the mass-transfer rates are

$$\Gamma^{I(k)}_{L1,SK(k)} = \frac{q^{I}_{L1,km}}{i_{L1} - i_{Sol,1}}, \qquad q^{I}_{L1,km} > 0, \quad \text{for crust formation, and} \tag{2-89}$$

$$\Gamma^{I(k)}_{km,L2} = -\frac{q^{I}_{L1,km}}{i_{Liq,2} - i_{km}}, \qquad q^{I}_{L1,km} < 0, \qquad \text{for can-wall ablation,} \tag{2-90}$$

where SK(k) for k = 2 and 3 is the energy component of crust fuel, S2 and S3, respectively.

Liquid-steel/Can-wall (or fuel crust) interface: For a can-wall surface, non-equilibrium M/F of steel can occur. This process is treated similarly to the liquid-steel/steel-particle interface, and hence the interface temperatures can be expressed by

$$T^{I}_{L2,km} = \min[T_{Liq,2}, \max(T_{L2km}, T_{Sol,2})], \tag{2-91}$$

where km for m = 2 and 3 is active for the left can-wall surface, SK(2) = S5 or S6, and the right can-wall surface, SK(3) = S7 or S8, respectively. The interface temperature, T_{L2km}, with no mass transfer is given by

$$T_{L2km} = \frac{h_{L2,S} T_{L2} + h_{km} T_{km}}{h_{L2,S} + h_{km}}. \tag{2-92}$$

Then, the interfacial energy transfer rate is given by

$$q^{I}_{L2,km} = a_{L2,km}[h_{L2,S}(T^{I}_{L2,km} - T_{L2}) + h_{km}(T^{I}_{L2,km} - T_{km})]. \tag{2-93}$$

Once the interfacial energy transfer rate is known, the mass-transfer rates are

$$\Gamma^{I(k)}_{L2,km} = \frac{q^{I}_{L2,km}}{i_{L2} - i_{Sol,2}}, \qquad q^{I}_{L2,km} > 0, \qquad \text{for steel freezing, and} \tag{2-94}$$

$$\Gamma^{I(k)}_{km,L2} = -\frac{q^{I}_{L2,km}}{i_{Liq,2} - i_{km}}, \qquad q^{I}_{L2,km} < 0, \qquad \text{for cladding melting,} \tag{2-95}$$

where I(k) for k = 2 and 3 represents I33 and I34, respectively.

For a crust surface, the case of no mass transfer is applied to the interface between liquid steel and can wall. Therefore, the interface temperatures are given by

$$T^{I}_{L2,km} = \frac{h_{L2,S} T_{L2} + h_{km} T_{km}}{h_{L2,S} + h_{km}}, \tag{2-96}$$

where km for m = 2 and 3 is active for the crust surface, SK(2) = S2 and SK(3) = S3, respectively.

Interfaces without non-equilibrium mass transfer: According to the limitation of non-equilibrium mass transfer, only the case of no mass transfer is applied to the following interfaces. At these interfaces, the interface temperature with no mass transfer, which is

defined by Eq. (2-8), is assigned.

For liquid-steel/fuel-particle interface

$$T^{I}_{L2,L4} = \frac{h_{L2,L4}T_{L2} + h_{L4}T_{L4}}{h_{L2,L4} + h_{L4}}. \tag{2-97}$$

For liquid-sodium/fuel-particle interface

$$T^{I}_{L3,L4} = \frac{h_{L3,L4}T_{L3} + h_{L4}T_{L4}}{h_{L3,L4} + h_{L4}}. \tag{2-98}$$

For liquid-sodium/steel-particle interface

$$T^{I}_{L3,L5} = \frac{h_{L3,L5}T_{L3} + h_{L5}T_{L5}}{h_{L3,L5} + h_{L5}}. \tag{2-99}$$

For real-liquid/control-particle interface

$$T^{I}_{Lm,L6} = \frac{h_{Lm,L6}T_{Lm} + h_{L6}T_{L6}}{h_{Lm,L6} + h_{L6}}, \text{ m} = 1, 2 \text{ and } 3. \tag{2-100}$$

For particle/particle interface

$$T^{I}_{Lm,Lm'} = \frac{h_{Lm,Lm'}T_{Lm} + h_{Lm'}T_{Lm'}}{h_{Lm,Lm'} + h_{Lm'}}, \text{ m} = 4, 5 \text{ and } 6, \text{ and m'} = 4, 5 \text{ and } 6 \text{ (m'} \neq \text{m)}. \tag{2-101}$$

For particle/structure interface

$$T^{I}_{Lm,km'} = \frac{h_{Lm,S}T_{Lm} + h_{km'}T_{km'}}{h_{Lm,S} + h_{km'}}, \text{ m} = 4, 5 \text{ and } 6, \text{ and m'} = 1, 2 \text{ and } 3. \tag{2-102}$$

For liquid-sodium/structure interface

$$T^{I}_{L3,km} = \frac{h_{L3,S}T_{L3} + h_{km}T_{km}}{h_{L3,S} + h_{km}}, \text{ m} = 4, 5 \text{ and } 6. \tag{2-103}$$

2.4. Equilibrium transfers

The equilibrium mass-transfer rate is determined from the bulk energy level exceeding the phase-transition energy. The freezing rate is proportional to the difference between the liquid energy and its liquidus energy. The melting rate is proportional to the difference between the solid energy and its solidus energy. In the case of freezing, the remaining liquid energy is assumed to be at its liquidus energy, and the solid energy is calculated to ensure energy conservation in the liquid-solid system. Similarly, in the case of melting, the

remaining solids have its solidus energy. The eight (and three optional) equilibrium mass-transfer rates are defined as follows:

for fuel crust melting

$$\Gamma^{EQ}_{Sm,L1} = \frac{1}{\Delta t}\frac{e_{S2} - e_{Sol,M(Sm)}}{h_{f,M(Sm)}}\overline{\rho}_{Sm}, \qquad e_{Sm} > e_{Sol,M(Sm)}, \qquad m = 2 \text{ and } 3, \tag{2-104}$$

for can-wall surface melting

$$\Gamma^{EQ}_{Sm,L2} = \frac{1}{\Delta t}\frac{e_{km} - e_{Sol,M(Sm)}}{h_{f,M(Sm)}}\overline{\rho}_{Sm}, \; e_{Sm} > e_{Sol,M(Sm)}, \qquad m = 5 \text{ and } 7, \tag{2-105}$$

for fuel particle melting

$$\Gamma^{EQ}_{L4,L1} = \frac{1}{\Delta t}\frac{e_{L4} - e_{Sol,M(L4)}}{h_{f,M(L4)}}\overline{\rho}_{L4}, \qquad e_{L4} > e_{Sol,M(L4)}, \tag{2-106}$$

for steel particle melting

$$\Gamma^{EQ}_{L5,L2} = \frac{1}{\Delta t}\frac{e_{L5} - e_{Sol,M(L5)}}{h_{f,M(L5)}}\overline{\rho}_{L5}, \qquad e_{L5} > e_{Sol,M(L5)}, \tag{2-107}$$

for fuel particle formation

$$\Gamma^{EQ}_{L1,L4} = \frac{1}{\Delta t}\frac{e_{Liq,M(L1)} - e_{L1}}{h_{f,M(L1)}}\overline{\rho}_{L1}, \qquad e_{L1} < e_{Liq,M(L1)}, \text{ and} \tag{2-108}$$

for steel particle formation and liquid steel film freezing into structures (optional paths)

$$\Gamma^{EQ}_{L2,L5} = \frac{1}{\Delta t}\frac{e_{Liq,M(L2)} - e_{L2}}{h_{f,M(L2)}}\overline{\rho}_{L2}, \qquad e_{L2} < e_{Liq,M(L2)}, \tag{2-109}$$

where the heat of fusion, $h_{f,M}$, is defined by $e_{Liq,M} - e_{Sol,M}$.

Table 2-1. Possible non-equilibrium mass-transfer processes.

ID	Interface	Process	Mass-transfer rate
I1	Liquid Fuel -Vapor	• Condense Fuel Vapor	$\Gamma^{I1}_{G,L1}$
		• Form Fuel Particles	$\Gamma^{I1}_{L1,L4}$
		• Vaporize Liquid Fuel	$\Gamma^{I1}_{L1,G}$
I2	Liquid Steel -Vapor	• Condense Fuel and Steel Vapor	$\Gamma^{I2}_{G,Lm}$ (m = 1 and 2)
		• Form Steel Particles	$\Gamma^{I2}_{L2,L5}$
		• Vaporize Liquid Steel	$\Gamma^{I2}_{L2,G}$
I3	Liquid Sodium -Vapor	• Condense Fuel, Steel, and Sodium Vapor	$\Gamma^{I3}_{G,Lm}$ (m = 1, 2 and 3)
		• Vaporize Liquid Sodium	$\Gamma^{I3}_{L3,G}$
I4	Fuel Particles -Vapor	• Condense Fuel, Steel, and Sodium Vapor	$\Gamma^{I4}_{G,Lm}$ (m = 1, 2 and 3)
		• Melt Fuel Particles	$\Gamma^{I4}_{L4,L1}$
I5	Steel Particles -Vapor	• Condense Fuel, Steel, and Sodium Vapor	$\Gamma^{I5}_{G,Lm}$ (m = 1, 2 and 3)
		• Melt Steel Particles	$\Gamma^{I5}_{L5,L2}$
I6	Control Particles -Vapor	• Condense Fuel, Steel, and Sodium Vapor	$\Gamma^{I6}_{G,Lm}$ (m = 1, 2 and 3)
I7	Liquid Fuel -Liquid Steel	• Form Fuel Particles	$\Gamma^{I7}_{L1,L4}$
		• Vaporize Liquid Steel	$\Gamma^{I7}_{L2,G}$
I8	Liquid Fuel -Liquid Sodium	• Form Fuel Particles	$\Gamma^{I8}_{L1,L4}$
		• Vaporize Liquid Sodium	$\Gamma^{I8}_{L3,G}$
I9	Liquid Fuel -Fuel Particles	• Form Fuel Particles	$\Gamma^{I9}_{L1,L4}$
		• Melt Fuel Particles	$\Gamma^{I9}_{L4,L1}$
I10	Liquid Fuel -Steel Particles	• Form Fuel Particles	$\Gamma^{I10}_{L1,L4}$
		• Melt Steel Particles	$\Gamma^{I10}_{L5,L2}$
I11	Liquid Fuel -Control Particles	• Form Fuel Particles	$\Gamma^{I11}_{L1,L4}$
		• Vaporize Liquid Fuel	$\Gamma^{I10}_{L2,G}$
I12	Liquid Steel -Liquid Sodium	• Form Steel Particles	$\Gamma^{I12}_{L2,L5}$
		• Vaporize Liquid Sodium	$\Gamma^{I12}_{L3,G}$

Table 2-1. (CONT)

ID	Interface	Process	Mass-transfer rate
I13	Liquid Steel -Fuel Particles	• Form Steel Particles	$\Gamma^{I13}_{L2,L5}$
		• Vaporize Liquid Steel	$\Gamma^{I13}_{L2,G}$
		• Melt Steel Particles	$\Gamma^{I13}_{L5,L2}$
I14	Liquid Steel -Steel Particles	• Form Steel Particles	$\Gamma^{I14}_{L2,L5}$
		• Melt Steel Particles	$\Gamma^{I14}_{L5,L2}$
I15	Liquid Steel -Control Particles	• Form Steel Particles	$\Gamma^{I15}_{LI,L4}$
		• Vaporize Liquid Steel	$\Gamma^{I15}_{L2,G}$
I16	Liquid Sodium -Fuel Particles	• Vaporize Liquid Sodium	$\Gamma^{I16}_{L3,G}$
I17	Liquid Sodium -Steel Particles	• Vaporize Liquid Sodium	$\Gamma^{I17}_{L3,G}$
		• Melt Steel Particles	$\Gamma^{I17}_{L5,L2}$
I18	Liquid Sodium -Control Particles	• Vaporize Liquid Sodium	$\Gamma^{I18}_{L3,G}$
I19	Fuel Particles -Steel Particles	• Melt Steel Particles	$\Gamma^{I19}_{L5,L2}$
I20	Fuel Particles - Control Particles	• Melt Fuel Particles	$\Gamma^{I20}_{L4,L1}$
I21	Steel Particles - Control Particles	• Melt Steel Particles	$\Gamma^{I21}_{L5,L2}$
I22	Pin -Vapor	• Condense Fuel, Steel, and Sodium Vapor	$\Gamma^{I22}_{G,Lm}$ (m = 1, 2 and 3)
		• Melt Cladding	$\Gamma^{I22}_{S4,L2}$
		• Melt Pin Fuel	$\Gamma^{I22}_{SI,L1}$
I23	Pin -Liquid Fuel	• Form Fuel Particles	$\Gamma^{I23}_{LI,L4}$
		• Melt Cladding	$\Gamma^{I23}_{S4,L2}$
		• Melt Pin Fuel	$\Gamma^{I23}_{SI,L1}$
		• Vaporize Liquid Fuel	$\Gamma^{I23}_{LI,G}$
I24	Pin -Liquid Steel	• Freeze Steel to Cladding	$\Gamma^{I24}_{L2,S4}$
		• Melt Cladding	$\Gamma^{I24}_{S4,L2}$
		• Vaporize Liquid Steel	$\Gamma^{I24}_{L2,G}$
		• Melt Pin Fuel	$\Gamma^{I24}_{SI,L1}$

Table 2-1. (CONT)

ID	Interface	Process	Mass-transfer rate
I25	Pin -Liquid Sodium	• Vaporize Liquid Sodium • Melt Cladding	$\Gamma_{L3,G}^{I25}$ $\Gamma_{S4,L2}^{I25}$
I26	Pin -Fuel Particles	• Melt Cladding • Melt Fuel Particles	$\Gamma_{S4,L2}^{I26}$ $\Gamma_{L4,L1}^{I26}$
I27	Pin -Steel Particles	• Melt Steel Particles	$\Gamma_{L5,L2}^{I27}$
I28	Pin -Control Particles	• Melt Cladding • Melt Pin Fuel	$\Gamma_{S4,L2}^{I28}$ $\Gamma_{SI,L1}^{I28}$
I29	Left Can Wall or Crust -Vapor	• Condense Fuel, Steel, and Sodium Vapor • Melt Can Wall • Melt Crust	$\Gamma_{G,Lm}^{I29}$ (m = 1, 2 and 3) $\Gamma_{S5,L2}^{I29}$ or $\Gamma_{S6,L2}^{I29}$ $\Gamma_{S2,L1}^{I29}$
I30	Right Can Wall or Crust -Vapor	• Condense Fuel, Steel, and Sodium Vapor • Melt Can Wall • Melt Crust	$\Gamma_{G,Lm}^{I30}$ (m = 1, 2 and 3) $\Gamma_{S7,L2}^{I30}$ or $\Gamma_{S8,L2}^{I30}$ $\Gamma_{S3,L1}^{I30}$
I31	Left Can Wall or Crust -Liquid Fuel	• Form Crust • Melt Crust • Melt Can Wall	$\Gamma_{L1,S2}^{I31}$ $\Gamma_{S2,L1}^{I31}$ $\Gamma_{S5,L2}^{I31}$ or $\Gamma_{S6,L2}^{I31}$
I32	Right Can Wall or Crust -Liquid Fuel	• Form Crust • Melt Crust • Melt Can Wall	$\Gamma_{L1,L3}^{I32}$ $\Gamma_{S3,L1}^{I32}$ $\Gamma_{S7,L2}^{I32}$ or $\Gamma_{S8,L2}^{I32}$
I33	Left Can Wall or Crust -Liquid Steel	• Freeze Steel to Can Wall • Melt Can Wall • Vaporize Liquid Steel • Melt Crust	$\Gamma_{L2,S5}^{I33}$ or $\Gamma_{L2,S6}^{I33}$ $\Gamma_{S5,L2}^{I33}$ or $\Gamma_{S6,L2}^{I33}$ $\Gamma_{L2,G}^{I33}$ $\Gamma_{S2,L1}^{I33}$
I34	Right Can Wall or Crust -Liquid Steel	• Freeze Steel to Can Wall • Melt Can Wall • Vaporize Liquid Steel • Melt Crust	$\Gamma_{L2,S7}^{I34}$ or $\Gamma_{L2,S8}^{I34}$ $\Gamma_{S7,L2}^{I34}$ or $\Gamma_{S8,L2}^{I34}$ $\Gamma_{L2,G}^{I34}$ $\Gamma_{S3,L1}^{I34}$
I35	Left Can Wall or Crust -Liquid Sodium	• Vaporize Liquid Sodium • Melt Can Wall	$\Gamma_{L3,G}^{I35}$ $\Gamma_{S5,L2}^{I35}$ or $\Gamma_{S6,L2}^{I35}$

Table 2-1. (CONT)

ID	Interface	Process	Mass-transfer rate
I36	Right Can Wall or Crust -Liquid Sodium	• Vaporize Liquid Sodium • Melt Can Wall	$\Gamma^{I36}_{L3,G}$ $\Gamma^{I36}_{S7,L2}$ or $\Gamma^{I36}_{S8,L2}$
I37	Left Can Wall or Crust -Fuel Particles	• Melt Can Wall	$\Gamma^{I37}_{S5,L2}$ or $\Gamma^{I37}_{S6,L2}$
I38	Right Can Wall or Crust -Fuel Particles	• Melt Can Wall	$\Gamma^{I38}_{S7,L2}$ or $\Gamma^{I38}_{S8,L2}$
I39	Left Can Wall or Crust -Steel Particles	• Melt Steel Particles	$\Gamma^{I39}_{L5,L2}$
I40	Right Can Wall or Crust -Steel Particles	• Melt Steel Particles	$\Gamma^{I40}_{L5,L2}$
I41	Left Can Wall or Crust -Control Particles	• Melt Can Wall • Melt Crust	$\Gamma^{I41}_{S5,L2}$ or $\Gamma^{I41}_{S6,L2}$ $\Gamma^{I41}_{S2,L1}$
I42	Right Can Wall or Crust -Control Particles	• Melt Can Wall • Melt Crust	$\Gamma^{I42}_{S7,L2}$ or $\Gamma^{I42}_{S8,L2}$ $\Gamma^{I32}_{S3,L1}$

Table 2-2. SIMMER-III non-equilibrium mass-transfer processes.

ID	Interface	Process	Mass-transfer rate
I1	Liquid Fuel -Vapor	• Condense Fuel Vapor • Vaporize Liquid Fuel	$\Gamma^{I1}_{G,L1}$ $\Gamma^{I1}_{L1,G}$
I2	Liquid Steel -Vapor	• Condense Fuel and Steel Vapor • Vaporize Liquid Steel	$\Gamma^{I2}_{G,Lm}$ (m = 1 and 2) $\Gamma^{I2}_{L2,G}$
I3	Liquid Sodium -Vapor	• Condense Fuel, Steel, and Sodium Vapor • Vaporize Liquid Sodium	$\Gamma^{I3}_{G,Lm}$ (m = 1, 2 and 3) $\Gamma^{I3}_{L3,G}$
I4	Fuel Particles -Vapor	• Condense Fuel, Steel, and Sodium Vapor	$\Gamma^{I4}_{G,Lm}$ (m = 1, 2 and 3)
I5	Steel Particles -Vapor	• Condense Fuel, Steel, and Sodium Vapor	$\Gamma^{I5}_{G,Lm}$ (m = 1, 2 and 3)
I6	Control Particles -Vapor	• Condense Fuel, Steel, and Sodium Vapor	$\Gamma^{I6}_{G,Lm}$ (m = 1, 2 and 3)
I7	Liquid Fuel -Liquid Steel	• Vaporize Liquid Steel	$\Gamma^{I7}_{L2,G}$
I8	Liquid Fuel -Liquid Sodium	• Vaporize Liquid Sodium	$\Gamma^{I8}_{L3,G}$
I9	Liquid Fuel -Fuel Particles	• Form Fuel Particles • Melt Fuel Particles	$\Gamma^{I9}_{L1,L4}$ $\Gamma^{I9}_{L4,L1}$
I10	Liquid Fuel -Steel Particles	• Form Fuel Particles • Melt Steel Particles	$\Gamma^{I10}_{L1,L4}$ $\Gamma^{I10}_{L5,L2}$
I12	Liquid Steel -Liquid Sodium	• Vaporize Liquid Sodium	$\Gamma^{I12}_{L3,G}$
I14	Liquid Steel -Steel Particles	• Form Steel Particles • Melt Steel Particles	$\Gamma^{I14}_{L2,L5}$ $\Gamma^{I14}_{L5,L2}$
I22	Pin -Vapor	• Condense Fuel, Steel, and Sodium Vapor	$\Gamma^{I22}_{G,Lm}$ (m = 1, 2 and 3)
I23	Pin -Liquid Fuel	• Form Fuel Particles • Melt Cladding	$\Gamma^{I23}_{L1,L4}$ $\Gamma^{I23}_{S4,L2}$

Table 2-2. (CONT)

ID	Interface	Process	Mass-transfer rate
I24	Pin -Liquid Steel	• Freeze Steel to Cladding • Melt Cladding	$\Gamma^{I24}_{L2,S4}$ $\Gamma^{I24}_{S4,L2}$
I29	Left Can Wall or Crust -Vapor	• Condense Fuel, Steel, and Sodium Vapor	$\Gamma^{I29}_{G,Lm}$ (m = 1, 2 and 3)
I30	Right Can Wall or Crust -Vapor	• Condense Fuel, Steel, and Sodium Vapor	$\Gamma^{I30}_{G,Lm}$ (m = 1, 2 and 3)
I31	Left Can Wall or Crust -Liquid Fuel	• Form Crust • Melt Crust • Melt Can Wall	$\Gamma^{I31}_{L1,S2}$ $\Gamma^{I31}_{S2,L1}$ $\Gamma^{I31}_{S5,L2}$ or $\Gamma^{I31}_{S6,L2}$
I32	Right Can Wall or Crust -Liquid Fuel	• Form Crust • Melt Crust • Melt Can Wall	$\Gamma^{I32}_{L1,L3}$ $\Gamma^{I32}_{S3,L1}$ $\Gamma^{I32}_{S7,L2}$ or $\Gamma^{I32}_{S8,L2}$
I33	Left Can Wall or Crust -Liquid Steel	• Freeze Steel to Can Wall • Melt Can Wall	$\Gamma^{I33}_{L2,S5}$ or $\Gamma^{I33}_{L2,S6}$ $\Gamma^{I33}_{S5,L2}$ or $\Gamma^{I33}_{S6,L2}$
I34	Right Can Wall or Crust -Liquid Steel	• Freeze Steel to Can Wall • Melt Can Wall	$\Gamma^{I34}_{L2,S7}$ or $\Gamma^{I34}_{L2,S8}$ $\Gamma^{I34}_{S7,L2}$ or $\Gamma^{I34}_{S8,L2}$

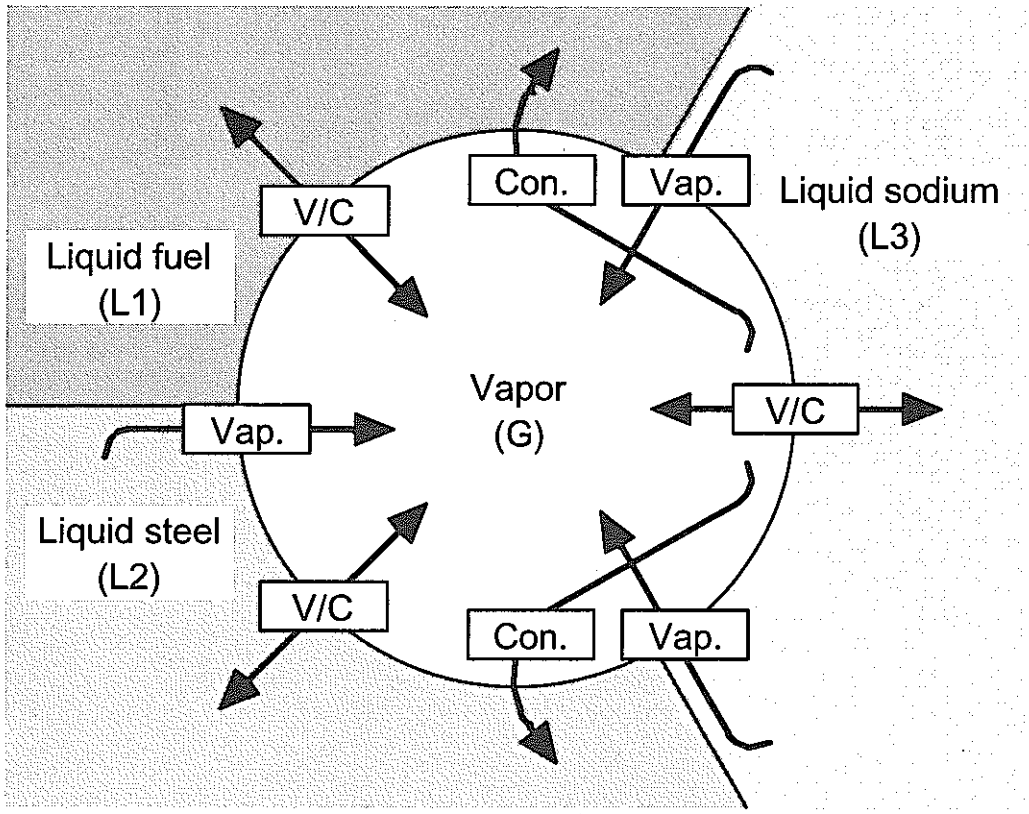

Figure 2-1. **Mass-transfer processes among liquid and vapor interfaces.**

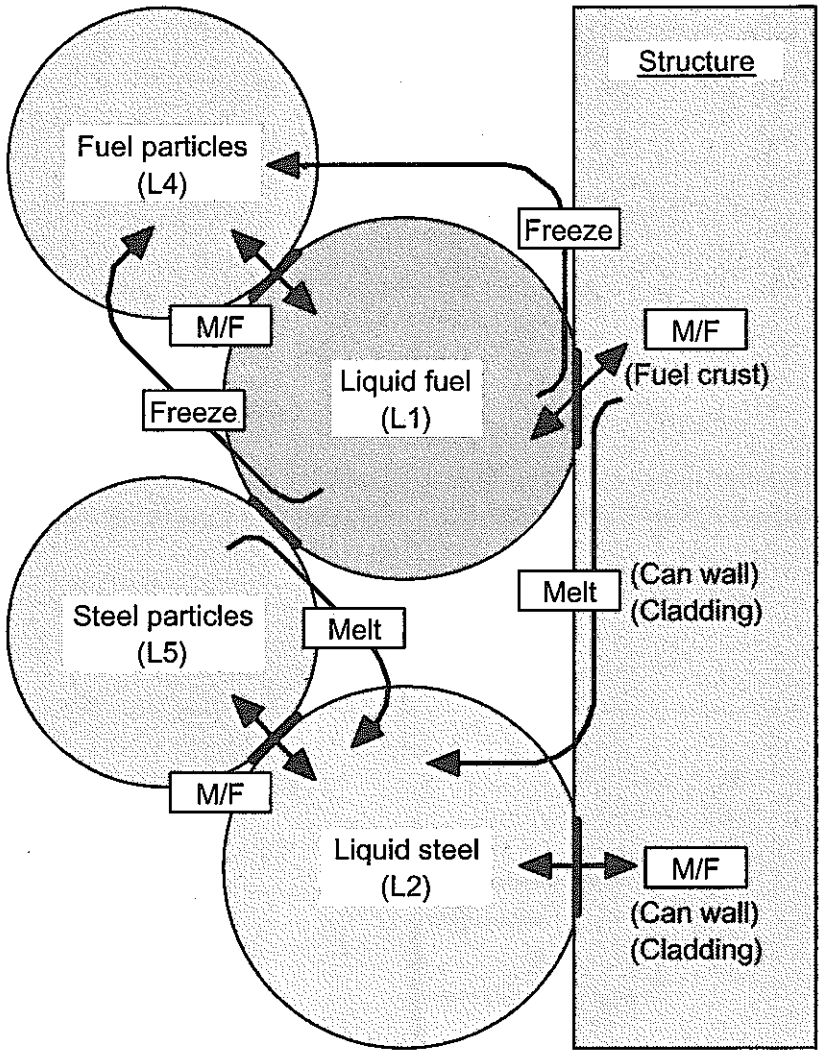

Figure 2-2. **Interface contacts and mass-transfer processes for fuel and steel droplets in non-equilibrium M/F model.**

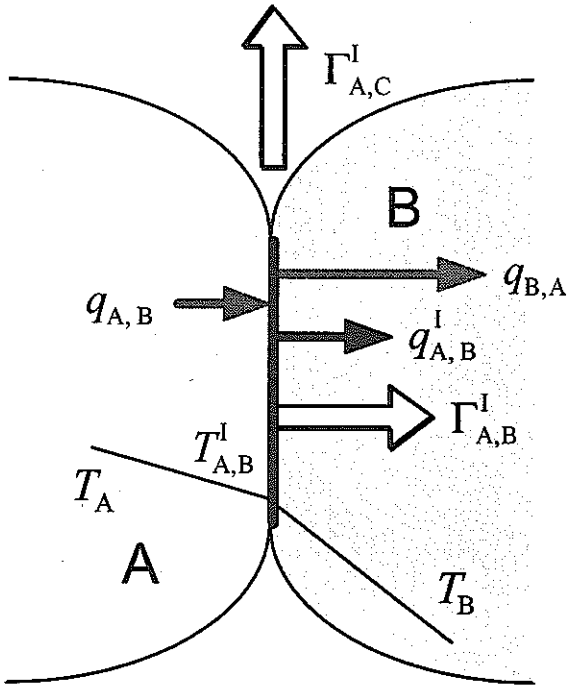

(a) Mass-transfer possibilities at an (A,B) interfaces with net heat flow to the interface toward Component B —— Component A condenses or freezes

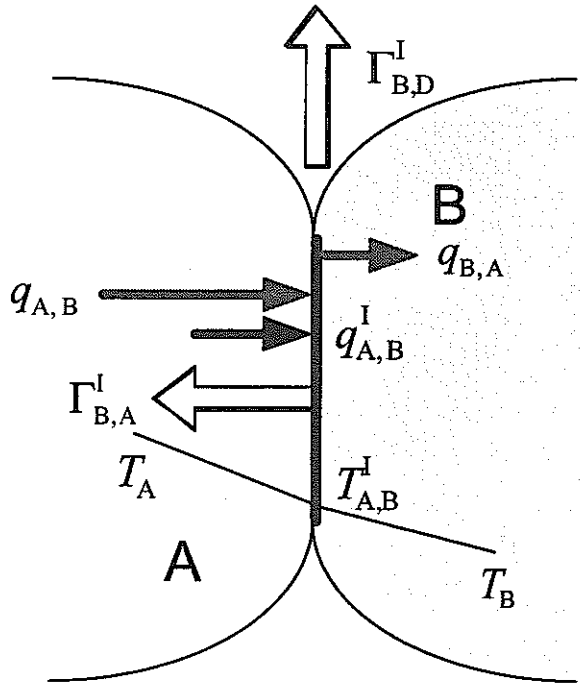

(b) Mass-transfer possibilities at an (A,B) interfaces with net heat flow to the interface from Component A —— Component B vaporizes or melts

Figure 2-3. Basis of non-equilibrium heat-transfer-limited process.

Chapter 3. Overall solution procedure

3.1. Mass- and energy-conservation equations

Once expressions for the heat and mass-transfer rates are known at each interface and/or component, the overall mass- and energy-conservation equations can be written for structure, particles, vapor, and liquids.

The mass-conservation equations for the structures are

$$\frac{\partial \overline{\rho}_{SK(k)}}{\partial t} = \sum_{m=1}^{2} [\Gamma^{NE}_{Lm,SK(k)} - \Gamma^{NE}_{SK(k),Lm}] - \sum_{m=1}^{2} \Gamma^{EQ}_{SK(k),Lm}, \tag{3-1}$$

where SK(k) for k = 1, 2 and 3 represents the energy components of pin, left and right can-wall surfaces, respectively, $\Gamma^{NE}_{Lm,SK(k)}$ is the non-equilibrium mass-transfer rate due to liquid freezing, $\Gamma^{NE}_{SK(k),Lm}$ is the non-equilibrium mass-transfer rate due to structure melting, and $\Gamma^{EQ}_{SK(k),Lm}$ is the equilibrium mass-transfer rate due to structure melting.

The mass-conservation equations for the fuel and steel particles are

$$\frac{\partial \overline{\rho}_{Lm}}{\partial t} = \sum_{m'=1}^{2} [\Gamma^{NE}_{Lm',Lm} - \Gamma^{NE}_{Lm,Lm'}] + \sum_{m'=1}^{2} [\Gamma^{EQ}_{Lm',Lm} - \Gamma^{EQ}_{Lm,Lm'}], \tag{3-2}$$

where Lm for m = 4 and 5 represents the energy components of fuel and steel particles, respectively, $\Gamma^{NE}_{Lm,Lm'}$ is the non-equilibrium mass-transfer rate due to liquid freezing, $\Gamma^{NE}_{Lm',Lm}$ is the non-equilibrium mass-transfer rate due to particle melting, $\Gamma^{EQ}_{Lm,Lm'}$ is the equilibrium mass-transfer rate due to liquid freezing, and $\Gamma^{EQ}_{Lm',Lm}$ is the equilibrium mass-transfer rate due to particle melting.

The mass-conservation equations for the real liquid components are

$$\frac{\partial \overline{\rho}_{Lm}}{\partial t} = \sum_{k=1}^{3} [\Gamma^{NE}_{SK(k),Lm} - \Gamma^{NE}_{Lm,SK(k)}] + \sum_{m'=4}^{5} [\Gamma^{NE}_{Lm',Lm} - \Gamma^{NE}_{Lm,Lm'}]$$

$$+ \sum_{k=1}^{3} \Gamma^{EQ}_{SK(k),Lm} + \sum_{m'=4}^{5} [\Gamma^{EQ}_{Lm',Lm} - \Gamma^{EQ}_{Lm,Lm'}] + \Gamma^{NE}_{G,Lm} - \Gamma^{NE}_{Lm,G}, \tag{3-3}$$

where Lm for m = 1, 2 and 3 represents the energy components of liquid fuel, steel and sodium, respectively, $\Gamma^{NE}_{G,Lm}$ is the mass-transfer rate due to condensation, and $\Gamma^{NE}_{Lm,G}$ is the mass-transfer rate due to vaporization.

For the three condensable vapor components only non-equilibrium mass transfer occurs.

The mass-conservation equations are

$$\frac{\partial \overline{\rho}_{Gm}}{\partial t} = \Gamma^{NE}_{Lm,G} - \Gamma^{NE}_{G,Lm}, \tag{3-4}$$

where Gm for m = 1, 2 and 3 represents the material components of condensable vapors, fuel, steel and sodium, respectively.

The energy-conservation equations for the structures are written in terms of specific enthalpy as follows:

$$\frac{\partial \overline{\rho}_{SK(k)} i_{SK(k)}}{\partial t} = \sum_{m=1}^{2} [\Gamma^{NE}_{Lm,SK(k)} i_{Sol,M(Lm)} - \Gamma^{NE}_{SK(k),Lm} i_{SK(k)}]$$

[Enthalpy gains from non-equilibrium M/F transfer]

$$-\sum_{m=1}^{2} \Gamma^{EQ}_{SK(k),Lm} i_{Liq,M(Lm)}$$

[Enthalpy gains from equilibrium M/F transfer]

$$+\sum_{m=1}^{6} [a_{Lm,SK(k)} h_{SK(k),Lm} (T^{1}_{Lm,SK(k)} - T_{SK(k)})]$$

[Heat transfer from liquid components]

$$+\sum_{m=1}^{4} [R_{Gm,SK(k)} a_{G,SK(k)} h_{SK(k),G} (T^{1}_{G,SK(k)} - T_{SK(k)})]$$

[Heat transfer from vapor field]

$$+Q_{Int,SK(k)} + Q_{N,SK(k)}$$

[Heat transfer from structure interior] + [Nuclear heating]

$$+\alpha_{SK(k)} \frac{\partial p}{\partial t}. \tag{3-5}$$

[Enthalpy gain from changing pressure]

The energy-conservation equations for the particles are written in terms of specific enthalpy as follows:

$$\frac{\partial \overline{\rho}_{Lm} i_{Lm}}{\partial t} = \sum_{m'=1}^{2} [\Gamma^{NE}_{Lm',Lm} i_{Sol,M(Lm')} - \Gamma^{NE}_{Lm,Lm'} i_{Lm}]$$

[Enthalpy gains from non-equilibrium M/F transfer]

$$+\sum_{m'=1}^{2}[\Gamma^{EQ}_{Lm',Lm} i_{Sol,M(Lm')} - \Gamma^{EQ}_{Lm,Lm'} i_{Liq,M(Lm)}]$$

[Enthalpy gains from equilibrium M/F transfer]

$$+\sum_{\substack{m'=1 \\ m'\neq m}}^{6}[a_{Lm,Lm'} h_{Lm,Lm'}(T^{I}_{Lm,Lm'} - T_{Lm})]$$

[Heat transfer from other liquid components]

$$+\sum_{k=1}^{3}[a_{Lm,SK(k)} h_{Lm,SK(k)}(T^{I}_{Lm,SK(k)} - T_{Lm})]$$

[Heat transfer from structures]

$$+\sum_{m'=1}^{4}[R_{Gm',Lm} a_{G,Lm} h_{Lm,G}(T^{I}_{Gm',Lm} - T_{Lm})]$$

[Heat transfer from vapor field]

$$+Q_{N,Lm} + \alpha_{Lm}\frac{\partial p}{\partial t}. \qquad (3\text{-}6)$$

[Nuclear heating + Enthalpy gain from changing pressure]

The energy-conservation equations for the real liquids are written in terms of specific enthalpy as follows:

$$\frac{\partial \overline{\rho}_{Lm} i_{Lm}}{\partial t} = \sum_{k=1}^{3}[\Gamma^{NE}_{SK(k),Lm} i_{Liq,M(SK(k))} - \Gamma^{NE}_{Lm,SK(k)} i_{Lm}] + \sum_{m'=4}^{5}[\Gamma^{NE}_{Lm',Lm} i_{Liq,M(Lm')} - \Gamma^{NE}_{Lm,Lm'} i_{Lm}]$$

[Enthalpy gains from non-equilibrium M/F transfer]

$$+\sum_{k=1}^{3}\Gamma^{EQ}_{SK(k),Lm} i_{Liq,M(SK(k))} + \sum_{m'=4}^{5}[\Gamma^{EQ}_{Lm',Lm} i_{Liq,M(Lm')} - \Gamma^{EQ}_{Lm,Lm'} i_{Sol,M(Lm)}]$$

[Enthalpy gains from equilibrium M/F transfer]

$$+\Gamma^{NE}_{G,Lm} i_{Con,Gm} - \Gamma^{NE}_{Lm,G} i_{Lm}$$

[Enthalpy gains from V/C transfer]

$$+\sum_{\substack{m'=1 \\ m'\neq m}}^{6}[a_{Lm,Lm'} h_{Lm,Lm'}(T^{I}_{Lm,Lm'} - T_{Lm})]$$

[Heat transfer from other liquid components]

$$+\sum_{k=1}^{3}[a_{Lm,SK(k)}h_{Lm,SK(k)}(T^{I}_{Lm,SK(k)}-T_{Lm})]$$

[Heat transfer from structures]

$$+\sum_{m'=1}^{4}[R_{Gm',Lm}a_{G,Lm}h_{Lm,G}(T^{I}_{Gm',Lm}-T_{Lm})]$$

[Heat transfer from vapor field]

$$+Q_{N,Lm}+\alpha_{Lm}\frac{\partial p}{\partial t}. \tag{3-7}$$

[Nuclear heating] + [Enthalpy gain from changing pressure]

The energy-conservation equation for the vapor mixture is written in terms of specific enthalpy as follows:

$$\frac{\partial \overline{\rho}_G i_G}{\partial t}=\sum_{m=1}^{3}[\Gamma^{NE}_{Lm,G}i_{Vap,Gm}-\Gamma^{NE}_{G,Lm}i_{Gm}]$$

[Enthalpy gains from V/C transfer]

$$+\sum_{m'=1}^{6}\sum_{m=1}^{4}[R_{Gm,Lm'}a_{G,Lm'}h_{G,Lm'}(T^{I}_{G,Lm'}-T_G)]$$

[Heat transfer from real liquids and particles]

$$+\sum_{k=1}^{3}\sum_{m=1}^{4}[R_{Gm,SK(k)}a_{G,SK(k)}h_{G,SK(k)}(T^{I}_{G,SK(k)}-T_G)]$$

[Heat transfer from structures]

$$+Q_{N,G}+\alpha_G\frac{\partial p}{\partial t}. \tag{3-8}$$

[Nuclear heating] + [Enthalpy gain from changing pressure]

3.2. Numerical algorithm

After the interfacial areas and heat-transfer coefficients are obtained, the conservation equations without convection are solved for intra-cell heat and mass transfer using a multiple-step approach because a simultaneous solution of them would be complex and inefficient. Actually, the equations presented in the previous section are not directly solved for all the modes of heat and mass transfers to obtain the end-of-time step variables. Instead, they are treated stepwise in the following procedure.

First, the M/F rates are determined based on the departure from equilibrium resulting from the heat transfer calculation. Second, the V/C rates are determined simultaneously with the intra-cell liquid and vapor heat-transfer rates. Third, the equilibrium model obtains the rate of M/F. Finally, velocity fields are updated from mass transfer. In these operations, the fuel and steel components in particles, liquids and structures are treated explicitly, and the liquid sodium and the vapor field are treated implicitly.

In the V/C calculation, the energy- and mass-conservation equations are solved implicitly and simultaneously with the EOS. This is because of strong non-linearity in V/C processes and a probable large change in the vapor thermodynamic state. In the V/C iteration, based on a multivariate Newton-Raphson method, five sensitive variables (three condensable vapor densities, coolant energy and vapor temperature) are updated implicitly, whereas the remaining less sensitive variables are updated explicitly following the convergence of the iteration. In a single-phase cell, vapor is assumed to always exist in a non-zero small volume, $\alpha_0(1-\alpha_S)$, and its density and energy are calculated consistently with two-phase cells to avoid numerical difficulties. The single-phase V/C calculation is performed using the same procedure as two-phase cells except for the energy transfer between liquids. At a liquid/liquid interface in a two-phase cell, vaporization can occur, and the interface temperature is defined as the saturation temperature of a vaporizing material. However, in a single-phase cell, the interface temperature of the liquid/liquid contact is defined such that the energy transfer between the liquids causes no vaporization. Instead, phase transition occurs only when the liquid temperature increases sufficiently to cause vaporization at a liquid/vapor interface.

The M/F calculation is based on the two modes: non-equilibrium and equilibrium processes. The former is similar to the V/C processes; however all the variables are updated explicitly except for the coolant energy, which is identified as sensitive. After calculating nuclear heating, heat and mass transfers resulting from non-equilibrium processes, and structure heat transfer, the equilibrium M/F rates are determined by comparing the updated component energy with its liquidus energy for freezing or its solidus energy for melting.

Chapter 4. Non-equilibrium M/F transfers

4.1. Mass- and energy-conservation equations

The non-equilibrium M/F operation performs particle-liquid-structure heat transfer with non-equilibrium M/F, which does not involve the V/C. The mass- and energy-conservation equations to be solved are written for three structure surfaces, three real liquids, and three solid particles.

The mass and energy conservation for structure surfaces is

$$\frac{\partial \overline{\rho}_{k1}}{\partial t} = (\Gamma^{I24}_{L2,k1} - \Gamma^{I23}_{k1,L2} - \Gamma^{I24}_{k1,L2})\delta(SK(1),S4), \tag{4-1}$$

$$\frac{\partial \overline{\rho}_{k2}}{\partial t} = (\Gamma^{I31}_{L1,k2} - \Gamma^{I31}_{k2,L1})\delta(SK(2),S2)$$

$$+(\Gamma^{I33}_{L2,k2} - \Gamma^{I31}_{k2,L2} - \Gamma^{I33}_{k2,L2})[\delta(SK(2),S5) + \delta(SK(2),S6)], \tag{4-2}$$

$$\frac{\partial \overline{\rho}_{k3}}{\partial t} = (\Gamma^{I32}_{L1,k3} - \Gamma^{I32}_{k3,L1})\delta(SK(3),S3)$$

$$+(\Gamma^{I34}_{L2,k3} - \Gamma^{I32}_{k3,L2} - \Gamma^{I34}_{k3,L2})[\delta(SK(3),S7) + \delta(SK(3),S8)], \tag{4-3}$$

$$\frac{\partial \overline{\rho}_{k1} e_{k1}}{\partial t} = \left[\Gamma^{I24}_{L2,k1} e_{Sol,M(k1)} - (\Gamma^{I23}_{k1,L2} + \Gamma^{I24}_{k1,L2}) e_{k1}\right]\delta(SK(1),S4)$$

$$+\sum_{m=1}^{6} a_{Lm,k1} h_{k1}(T^{I}_{k1,Lm} - T_{k1}), \tag{4-4}$$

$$\frac{\partial \overline{\rho}_{k2} e_{k2}}{\partial t} = (\Gamma^{I31}_{L1,k2} e_{Sol,M(k2)} - \Gamma^{I31}_{k2,L1} e_{k2})\delta(SK(2),S2)$$

$$+\left[\Gamma^{I33}_{L2,k2} e_{Sol,M(k2)} - (\Gamma^{I31}_{k2,L2} + \Gamma^{I33}_{k2,L2}) e_{k2}\right][\delta(SK(2),S5) + \delta(SK(2),S6)]$$

$$+\sum_{m=1}^{6} a_{Lm,k2} h_{k2}(T^{I}_{k2,Lm} - T_{k2}), \text{ and} \tag{4-5}$$

$$\frac{\partial \overline{\rho}_{k3} e_{k3}}{\partial t} = (\Gamma^{I32}_{L1,k3} e_{Sol,M(k3)} - \Gamma^{I32}_{k3,L1} e_{k3})\delta(SK(3),S3)$$

$$+\left[\Gamma^{I34}_{L2,k3} e_{Sol,M(k3)} - (\Gamma^{I32}_{k3,L2} + \Gamma^{I34}_{k3,L2}) e_{k3}\right][\delta(SK(3),S7) + \delta(SK(3),S8)]$$

$$+\sum_{m=1}^{6} a_{Lm,k3} h_{k3}(T^{I}_{k3,Lm} - T_{k3}), \tag{4-6}$$

where δ is the Kronecker symbol. When a fuel crust is newly formed on the can-wall

surface, the crust mass and energy equations are

$$\frac{\partial \overline{\rho}_{S2}}{\partial t} = \Gamma^{I31}_{L1,S2}[1-\delta(SK(2),S2)], \tag{4-7}$$

$$\frac{\partial \overline{\rho}_{S3}}{\partial t} = \Gamma^{I32}_{L1,S3}[1-\delta(SK(3),S3)], \tag{4-8}$$

$$\frac{\partial \overline{\rho}_{S2} e_{S2}}{\partial t} = \Gamma^{I31}_{L1,S2} e_{Sol,M(S2)}[1-\delta(SK(2),S2)], \text{ and} \tag{4-9}$$

$$\frac{\partial \overline{\rho}_{S3} e_{S3}}{\partial t} = \Gamma^{I32}_{L1,S3} e_{Sol,M(S3)}[1-\delta(SK(3),S3)]. \tag{4-10}$$

The mass and energy conservation for particles is

$$\frac{\partial \overline{\rho}_{L4}}{\partial t} = \Gamma^{I9}_{L1,L4} - \Gamma^{I9}_{L4,L1} + \Gamma^{I10}_{L1,L4} + \Gamma^{I23}_{L1,L4}\delta(SK(1),S4), \tag{4-11}$$

$$\frac{\partial \overline{\rho}_{L5}}{\partial t} = \Gamma^{I14}_{L2,L5} - \Gamma^{I10}_{L5,L2} - \Gamma^{I14}_{L5,L2}, \tag{4-12}$$

$$\frac{\partial \overline{\rho}_{L6}}{\partial t} = 0, \tag{4-13}$$

$$\begin{aligned}\frac{\partial \overline{\rho}_{L4} e_{L4}}{\partial t} = {} & \left[\Gamma^{I9}_{L1,L4} + \Gamma^{I10}_{L1,L4} + \Gamma^{I23}_{L1,L4}\delta(SK(1),S4)\right] e_{Sol,M(L4)} - \Gamma^{I9}_{L4,L1} e_{L4} \\ & + \sum_{m=1}^{3} a_{Lm,L4} h_{L4}(T^{I}_{Lm,L4} - T_{L4}) + \sum_{m=5}^{6} a_{Lm,L4} h_{L4}(T^{I}_{Lm,L4} - T_{L4}) \\ & + \sum_{m=1}^{3} a_{km,L4} h_{L4,S}(T^{I}_{km,L4} - T_{L4}),\end{aligned} \tag{4-14}$$

$$\begin{aligned}\frac{\partial \overline{\rho}_{L5} e_{L5}}{\partial t} = {} & \Gamma^{I14}_{L2,L5} e_{Sol,M(L5)} - (\Gamma^{I10}_{L5,L2} + \Gamma^{I14}_{L5,L2}) e_{L5} \\ & + \sum_{m=1}^{3} a_{Lm,L5} h_{L5}(T^{I}_{Lm,L5} - T_{L5}) + a_{L4,L5} h_{L5}(T^{I}_{L4,L5} - T_{L5}) + a_{L6,L5} h_{L5}(T^{I}_{L6,L5} - T_{L5}) \\ & + \sum_{m=1}^{3} a_{km,L5} h_{L5,S}(T^{I}_{km,L5} - T_{L5}), \text{ and}\end{aligned} \tag{4-15}$$

$$\frac{\partial \overline{\rho}_{L6} e_{L6}}{\partial t} = \sum_{m=1}^{5} a_{Lm,L6} h_{L6}(T^{I}_{Lm,L6} - T_{L6}) + \sum_{m=1}^{3} a_{km,L6} h_{L6,S}(T^{I}_{km,L6} - T_{L6}). \tag{4-16}$$

The mass and energy conservation for real liquids is

$$\frac{\partial \overline{\rho}_{L1}}{\partial t} = \Gamma^{I9}_{L4,L1} - \Gamma^{I9}_{L1,L4} - \Gamma^{I10}_{L1,L4} - \Gamma^{I31}_{L1,S2} - \Gamma^{I32}_{L1,S3}$$

$$+\Gamma^{I31}_{k2,L1}\delta(SK(2),S2) + \Gamma^{I32}_{k3,L1}\delta(SK(3),S3) - \Gamma^{I23}_{L1,L4}\delta(SK(1),S4), \quad (4\text{-}17)$$

$$\frac{\partial \overline{\rho}_{L2}}{\partial t} = \Gamma^{I10}_{L5,L2} + \Gamma^{I14}_{L5,L2} - \Gamma^{I14}_{L2,L5}$$

$$+(\Gamma^{I23}_{k1,L2} + \Gamma^{I24}_{k1,L2} - \Gamma^{I24}_{L2,k1})\delta(SK(1),S4)$$

$$+(\Gamma^{I31}_{k2,L2} + \Gamma^{I33}_{k2,L2} - \Gamma^{I33}_{L2,k2})[\delta(SK(2),S5) + \delta(SK(2),S6)]$$

$$+(\Gamma^{I32}_{k3,L2} + \Gamma^{I34}_{k3,L2} - \Gamma^{I34}_{L2,k3})[\delta(SK(3),S7) + \delta(SK(3),S8)], \quad (4\text{-}18)$$

$$\frac{\partial \overline{\rho}_{L3}}{\partial t} = 0, \quad (4\text{-}19)$$

$$\frac{\partial \overline{\rho}_{L1} e_{L1}}{\partial t} = \left[\Gamma^{I9}_{L4,L1} + \Gamma^{I31}_{k2,L1}\delta(SK(2),S2) + \Gamma^{I32}_{k3,L1}\delta(SK(3),S3)\right] e_{Liq,M(L1)}$$

$$-\left[\Gamma^{I9}_{L1,L4} + \Gamma^{I10}_{L1,L4} + \Gamma^{I23}_{L1,L4}\delta(SK(1),S4) + \Gamma^{I31}_{L1,S2} + \Gamma^{I32}_{L1,S3}\right] e_{L1}$$

$$+\sum_{m=4}^{6} a_{L1,Lm} h_{L1,Lm}(T^{I}_{L1,Lm} - T_{L1}) + \sum_{m=1}^{3} a_{L1,km} h_{L1,S}(T^{I}_{L1,km} - T_{L1}), \quad (4\text{-}20)$$

$$\frac{\partial \overline{\rho}_{L2} e_{L2}}{\partial t} = \left\{\Gamma^{I10}_{L5,L2} + \Gamma^{I14}_{L5,L2} + (\Gamma^{I23}_{k1,L2} + \Gamma^{I24}_{k1,L2})\delta(SK(1),S4)\right.$$

$$+(\Gamma^{I31}_{k2,L2} + \Gamma^{I33}_{k2,L2})[\delta(SK(2),S5) + \delta(SK(2),S6)]$$

$$\left.+(\Gamma^{I32}_{k3,L2} + \Gamma^{I34}_{k3,L2})[\delta(SK(3),S7) + \delta(SK(3),S8)]\right\} e_{Liq,M(L2)}$$

$$-\left\{\Gamma^{I14}_{L2,L5} + \Gamma^{I24}_{L2,k1}\delta(SK(1),S4)\right.$$

$$+\Gamma^{I33}_{L2,k2}[\delta(SK(2),S5) + \delta(SK(2),S6)]$$

$$\left.+\Gamma^{I34}_{L2,k3}[\delta(SK(3),S7) + \delta(SK(3),S8)]\right\} e_{L2}$$

$$+\sum_{m=4}^{6} a_{L2,Lm} h_{L2,Lm}(T^{I}_{L2,Lm} - T_{L2}) + \sum_{m=1}^{3} a_{L2,km} h_{L2,S}(T^{I}_{L2,km} - T_{L2}), \text{ and} \quad (4\text{-}21)$$

$$\frac{\partial \overline{\rho}_{L3} e_{L3}}{\partial t} = \sum_{m=4}^{6} a_{L3,Lm} h_{L3,Lm}(T^{I}_{L3,Lm} - T_{L3}) + \sum_{m=1}^{3} a_{km,L3} h_{L3,S}(T^{I}_{km,L3} - T_{L3}). \quad (4\text{-}22)$$

4.2. Solution procedure

In the non-equilibrium M/F operation, the mass- and energy-conservation equations are

solved explicitly using beginning-of-time-step values except for liquid sodium. The implicit treatment of sodium energy could mitigate its excessive change due to high thermal conductivity. The solution procedure is to update first the macroscopic densities of structure surfaces, solid particles, and real liquids. Second their energies are evaluated using the updated densities.

The finite-difference representations of the mass-conservation equations to be solved are

$$\frac{\tilde{\bar{\rho}}_{k1}^{n+1}-\tilde{\bar{\rho}}_{k1}^{n}}{\Delta t}=(\Gamma_{L2,k1}^{I24}-\Gamma_{k1,L2}^{I23}-\Gamma_{k1,L2}^{I24})\delta(SK(1),S4), \tag{4-23}$$

$$\frac{\tilde{\bar{\rho}}_{k2}^{n+1}-\tilde{\bar{\rho}}_{k2}^{n}}{\Delta t}=(\Gamma_{L1,k2}^{I31}-\Gamma_{k2,L1}^{I31})\delta(SK(2),S2)$$
$$+(\Gamma_{L2,k2}^{I33}-\Gamma_{k2,L2}^{I31}-\Gamma_{k2,L2}^{I33})[\delta(SK(2),S5)+\delta(SK(2),S6)], \tag{4-24}$$

$$\frac{\tilde{\bar{\rho}}_{k3}^{n+1}-\tilde{\bar{\rho}}_{k3}^{n}}{\Delta t}=(\Gamma_{L1,k3}^{I32}-\Gamma_{k3,L1}^{I32})\delta(SK(3),S3)$$
$$+(\Gamma_{L2,k3}^{I34}-\Gamma_{k3,L2}^{I32}-\Gamma_{k3,L2}^{I34})[\delta(SK(3),S7)+\delta(SK(3),S8)], \tag{4-25}$$

$$\frac{\tilde{\bar{\rho}}_{L4}^{n+1}-\tilde{\bar{\rho}}_{L4}^{n}}{\Delta t}=\Gamma_{L1,L4}^{I9}+\Gamma_{L1,L4}^{I10}-\Gamma_{L4,L1}^{I9}+\Gamma_{L1,L4}^{I23}\delta(SK(1),S4), \tag{4-26}$$

$$\frac{\tilde{\bar{\rho}}_{L5}^{n+1}-\tilde{\bar{\rho}}_{L5}^{n}}{\Delta t}=\Gamma_{L2,L5}^{I14}-\Gamma_{L5,L2}^{I10}-\Gamma_{L5,L2}^{I14}, \tag{4-27}$$

$$\frac{\tilde{\bar{\rho}}_{L1}^{n+1}-\tilde{\bar{\rho}}_{L1}^{n}}{\Delta t}=-\frac{\tilde{\bar{\rho}}_{L4}^{n+1}-\tilde{\bar{\rho}}_{L4}^{n}}{\Delta t}-\frac{\tilde{\bar{\rho}}_{S2}^{n+1}-\tilde{\bar{\rho}}_{S2}^{n}}{\Delta t}-\frac{\tilde{\bar{\rho}}_{S3}^{n+1}-\tilde{\bar{\rho}}_{S3}^{n}}{\Delta t}, \text{ and} \tag{4-28}$$

$$\frac{\tilde{\bar{\rho}}_{L2}^{n+1}-\tilde{\bar{\rho}}_{L2}^{n}}{\Delta t}=-\frac{\tilde{\bar{\rho}}_{L5}^{n+1}-\tilde{\bar{\rho}}_{L5}^{n}}{\Delta t}-\sum_{m=4}^{8}\frac{\tilde{\bar{\rho}}_{Sm}^{n+1}-\tilde{\bar{\rho}}_{Sm}^{n}}{\Delta t}. \tag{4-29}$$

Here, the mass-transfer rates in Eqs. (4-23) – (4-29) are evaluated using beginning-of-time-step values of temperatures, and then these equations are solved with respect to $\tilde{\bar{\rho}}^{n+1}$.

The finite-difference representations of the energy-conservation equations to be solved are

$$\frac{\tilde{\bar{\rho}}_{k1}^{n+1}\tilde{e}_{k1}^{n+1}-\tilde{\bar{\rho}}_{k1}^{n}\tilde{e}_{k1}^{n}}{\Delta t}=[\Gamma_{L2,k1}^{I24}e_{Sol,M(k1)}-(\Gamma_{k1,L2}^{I23}+\Gamma_{k1,L2}^{I24})\tilde{e}_{k1}^{n}]\delta(SK(1),S4)$$
$$+\sum_{m=1}^{6}a_{Lm,k1}h_{k1}(T_{k1,Lm}^{I}-\tilde{T}_{k1}^{n}), \tag{4-30}$$

$$\frac{\tilde{\rho}_{k2}^{n+1}\tilde{e}_{k2}^{n+1}-\tilde{\rho}_{k2}^{n}\tilde{e}_{k2}^{n}}{\Delta t}=(\Gamma_{L1,k2}^{I31}e_{Sol,M(k2)}-\Gamma_{k2,L1}^{I31}\tilde{e}_{k2}^{n})\delta(SK(2),S2)$$

$$+\left[\Gamma_{L2,k2}^{I33}e_{Sol,M(k2)}-(\Gamma_{k2,L2}^{I31}+\Gamma_{k2,L2}^{I33})\tilde{e}_{k2}^{n}\right]\delta(SK(2),S5)+\delta(SK(2),S6)]$$

$$+\sum_{m=1}^{6}a_{Lm,k2}h_{k2}(T_{k2,Lm}^{I}-\tilde{T}_{k2}^{n}), \qquad (4\text{-}31)$$

$$\frac{\tilde{\rho}_{k3}^{n+1}\tilde{e}_{k3}^{n+1}-\tilde{\rho}_{k3}^{n}\tilde{e}_{k3}^{n}}{\Delta t}=(\Gamma_{L1,k3}^{I32}e_{Sol,M(k3)}-\Gamma_{k3,L1}^{I32}\tilde{e}_{k3}^{n})\delta(SK(3),S3)$$

$$+\left[\Gamma_{L2,k3}^{I34}e_{Sol,M(k3)}-(\Gamma_{k3,L2}^{I32}+\Gamma_{k3,L2}^{I34})\tilde{e}_{k3}^{n}\right]\delta(SK(3),S7)+\delta(SK(3),S8)]$$

$$+\sum_{m=1}^{6}a_{Lm,k3}h_{k3}(T_{k3,Lm}^{I}-\tilde{T}_{k3}^{n}), \qquad (4\text{-}32)$$

$$\frac{\tilde{e}_{L4}^{n+1}\tilde{\rho}_{L4}^{n+1}-\tilde{\rho}_{L4}^{n}\tilde{e}_{L4}^{n}}{\Delta t}=(\Gamma_{L1,L4}^{I9}+\Gamma_{L1,L4}^{I10})e_{Sol,M(L4)}-\Gamma_{L4,L1}^{I9}\tilde{e}_{L4}^{n}$$

$$+\sum_{m=1}^{3}a_{Lm,L4}h_{L4}(T_{Lm,L4}^{I}-\tilde{T}_{L4}^{n})+\sum_{m=5}^{6}a_{Lm,L4}h_{L4}(T_{Lm,L4}^{I}-\tilde{T}_{L4}^{n})$$

$$+\sum_{m=1}^{3}a_{km,L4}h_{L4,S}(T_{km,L4}^{I}-\tilde{T}_{L4}^{n}), \qquad (4\text{-}33)$$

$$\frac{\tilde{\rho}_{L5}^{n+1}\tilde{e}_{L5}^{n+1}-\tilde{\rho}_{L5}^{n}\tilde{e}_{L5}^{n}}{\Delta t}=\Gamma_{L2,L5}^{I14}e_{Sol,M(L5)}-(\Gamma_{L5,L2}^{I10}+\Gamma_{L5,L2}^{I14})\tilde{e}_{L5}^{n}$$

$$+\sum_{m=1}^{3}a_{Lm,L5}h_{L5}(T_{Lm,L5}^{I}-\tilde{T}_{L5}^{n})$$

$$+a_{L4,L5}h_{L5}(T_{L4,L5}^{I}-\tilde{T}_{L5}^{n})+a_{L6,L5}h_{L5}(T_{L6,L5}^{I}-\tilde{T}_{L5}^{n})$$

$$+\sum_{m=1}^{3}a_{km,L5}h_{L5,S}(T_{km,L5}^{I}-T_{L5}), \text{ and} \qquad (4\text{-}34)$$

$$\frac{\tilde{\rho}_{L6}^{n}\tilde{e}_{L6}^{n+1}-\tilde{\rho}_{L6}^{n}\tilde{e}_{L6}^{n}}{\Delta t}=\sum_{m=1}^{5}a_{Lm,L6}h_{L6}(T_{Lm,L6}^{I}-\tilde{T}_{L6}^{n})+\sum_{m=1}^{3}a_{km,L6}h_{L6,S}(T_{km,L6}^{I}-\tilde{T}_{L6}^{n}), \qquad (4\text{-}35)$$

$$\frac{\tilde{\rho}_{L1}^{n+1}\tilde{e}_{L1}^{n+1}-\tilde{\rho}_{L1}^{n}\tilde{e}_{L1}^{n}}{\Delta t}=\left[\Gamma_{L4,L1}^{I9}+\Gamma_{k2,L1}^{I31}\delta(SK(2),S2)+\Gamma_{k3,L1}^{I32}\delta(SK(3),S3)\right]e_{Liq,M(L1)}$$

$$-\left[\Gamma_{L1,L4}^{I9}+\Gamma_{L1,L4}^{I10}+\Gamma_{L1,L4}^{I23}\delta(SK(1),S4)+\Gamma_{L1,S2}^{I31}+\Gamma_{L1,S3}^{I32}\right]\tilde{e}_{L1}^{n}$$

$$+\sum_{m=4}^{6}a_{L1,Lm}h_{Lm}(T_{L1,Lm}^{I}-\tilde{T}_{L1}^{n})+\sum_{m=1}^{3}a_{L1,km}h_{L1,S}(T_{L1,km}^{I}-\tilde{T}_{L1}^{n}), \qquad (4\text{-}36)$$

$$\frac{\tilde{\bar{\rho}}_{L2}^{n+1}\tilde{e}_{L2}^{n+1}-\tilde{\bar{\rho}}_{L2}^{n}\tilde{e}_{L2}^{n}}{\Delta t}=\{\Gamma_{L5,L2}^{I10}+\Gamma_{L5,L2}^{I14}+(\Gamma_{k1,L2}^{I23}+\Gamma_{k1,L2}^{I24})\delta(SK(1),S4)$$

$$+(\Gamma_{k2,L2}^{I31}+\Gamma_{k2,L2}^{I33})[\delta(SK(2),S5)+\delta(SK(2),S6)]$$

$$+(\Gamma_{k3,L2}^{I32}+\Gamma_{k3,L2}^{I34})[\delta(SK(3),S7)+\delta(SK(3),S8)]\}e_{Liq,M(L2)}$$

$$-\{\Gamma_{L2,L5}^{I14}+\Gamma_{L2,k1}^{I24}\delta(SK(1),S4)$$

$$+\Gamma_{L2,k2}^{I33}[\delta(SK(2),S5)+\delta(SK(2),S6)]$$

$$+\Gamma_{L2,k3}^{I34}[\delta(SK(3),S7)+\delta(SK(3),S8)]\}\tilde{e}_{L2}^{n}$$

$$+\sum_{m=4}^{6}a_{L2,Lm}h_{Lm}(T_{L2,Lm}^{I}-\tilde{T}_{L2}^{n})+\sum_{m=1}^{3}a_{L2,km}h_{L2,S}(T_{L2,km}^{I}-\tilde{T}_{L2}^{n}),\text{ and} \tag{4-37}$$

$$\tilde{\bar{\rho}}_{L3}^{n}\frac{\tilde{e}_{L3}^{n+1}-\tilde{e}_{L3}^{n}}{\Delta t}=\sum_{m=4}^{6}a_{L3,Lm}h_{L3,Lm}(T_{L3,Lm}^{I}-\tilde{T}_{L3}^{n+1})+\sum_{m=1}^{3}a_{km,L3}h_{L3,S}(T_{km,L3}^{I}-\tilde{T}_{L3}^{n+1}). \tag{4-38}$$

Equation (4-8) is expanded further with respect to $\tilde{e}_{L3}^{n+1}$ using the following relation:

$$\tilde{T}_{L3}^{n+1}=\tilde{T}_{L3}^{n}+\frac{\partial T_{L3}}{\partial e_{L3}}(\tilde{e}_{L3}^{n+1}-\tilde{e}_{L3}^{n}). \tag{4-39}$$

The resulting expression to update the sodium energy is

$$\tilde{e}_{L3}^{n+1}=\tilde{e}_{L3}^{n}+\frac{\Delta t\left[\sum_{m=4}^{6}a_{L3,Lm}h_{L3,Lm}(T_{L3,Lm}^{I}-\tilde{T}_{L3}^{n})+\sum_{m=1}^{3}a_{km,L3}h_{L3,S}(T_{km,L3}^{I}-\tilde{T}_{L3}^{n})\right]}{\tilde{\bar{\rho}}_{L3}^{n}+\Delta t\left(\frac{\partial T_{L3}}{\partial e_{L3}}\right)_{p}\left[\sum_{m=1}^{3}a_{km,L3}h_{L3,S}+\sum_{m=4}^{6}a_{L3,Lm}h_{L3,Lm}\right]}. \tag{4-40}$$

Equation (4-40) is evaluated first such that its temperatures are to be obtained implicitly, and then Eqs. (4-30) – (4-37) are solved with respect to $\tilde{e}^{n+1}$. The interface temperatures in Eqs. (4-30) – (4-38) are evaluated using beginning-of-time-step values of temperatures except for the liquid sodium.

When a fuel crust is newly formed on the can-wall surface, the crust mass and energy are evaluated by

$$\tilde{\bar{\rho}}_{S2}^{n+1}=\Delta t\Gamma_{L1,S2}^{I31}[1-\delta(SK(2),S2)], \tag{4-41}$$

$$\tilde{\bar{\rho}}_{S3}^{n+1}=\Delta t\Gamma_{L1,S3}^{I32}[1-\delta(SK(3),S3)], \tag{4-42}$$

$$\tilde{e}_{S2}^{n+1}=e_{Sol,M(S2)}H(\Gamma_{L1,S2}^{I31})[1-\delta(SK(2),S2)],\text{ and} \tag{4-43}$$

$$\tilde{e}_{S3}^{n+1} = e_{Sol,M(S3)} H(\Gamma_{L1,S3}^{I32})[1-\delta(SK(3),S3)]. \quad (4\text{-}44)$$

4.3. Special case treatments

4.3.1. Heat-transfer coefficients

To achieve numerical stability in the explicit solution, some limiters for heat-transfer coefficients are defined based on the thermal capacity. For liquid-fuel and liquid-steel side coefficients, each heat-transfer coefficient is reduced proportionally such that the following inequalities are satisfied:

$$\frac{\bar{\rho}_{L1}}{\Delta t}\left(\frac{dT_{L1}^{+}}{de_{L1}}\right)^{-1} \geq \sum_{m=2}^{6} a_{L1,Lm} h_{L1,Lm} H(T_{L1}-T_{Lm}) + \sum_{m=1}^{3} a_{L1,km} h_{L1,km} H(T_{L1}-T_{km}), \quad (4\text{-}45)$$

$$\frac{\bar{\rho}_{L1}}{\Delta t}\left(\frac{dT_{L1}^{+}}{de_{L1}}\right)^{-1} \geq \sum_{m=2}^{6} a_{L1,Lm} h_{L1,Lm} H(T_{Lm}-T_{L1}) + \sum_{m=1}^{3} a_{L1,km} h_{L1,km} H(T_{km}-T_{L1}), \quad (4\text{-}46)$$

$$\frac{\bar{\rho}_{L2}}{\Delta t}\left(\frac{dT_{L2}^{+}}{de_{L2}}\right)^{-1} \geq a_{L2,L1} h_{L2,L1} H(T_{L2}-T_{L1}) + \sum_{m=3}^{6} a_{L2,Lm} h_{L2,Lm} H(T_{L2}-T_{Lm})$$

$$+\sum_{m=1}^{3} a_{L2,km} h_{L2,km} H(T_{L2}-T_{km}), \text{ and} \quad (4\text{-}47)$$

$$\frac{\bar{\rho}_{L2}}{\Delta t}\left(\frac{dT_{L2}^{+}}{de_{L2}}\right)^{-1} \geq a_{L2,L1} h_{L2,L1} H(T_{L1}-T_{L2}) + \sum_{m=3}^{6} a_{L2,Lm} h_{L2,Lm} H(T_{Lm}-T_{L2})$$

$$+\sum_{m=1}^{3} a_{L2,km} h_{L2,km} H(T_{km}-T_{L2}). \quad (4\text{-}48)$$

For particle side, the following inequalities are assumed sufficient:

$$\frac{\bar{\rho}_{L4}}{\Delta t}\left(\frac{dT_{L4}^{+}}{de_{L4}}\right)^{-1} \geq \sum_{m=1}^{3} a_{L4,Lm} h_{L4} + \sum_{m=5}^{6} a_{L4,Lm} h_{L4}, \quad (4\text{-}49)$$

$$\frac{\bar{\rho}_{L5}}{\Delta t}\left(\frac{dT_{L5}^{+}}{de_{L5}}\right)^{-1} \geq \sum_{m=1}^{4} a_{L5,Lm} h_{L5} + a_{L4,L6} h_{L5}, \quad (4\text{-}50)$$

$$\frac{\bar{\rho}_{L6}}{\Delta t}\left(\frac{dT_{L6}^{+}}{de_{L6}}\right)^{-1} \geq \sum_{m=1}^{5} a_{L6,Lm} h_{L6}, \text{ and} \quad (4\text{-}51)$$

$$\frac{\bar{\rho}_{Lm}}{\Delta t}\left(\frac{dT_{Lm}^{+}}{de_{Lm}}\right)^{-1} \geq \sum_{r=k1}^{k3} a_{Lm,r} h_{Lm,S}, \text{ m} = 4, 5 \text{ and } 6. \quad (4\text{-}52)$$

4.3.2. Overshooting of updated macroscopic densities

It is unlikely but possible that an updated macroscopic density becomes negative ($\tilde{\bar{\rho}}^{n+1} < 0$), because the mass-transfer rates depend on conditions on both sides of an interface and the heat-transfer coefficients have only been limited on one side. To avoid the overshooting of the updated macroscopic densities, the relevant interfacial areas are reduced proportionally such that $\tilde{\bar{\rho}}^{n+1} \geq \phi\tilde{\bar{\rho}}^{n}$, where ϕ is a constant specified by the input PHI in the Namelist /XHMT/. Then, the mass-transfer rates in Eqs. (4-23) – (4-27) are evaluated. If $\tilde{\bar{\rho}}^{n+1} \geq \phi\tilde{\bar{\rho}}^{n}$ are still not satisfied after the reduction of interfacial areas, all appropriate interfacial areas are reduced using a minimum of the reduction factors that restrict the fractional decrease in densities to $1-\phi$.

Chapter 5. Non-equilibrium V/C transfers

5.1. Mass- and energy-conservation equations

The non-equilibrium V/C operation performs liquid-vapor-solid heat transfer with non-equilibrium V/C, which does not involve the M/F. The mass- and energy-conservation equations to be solved are written for vapor mixture, three real liquids, and six solid components.

The mass-conservation equations for solid components such as a structure surface and particles are

$$\frac{\partial \overline{\rho}_{K(k)}}{\partial t} = 0, \tag{5-1}$$

where K(k) for k = 1 – 6 represents L4, L5 and L6 for particles, and k1, k2 and k3 for structure surfaces, respectively.

The mass-conservation equations for real liquids and vapor mixture are

$$\frac{\partial \overline{\rho}_{Lm}}{\partial t} = \Gamma^{NE}_{G,Lm} - \Gamma^{NE}_{Lm,G}, \text{ m = 1, 2 and 3, and} \tag{5-2}$$

$$\frac{\partial \overline{\rho}_{Gm}}{\partial t} = \Gamma^{NE}_{Lm,G} - \Gamma^{NE}_{G,Lm}, \tag{5-3}$$

where the mass-transfer rates are given by

$$\Gamma^{NE}_{G,L1} = \Gamma^{I1}_{G,L1} + \Gamma^{I2}_{G,L1} + \Gamma^{I3}_{G,L1} + \sum_{k=1}^{6} \Gamma^{I(k)}_{G,L1}, \tag{5-4}$$

$$\Gamma^{NE}_{G,L2} = \Gamma^{I2}_{G,L2} + \Gamma^{I3}_{G,L2} + \sum_{k=1}^{6} \Gamma^{I(k)}_{G,L2}, \tag{5-5}$$

$$\Gamma^{NE}_{G,L3} = \Gamma^{I3}_{G,L3} + \sum_{k=1}^{6} \Gamma^{I(k)}_{G,L3}, \tag{5-6}$$

$$\Gamma^{NE}_{L1,G} = \Gamma^{I1}_{L1,G}, \tag{5-7}$$

$$\Gamma^{NE}_{L2,G} = \Gamma^{I2}_{L2,G} + \Gamma^{I7}_{L2,G}, \text{ and} \tag{5-8}$$

$$\Gamma^{NE}_{L3,G} = \Gamma^{I3}_{L3,G} + \Gamma^{I8}_{L3,G} + \Gamma^{I12}_{L3,G}. \tag{5-9}$$

The energy-conservation equations are expressed in terms of specific internal energy:

for solid components

$$\frac{\partial \overline{\rho}_{K(k)} e_{K(k)}}{\partial t} = \sum_{m=1}^{4} R_{Gm,K(k)} a_{G,K(k)} h_{K(k)} (T^{I}_{Gm,K(k)} - T_{K(k)}), \tag{5-10}$$

for real liquids

$$\begin{aligned}\frac{\partial \overline{\rho}_{L1} e_{L1}}{\partial t} &= \Gamma^{NE}_{G,L1} i_{Con,G1} - \Gamma^{NE}_{L1,G} i_{L1} \\ &+ \sum_{m=2}^{3} a_{L1,Lm} h_{L1,Lm} (T^{I}_{L1,Lm} - T_{L1}) \\ &+ R_{G1,L1} a_{G,L1} h_{L1,G} (T^{I}_{G1,L1} - T_{L1}) + R_{G4,L1} a_{G,L1} h_{L1,G} (T^{I}_{G4,L1} - T_{L1}),\end{aligned} \tag{5-11}$$

$$\begin{aligned}\frac{\partial \overline{\rho}_{L2} e_{L2}}{\partial t} &= \Gamma^{NE}_{G,L2} i_{Con,G2} - \Gamma^{NE}_{L2,G} i_{L2} \\ &+ a_{L1,L2} h_{L2,L1} (T^{I}_{L1,L2} - T_{L2}) + a_{L2,L3} h_{L2,L3} (T^{I}_{L2,L3} - T_{L2}) \\ &+ \sum_{m=1}^{2} R_{Gm,L2} a_{G,L2} h_{L2,G} (T^{I}_{Gm,L2} - T_{L2}) + R_{G4,L2} a_{G,L2} h_{L2,G} (T^{I}_{G4,L2} - T_{L2}),\end{aligned} \tag{5-12}$$

$$\begin{aligned}\frac{\partial \overline{\rho}_{L3} e_{L3}}{\partial t} &= \Gamma^{NE}_{G,L3} i_{Con,G3} - \Gamma^{NE}_{L3,G} i_{L3} \\ &+ \sum_{m=1}^{2} a_{Lm,L3} h_{L3,Lm} (T^{I}_{Lm,L3} - T_{L3}) + \sum_{m=1}^{4} R_{Gm,L3} a_{G,L3} h_{L3,G} (T^{I}_{Gm,L3} - T_{L3}), \text{ and}\end{aligned} \tag{5-13}$$

for vapor mixture

$$\begin{aligned}\frac{\partial \overline{\rho}_{G} e_{G}}{\partial t} &= \sum_{m=1}^{3} \Gamma^{NE}_{Lm,G} i_{Vap,Gm} - \Gamma^{NE}_{G,Lm} i_{Gm} \\ &+ \sum_{m=1}^{3} R_{Gm,Lm} a_{G,Lm} h_{G,Lm} (T^{I}_{Gm,Lm} - T_{G}) \\ &+ R_{G1,L2} a_{G,L2} h_{G,L2} (T^{I}_{G1,L2} - T_{G}) + \sum_{m=1}^{2} R_{Gm,L3} a_{G,L3} h_{G,L3} (T^{I}_{Gm,L3} - T_{G}) \\ &+ \sum_{m=1}^{4} \sum_{k=1}^{6} R_{Gm,K(k)} a_{G,K(k)} h_{G,K(k)} (T^{I}_{Gm,K(k)} - T_{G}).\end{aligned} \tag{5-14}$$

The mass-conservation equations are multiplied by the component energies and subtracted from the energy-conservation equations to obtain expressions only involving the energy time derivative. The resulting system of energy-conservation equations to be solved is

for solid components

$$\bar{\rho}_{K(k)}\frac{\partial e_{K(k)}}{\partial t}=\sum_{m=1}^{4}R_{Gm,K(k)}a_{G,K(k)}h_{K(k)}(T^{I}_{Gm,K(k)}-T_{K(k)}), \tag{5-15}$$

for real liquids

$$\begin{aligned}\bar{\rho}_{L1}\frac{\partial e_{L1}}{\partial t}&=\Gamma^{NE}_{G,L1}(i_{Con,G1}-e_{L1})\\&+\sum_{m=2}^{3}a_{L1,Lm}h_{L1,Lm}(T^{I}_{L1,Lm}-T_{L1})\\&+R_{G1,L1}a_{G,L1}h_{L1,G}(T^{I}_{G1,L1}-T_{L1})+R_{G4,L1}a_{G,L1}h_{L1,G}(T^{I}_{G4,L1}-T_{L1}),\end{aligned} \tag{5-16}$$

$$\begin{aligned}\bar{\rho}_{L2}\frac{\partial e_{L2}}{\partial t}&=\Gamma^{NE}_{G,L2}(i_{Con,G2}-e_{L2})\\&+a_{L1,L2}h_{L2,L1}(T^{I}_{L1,L2}-T_{L2})+a_{L2,L3}h_{L2,L3}(T^{I}_{L2,L3}-T_{L2})\\&+\sum_{m=1}^{2}R_{Gm,L2}a_{G,L2}h_{L2,G}(T^{I}_{Gm,L2}-T_{L2})+R_{G4,L2}a_{G,L2}h_{L2,G}(T^{I}_{G4,L2}-T_{L2}),\end{aligned} \tag{5-17}$$

$$\begin{aligned}\bar{\rho}_{L3}\frac{\partial e_{L3}}{\partial t}&=\Gamma^{NE}_{G,L3}(i_{Con,G3}-e_{L3})\\&+\sum_{m=1}^{2}a_{Lm,L3}h_{L3,Lm}(T^{I}_{Lm,L3}-T_{L3})+\sum_{m=1}^{4}R_{Gm,L3}a_{G,L3}h_{L3,G}(T^{I}_{Gm,L3}-T_{L3}),\ \text{and}\end{aligned} \tag{5-18}$$

for vapor mixture

$$\begin{aligned}e_{G}\frac{\partial\bar{\rho}_{G}}{\partial t}&=\sum_{m=1}^{3}\left[\Gamma^{NE}_{Lm,G}(i_{Vap,Gm}-e_{G})-\Gamma^{NE}_{G,Lm}(i_{Gm}-e_{G})\right]\\&+\sum_{m=1}^{3}R_{Gm,Lm}a_{G,Lm}h_{G,Lm}(T^{I}_{Gm,Lm}-T_{G})\\&+R_{G1,L2}a_{G,L2}h_{G,L2}(T^{I}_{G1,L2}-T_{G})+\sum_{m=1}^{2}R_{Gm,L3}a_{G,L3}h_{G,L3}(T^{I}_{Gm,L3}-T_{G})\\&+\sum_{m=1}^{4}\sum_{k=1}^{6}R_{Gm,K(k)}a_{G,K(k)}h_{G,K(k)}(T^{I}_{Gm,K(k)}-T_{G}).\end{aligned} \tag{5-19}$$

Note that the above energy-conservation equations of the real liquid energies are derived on the assumption that $i_{Lm}\cong e_{Lm}$. This means that terms $\Gamma^{NE}_{Lm,G}(i_{Lm}-e_{Lm})$ appearing on the right side of the energy-conservation equations are ignored.

5.2. Solution procedure

To solve Eqs. (5-3) and (5-15) – (5-19) two types of variables are defined: "sensitive" and "less sensitive." The sensitive variables are comprised of the condensable vapor densities, the coolant energy, and the vapor temperature. Vapor components participate directly in mass transfer. Changes in their values were judged to be best evaluated implicitly. The liquid fuel, liquid steel, particle and structure energies are the less sensitive variables. The procedure is to finite-difference Eqs. (5-3) and (5-15) – (5-19) and then solve first for the sensitive variables using a multivariate Newton-Raphson method. Once convergence is obtained, an explicit solution procedure is used for the less sensitive variables. The finite-difference representations of Eqs. (5-3) and (5-15) – (5-19) are

$$\frac{\tilde{\rho}_{Gm}^{n+1}-\tilde{\rho}_{Gm}^{n}}{\Delta t}=\Gamma_{Lm,G}^{NE}-\Gamma_{G,Lm}^{NE},\ m=1,\ 2\ \text{and}\ 3, \tag{5-20}$$

$$\begin{aligned}\tilde{\rho}_{L3}^{n}\frac{\tilde{e}_{L3}^{n+1}-\tilde{e}_{L3}^{n}}{\Delta t}&=\Gamma_{G,L3}^{NE}(\tilde{i}_{Con,G3}^{n+1}-\tilde{e}_{L3}^{n+1})\\&+\sum_{m=1}^{2}a_{L3,Lm}h_{L3,Lm}(T_{Lm,L3}^{I}-\tilde{T}_{L3}^{n+1})+\sum_{m=1}^{4}R_{Gm,L3}a_{G,L3}h_{L3,G}(T_{Gm,L3}^{I}-\tilde{T}_{L3}^{n+1}),\end{aligned} \tag{5-21}$$

$$\begin{aligned}\tilde{\rho}_{G}^{n}\frac{\tilde{e}_{G}^{n+1}-\tilde{e}_{G}^{n}}{\Delta t}&=\sum_{m=1}^{3}\left[\Gamma_{Lm,G}^{NE}(\tilde{i}_{Vap,Gm}^{n+1}-\tilde{e}_{G}^{n+1})-\Gamma_{G,Lm}^{NE}(\tilde{i}_{Gm}^{n+1}-\tilde{e}_{G}^{n+1})\right]\\&+\sum_{m=1}^{3}R_{Gm,Lm}a_{G,Lm}h_{G,Lm}(T_{Gm,Lm}^{I}-\tilde{T}_{G}^{n+1})\\&+R_{G1,L2}a_{G,L2}h_{G,L2}(T_{G1,L2}^{I}-\tilde{T}_{G}^{n+1})+\sum_{m=1}^{2}R_{Gm,L3}a_{G,L3}h_{G,L3}(T_{Gm,L3}^{I}-\tilde{T}_{G}^{n+1})\\&+\sum_{m=1}^{4}\sum_{k=1}^{6}R_{Gm,K(k)}a_{G,K(k)}h_{G,K(k)}(T_{Gm,K(k)}^{I}-\tilde{T}_{G}^{n+1}),\end{aligned} \tag{5-22}$$

$$\begin{aligned}\tilde{\rho}_{L1}^{n+1}\frac{\tilde{e}_{L1}^{n+1}-\tilde{e}_{L1}^{n}}{\Delta t}&=\Gamma_{G,L1}^{NE}(\tilde{i}_{Con,G1}^{n+1}-\tilde{e}_{L1}^{n})\\&+\sum_{m=2}^{3}a_{L1,Lm}h_{L1,Lm}(T_{L1,Lm}^{I}-\tilde{T}_{L1}^{n})\\&+R_{G1,L1}a_{G,L1}h_{L1,G}(T_{G1,L1}^{I}-\tilde{T}_{L1}^{n})+R_{G4,L1}a_{G,L1}h_{L1,G}(T_{G4,L1}^{I}-\tilde{T}_{L1}^{n}),\end{aligned} \tag{5-23}$$

$$\tilde{\rho}_{L2}^{n+1}\frac{\tilde{e}_{L2}^{n+1}-\tilde{e}_{L2}^{n}}{\Delta t}=\Gamma_{G,L2}^{NE}(\tilde{i}_{Con,G2}^{n+1}-\tilde{e}_{L2}^{n})$$

$$+a_{L2,L1}h_{L2,L1}(T^{I}_{L2,L1}-\tilde{T}^{n}_{L2})+a_{L2,L3}h_{L2,L3}(T^{I}_{L2,L3}-\tilde{T}^{n}_{L2})$$

$$+\sum_{m=1}^{2}R_{Gm,L2}a_{G,L2}h_{L2,G}(T^{I}_{Gm,L2}-\tilde{T}^{n}_{L2})+R_{G4,L2}a_{G,L2}h_{L2,G}(T^{I}_{G4,L2}-\tilde{T}^{n}_{L2}),\ \text{and} \qquad (5\text{-}24)$$

$$\tilde{\bar{\rho}}^{n}_{K(k)}\frac{\tilde{e}^{n+1}_{K(k)}-\tilde{e}^{n}_{K(k)}}{\Delta t}=\sum_{m=1}^{4}R_{Gm,K(k)}a_{G,K(k)}h_{K(k)}(T^{I}_{Gm,K(k)}-\tilde{T}^{n}_{K(k)}),\ k=1,2,3,4,5\ \text{and}\ 6. \qquad (5\text{-}25)$$

The energy-conservation equations (5-23) – (5-25) for liquid fuel and steel, particles, and structure surfaces are explicitly solved with respect to $\tilde{e}^{n+1}$ after the convergence of V/C iteration.

The objective of the multivariate Newton-Raphson method is to perform iteration until convergence is achieved. The approach is first to perform an expansion of Eqs. (5-20) – (5-22) with respect to the sensitive variables, keeping only the linear terms. The sensitive variables are then updated using the five "fundamental" variables $\Delta\bar{\rho}_{G1}$, $\Delta\bar{\rho}_{G2}$, $\Delta\bar{\rho}_{G3}$, Δe_{L3} and ΔT_G as follows:

$$\bar{\rho}^{\kappa+1}_{Gm}=\bar{\rho}^{\kappa}_{Gm}+\Delta\bar{\rho}_{Gm},\ m=1,2\ \text{and}\ 3, \qquad (5\text{-}26)$$

$$e^{\kappa+1}_{L3}=e^{\kappa}_{L3}+\Delta e_{L3},\ \text{and} \qquad (5\text{-}27)$$

$$T^{\kappa+1}_{G}=T^{\kappa}_{G}+\Delta T_{G}, \qquad (5\text{-}28)$$

where κ is the initiation index. The liquid-density changes are determined from

$$\Delta\bar{\rho}_{Lm}=-\Delta\bar{\rho}_{Gm},\ m=1,2\ \text{and}\ 3. \qquad (5\text{-}29)$$

The solutions to the finite-difference representations of Eqs. (5-20) – (5-22) are

$$\tilde{\bar{\rho}}^{n+1}_{Gm}=\lim(\bar{\rho}^{\kappa+1}_{Gm}),\ m=1,2\ \text{and}\ 3, \qquad (5\text{-}30)$$

$$\tilde{e}^{n+1}_{L3}=\lim(e^{\kappa+1}_{L3}),\ \text{and} \qquad (5\text{-}31)$$

$$\tilde{T}^{n+1}_{G}=\lim(T^{\kappa+1}_{G}). \qquad (5\text{-}32)$$

The less sensitive variables remain constant during the iteration process.

The expansion representations of Eqs. (5-20) – (5-22) result in

$$\bar{\rho}^{\kappa}_{Gm}+\Delta\bar{\rho}_{Gm}-\tilde{\bar{\rho}}^{n}_{Gm}=\Delta t(\Gamma^{NE}_{Lm,G}+\Delta\Gamma^{NE}_{Lm,G}-\Gamma^{NE}_{G,Lm}-\Delta\Gamma^{NE}_{G,Lm}),\ m=1,2\ \text{and}\ 3, \qquad (5\text{-}33)$$

$$\tilde{\bar{\rho}}^{n}_{L3}(e^{\kappa}_{L3}+\Delta e_{L3}-\tilde{e}^{n}_{L3})=\Delta t(\Gamma^{NE}_{G,L3}+\Delta\Gamma^{NE}_{G,L3})(i^{\kappa}_{Con,G3}+\Delta i_{Con,G3}-e^{\kappa}_{L3}-\Delta e_{L3})$$

$$+\Delta t\sum_{m=1}^{2} a_{L3,Lm} h_{L3,Lm}(T^{I}_{Lm,L3} + \Delta T^{I}_{Lm,L3} - T^{\kappa}_{L3} - \Delta T_{L3})$$

$$+\Delta t\sum_{m=1}^{4} R_{Gm,L3} a_{G,L3} h_{L3,G}(T^{I}_{Gm,L3} + \Delta T^{I}_{Gm,L3} - T^{\kappa}_{L3} - \Delta T_{L3}), \text{ and} \quad (5\text{-}34)$$

$$\tilde{\bar{\rho}}^{n}_{G}(e^{\kappa}_{G} + \Delta e_{G} - \tilde{e}^{n}_{G}) = \Delta t\sum_{m=1}^{3}\Big[(\Gamma^{NE}_{Lm,G} + \Delta\Gamma^{NE}_{Lm,G})(i^{\kappa}_{Vap,Gm} + \Delta i_{Vap,Gm} - e^{\kappa}_{G} - \Delta e_{G})$$

$$-(\Gamma^{NE}_{G,Lm} + \Delta\Gamma^{NE}_{G,Lm})(i^{\kappa}_{Gm} + \Delta i_{Gm} - e^{\kappa}_{G} - \Delta e_{G})\Big]$$

$$+\Delta t\sum_{m=1}^{3}(R_{Gm,Lm} + \Delta R_{Gm,Lm}) a_{G,Lm} h_{G,Lm}(T^{I}_{Gm,Lm} + \Delta T^{I}_{Gm,Lm} - T^{\kappa}_{G} - \Delta T_{G})$$

$$+\Delta t\Big[(R_{G1,L2} + \Delta R_{G1,L2}) a_{G,L2} h_{G,L2}(T^{I}_{G1,L2} + \Delta T^{I}_{G1,L2} - T^{\kappa}_{G} - \Delta T_{G})\Big]$$

$$+\Delta t\sum_{m=1}^{2}(R_{Gm,L3} + \Delta R_{Gm,L3}) a_{G,L3} h_{G,L3}(T^{I}_{Gm,L3} + \Delta T^{I}_{Gm,L3} - T^{\kappa}_{G} - \Delta T_{G})$$

$$+\Delta t\sum_{k=1}^{6}\sum_{m=1}^{4}(R_{Gm,K(k)} + \Delta R_{Gm,K(k)}) a_{G,K(k)} h_{G,K(k)}(T^{I}_{Gm,K(k)} + \Delta T^{I}_{Gm,K(k)} - T^{\kappa}_{G} - \Delta T_{G}). \quad (5\text{-}35)$$

The expressions of $\Delta\Gamma^{NE}_{G,Lm}$, $\Delta\Gamma^{NE}_{Lm,G}$, $\Delta T^{I}_{Gm,Lm'}$, $\Delta T^{I}_{Gm,SK(k)}$, $\Delta R_{Gm,Lm'}$ and $\Delta R_{Gm,K(k)}$ are given by

$$\Delta\Gamma^{NE}_{G,Lm} = \sum_{l=1}^{3}\frac{\partial\Gamma^{NE}_{G,Lm}}{\partial\bar{\rho}_{Gl}}\Delta\bar{\rho}_{Gl} + \frac{\partial\Gamma^{NE}_{G,Lm}}{\partial e_{L3}}\Delta e_{L3} + \frac{\partial\Gamma^{NE}_{G,Lm}}{\partial T_{G}}\Delta T_{G}, \quad (5\text{-}36)$$

$$\Delta\Gamma^{NE}_{Lm,G} = \sum_{l=1}^{3}\frac{\partial\Gamma^{NE}_{Lm,G}}{\partial\bar{\rho}_{Gl}}\Delta\bar{\rho}_{Gl} + \frac{\partial\Gamma^{NE}_{Lm,G}}{\partial e_{L3}}\Delta e_{L3} + \frac{\partial\Gamma^{NE}_{Lm,G}}{\partial T_{G}}\Delta T_{G}, \quad (5\text{-}37)$$

$$\Delta T^{I}_{Gm,Lm'} = \sum_{l=1}^{3}\frac{\partial T^{I}_{Gm,Lm'}}{\partial\bar{\rho}_{Gl}}\Delta\bar{\rho}_{Gl} + \frac{\partial T^{I}_{Gm,Lm'}}{\partial e_{L3}}\Delta e_{L3} + \frac{\partial T^{I}_{Gm,Lm'}}{\partial T_{G}}\Delta T_{G}, \quad (5\text{-}38)$$

$$\Delta T^{I}_{Gm,K(k)} = \sum_{l=1}^{3}\frac{\partial T^{I}_{Gm,K(k)}}{\partial\bar{\rho}_{Gl}}\Delta\bar{\rho}_{Gl} + \frac{\partial T^{I}_{Gm,K(k)}}{\partial T_{G}}\Delta T_{G}, \quad (5\text{-}39)$$

$$\Delta R_{Gm,Lm'} = \sum_{l=1}^{3}\frac{\partial R_{Gm,Lm'}}{\partial\bar{\rho}_{Gl}}\Delta\bar{\rho}_{Gl} + \frac{\partial R_{Gm,Lm'}}{\partial T_{G}}\Delta T_{G}, \text{ and} \quad (5\text{-}40)$$

$$\Delta R_{Gm,K(k)} = \sum_{l=1}^{3}\frac{\partial R_{Gm,K(k)}}{\partial\bar{\rho}_{Gl}}\Delta\bar{\rho}_{Gl} + \frac{\partial R_{Gm,K(k)}}{\partial T_{G}}\Delta T_{G}. \quad (5\text{-}41)$$

The derivatives on the right side of Eqs. (5-36) – (5-41) are defined in Appendix A. The

variables, ΔT_{L3}, Δe_G, Δi_{Gm}, $\Delta i_{Vap,Gm}$ and $\Delta i_{Con,Gm}$, are further expanded into the fundamental variables. The expressions of ΔT_{L3}, Δe_G and Δi_{Gm} are given by

$$\Delta T_{L3} = \frac{\partial T_{L3}}{\partial e_{L3}} \Delta e_{L3}, \tag{5-42}$$

$$\Delta e_G = \sum_{l=1}^{3} \frac{\partial e_G}{\partial \bar{\rho}_{Gl}} \Delta \bar{\rho}_{Gl} + \frac{\partial e_G}{\partial T_G} \Delta T_G, \text{ and} \tag{5-43}$$

$$\Delta i_{Gm} = \sum_{l=1}^{3} \frac{\partial i_{Gm}}{\partial \bar{\rho}_{Gl}} \Delta \bar{\rho}_{Gl} \delta(m,l) + \frac{\partial i_{Gm}}{\partial T_G} \Delta T_G. \tag{5-44}$$

As discussed later in Section 5.6, to adjust the effective latent heats $i_{Vap,Gm}$ and $i_{Con,Gm}$ are replaced with variables $i^*_{Vap,Gm}$ and $i^*_{Con,Gm}$, respectively. The resulting expressions of $\Delta i^*_{Vap,Gm}$ and $\Delta i^*_{Con,Gm}$ are given by

$$\Delta i^*_{Vap,Gm} = \sum_{l=1}^{3} \frac{\partial i^*_{Vap,Gm}}{\partial \bar{\rho}_{Gl}} \Delta \bar{\rho}_{Gl} + \frac{\partial i^*_{Vap,Gm}}{\partial e_{L3}} \Delta e_{L3} \delta(m,3) + \frac{\partial i^*_{Vap,Gm}}{\partial T_G} \Delta T_G, \text{ and} \tag{5-45}$$

$$\Delta i^*_{Con,Gm} = \sum_{l=1}^{3} \frac{\partial i^*_{Con,Gm}}{\partial \bar{\rho}_{Gl}} \Delta \bar{\rho}_{Gl} + \frac{\partial i^*_{Con,Gm}}{\partial T_G} \Delta T_G. \tag{5-46}$$

5.3. V/C iteration scheme

5.3.1. Linearized equations to be solved

By differencing Eqs. (5-33) – (5-35), we construct a linear system of five equations in five unknowns, which can be represented by the following matrix equations:

$$[B] \begin{bmatrix} \Delta \bar{\rho}_{G1} \\ \Delta \bar{\rho}_{G2} \\ \Delta \bar{\rho}_{G3} \\ \Delta e_{L3} \\ \Delta T_G \end{bmatrix} = \{C\}, \tag{5-47}$$

where $[B]$ is a 5×5 matrix and $\{C\}$ is a column vector. Significant algebra is required to obtain the expressions for the elements of $[B]$ and $\{C\}$. The derivation is described in Appendix A. Here, only the results are given. The first three rows of matrix Eq. (5-47) are obtained by differencing the mass-conservation equation for each of the condensable vapor-density components.

For m = 1, 2 and 3

$$B(\mathrm{m},1)=\delta(\mathrm{m},1)+\Delta t\left(\frac{\partial\Gamma^{\mathrm{NE}}_{\mathrm{G,Lm}}}{\partial\overline{\rho}_{\mathrm{G1}}}-\frac{\partial\Gamma^{\mathrm{NE}}_{\mathrm{Lm,G}}}{\partial\overline{\rho}_{\mathrm{G1}}}\right), \tag{5-48}$$

$$B(\mathrm{m},2)=\delta(\mathrm{m},2)+\Delta t\left(\frac{\partial\Gamma^{\mathrm{NE}}_{\mathrm{G,Lm}}}{\partial\overline{\rho}_{\mathrm{G2}}}-\frac{\partial\Gamma^{\mathrm{NE}}_{\mathrm{Lm,G}}}{\partial\overline{\rho}_{\mathrm{G2}}}\right), \tag{5-49}$$

$$B(\mathrm{m},3)=\delta(\mathrm{m},3)+\Delta t\left(\frac{\partial\Gamma^{\mathrm{NE}}_{\mathrm{G,Lm}}}{\partial\overline{\rho}_{\mathrm{G3}}}-\frac{\partial\Gamma^{\mathrm{NE}}_{\mathrm{Lm,G}}}{\partial\overline{\rho}_{\mathrm{G3}}}\right), \tag{5-50}$$

$$B(\mathrm{m},4)=\Delta t\left(\frac{\partial\Gamma^{\mathrm{NE}}_{\mathrm{G,Lm}}}{\partial e_{\mathrm{L3}}}-\frac{\partial\Gamma^{\mathrm{NE}}_{\mathrm{Lm,G}}}{\partial e_{\mathrm{L3}}}\right), \tag{5-51}$$

$$B(\mathrm{m},5)=\Delta t\left(\frac{\partial\Gamma^{\mathrm{NE}}_{\mathrm{G,Lm}}}{\partial T_{\mathrm{G}}}-\frac{\partial\Gamma^{\mathrm{NE}}_{\mathrm{Lm,G}}}{\partial T_{\mathrm{G}}}\right), \text{ and} \tag{5-52}$$

$$C(\mathrm{m})=\tilde{\overline{\rho}}^{\,\mathrm{n}}_{\mathrm{Gm}}-\overline{\rho}^{\kappa}_{\mathrm{Gm}}-\Delta t(\Gamma^{\mathrm{NE}}_{\mathrm{G,Lm}}-\Gamma^{\mathrm{NE}}_{\mathrm{Lm,G}}). \tag{5-53}$$

The fourth row of matrix Eq. (5-47) is obtained from the energy equation for coolant:

$$\begin{aligned}B(4,l)=&-\Delta t\left[\frac{\partial\Gamma^{\mathrm{NE}}_{\mathrm{G,L3}}}{\partial\overline{\rho}_{\mathrm{G}l}}(i^{*}_{\mathrm{Con,G3}}-e^{\kappa}_{\mathrm{L3}})+\Gamma^{\mathrm{NE}}_{\mathrm{G,L3}}\frac{\partial i^{*}_{\mathrm{Con,G3}}}{\partial\overline{\rho}_{\mathrm{G}l}}\delta(l,3)\right]\\&-\Delta t\sum_{\mathrm{m=1}}^{2}a_{\mathrm{L3,Lm}}h_{\mathrm{L3,Lm}}\frac{\partial T^{\mathrm{I}}_{\mathrm{L3,Lm}}}{\partial\overline{\rho}_{\mathrm{G}l}}\delta(l,3)\\&-\Delta t\sum_{\mathrm{m=1}}^{4}\left[\frac{\partial R_{\mathrm{Gm,L3}}}{\partial\overline{\rho}_{\mathrm{G}l}}a_{\mathrm{G,L3}}h_{\mathrm{L3,G}}(T^{\mathrm{I}}_{\mathrm{Gm,L3}}-T^{\kappa}_{\mathrm{L3}})\right.\\&\qquad\left.+R_{\mathrm{Gm,L3}}a_{\mathrm{G,L3}}h_{\mathrm{L3,G}}\frac{\partial T^{\mathrm{I}}_{\mathrm{Gm.L3}}}{\partial\overline{\rho}_{\mathrm{G}l}}\delta(\mathrm{m},l)\right],\ l=1,2\text{ and }3,\end{aligned} \tag{5-54}$$

$$\begin{aligned}B(4,4)=&\tilde{\overline{\rho}}^{\,\mathrm{n}}_{\mathrm{L3}}-\Delta t\left[\frac{\partial\Gamma^{\mathrm{NE}}_{\mathrm{G,L3}}}{\partial e_{\mathrm{L3}}}(i^{*}_{\mathrm{Con,G3}}-e^{\kappa}_{\mathrm{L3}})-\Gamma^{\mathrm{NE}}_{\mathrm{G,L3}}\right]\\&-\Delta t\sum_{\mathrm{m=1}}^{2}a_{\mathrm{L3,Lm}}h_{\mathrm{L3,Lm}}\left(\frac{\partial T^{\mathrm{I}}_{\mathrm{L3,Lm}}}{\partial e_{\mathrm{L3}}}-\frac{\partial T_{\mathrm{L3}}}{\partial e_{\mathrm{L3}}}\right)\\&-\Delta t\sum_{\mathrm{m=1}}^{4}R_{\mathrm{Gm,L3}}a_{\mathrm{G,L3}}h_{\mathrm{L3,G}}\left(\frac{\partial T^{\mathrm{I}}_{\mathrm{Gm,L3}}}{\partial e_{\mathrm{L3}}}-\frac{\partial T_{\mathrm{L3}}}{\partial e_{\mathrm{L3}}}\right),\end{aligned} \tag{5-55}$$

$$B(4,5)=-\Delta t\left[\frac{\partial\Gamma^{\mathrm{NE}}_{\mathrm{G,L3}}}{\partial T_{\mathrm{G}}}(i^{*}_{\mathrm{Con,G3}}-e^{\kappa}_{\mathrm{L3}})+\Gamma^{\mathrm{NE}}_{\mathrm{G,L3}}\frac{\partial i^{*}_{\mathrm{Con,G3}}}{\partial T_{\mathrm{G}}}\right]$$

$$-\Delta t\sum_{m=1}^{2} a_{L3,Lm} h_{L3,Lm} \frac{\partial T^{I}_{L3,Lm}}{\partial T_G}$$

$$-\Delta t\sum_{m=1}^{4}\left[\frac{\partial R_{Gm,L3}}{\partial T_G} a_{G,L3} h_{L3,G}(T^{I}_{Gm,L3} - T^{\kappa}_{L3}) + R_{Gm,L3} a_{G,L3} h_{L3,G} \frac{\partial T^{I}_{Gm,L3}}{\partial T_G}\right], \text{ and} \qquad (5\text{-}56)$$

$$C(4) = \tilde{\bar{\rho}}^{n}_{L3}(\tilde{e}^{n}_{L3} - e^{\kappa}_{L3}) + \Delta t\Gamma^{NE}_{G,L3}(i^{*}_{Con,G3} - e^{\kappa}_{L3})$$

$$+\Delta t\sum_{m=1}^{2} a_{L3,Lm} h_{L3,Lm}(T^{I}_{L3,Lm} - T^{\kappa}_{L3}) + \Delta t\sum_{m=1}^{4} R_{Gm,L3} a_{G,L3} h_{L3,G}(T^{I}_{Gm,L3} - T^{\kappa}_{L3}). \qquad (5\text{-}57)$$

The energy-conservation equation for the vapor field gives the coefficients for the fifth row of matrix Eq. (5-47).

$$B(5,l) = \tilde{\bar{\rho}}^{n}_{G}\frac{\partial e_G}{\partial \bar{\rho}_{Gl}} - \Delta t\sum_{m=1}^{3}\left[\Gamma^{NE}_{Lm,G}\left(\frac{\partial i^{*}_{Vap,Gm}}{\partial \bar{\rho}_{Gl}}\delta(m,l) - \frac{\partial e_G}{\partial \bar{\rho}_{Gl}}\right) + \frac{\partial \Gamma^{NE}_{Lm,G}}{\partial \bar{\rho}_{Gl}}(i^{*}_{Vap,Gm} - e^{\kappa}_{G})\right.$$

$$\left. -\Gamma^{NE}_{G,Lm}\left(\frac{\partial i_{Gm}}{\partial \bar{\rho}_{Gl}}\delta(m,l) - \frac{\partial e_G}{\partial \bar{\rho}_{Gl}}\right) + \frac{\partial \Gamma^{NE}_{G,Lm}}{\partial \bar{\rho}_{Gl}}(i^{\kappa}_{Gm} - e^{\kappa}_{G})\right]$$

$$-\Delta t\sum_{m=1}^{3} a_{G,Lm} h_{G,Lm}\left[R_{Gm,Lm}\frac{\partial T^{I}_{Gm,Lm}}{\partial \bar{\rho}_{Gl}}\delta(m,l) + \frac{\partial R_{Gm,Lm}}{\partial \bar{\rho}_{Gl}}(T^{I}_{Gm,Lm} - T^{\kappa}_{G})\right]$$

$$-\Delta t a_{G,L2} h_{G,L2}\left[R_{G1,L2}\frac{\partial T^{I}_{G1,L2}}{\partial \bar{\rho}_{Gl}}\delta(l,1) + \frac{\partial R_{G1,L2}}{\partial \bar{\rho}_{Gl}}(T^{I}_{G1,L2} - T^{\kappa}_{G})\right]$$

$$-\Delta t\sum_{m=1}^{2} a_{G,L3} h_{G,L3}\left[R_{Gm,L3}\frac{\partial T^{I}_{Gm,L3}}{\partial \bar{\rho}_{Gl}}\delta(m,l) + \frac{\partial R_{Gm,L3}}{\partial \bar{\rho}_{Gl}}(T^{I}_{Gm,L3} - T^{\kappa}_{G})\right]$$

$$-\Delta t\sum_{m=1}^{4}\sum_{k=1}^{6} a_{G,K(k)} h_{G,K(k)}\left[R_{Gm,K(k)}\frac{\partial T^{I}_{Gm,K(k)}}{\partial \bar{\rho}_{Gl}}\delta(m,l)\right.$$

$$\left. + \frac{\partial R_{Gm,K(k)}}{\partial \bar{\rho}_{Gl}}(T^{I}_{Gm,K(k)} - T^{\kappa}_{G})\right], \; l = 1, 2 \text{ and } 3, \qquad (5\text{-}58)$$

$$B(5,4) = -\Delta t\sum_{m=1}^{3}\left[\frac{\partial \Gamma^{NE}_{Lm,G}}{\partial e_{L3}}(i^{*}_{Vap,Gm} - e^{\kappa}_{G}) - \frac{\partial \Gamma^{NE}_{G,Lm}}{\partial e_{L3}}(i^{\kappa}_{Gm} - e^{\kappa}_{G})\right]$$

$$-\Delta t\sum_{m=1}^{4} a_{G,L3} h_{G,L3} R_{Gm,L3}\frac{\partial T^{I}_{Gm,L3}}{\partial e_{L3}}, \qquad (5\text{-}59)$$

$$B(5,5) = \tilde{\bar{\rho}}^{n}_{G}\frac{\partial e_G}{\partial T_G} - \Delta t\sum_{m=1}^{3}\left[\Gamma^{NE}_{Lm,G}\left(\frac{\partial i_{Vap,Gm}}{\partial T_G} - \frac{\partial e_G}{\partial T_G}\right) + \frac{\partial \Gamma^{NE}_{Lm,G}}{\partial T_G}(i^{\kappa}_{Vap,Gm} - \tilde{e}^{\kappa}_{G})\right.$$

$$-\Gamma^{NE}_{G,Lm}\left(\frac{\partial i_{Gm}}{\partial T_G}-\frac{\partial e_G}{\partial T_G}\right)+\frac{\partial \Gamma^{NE}_{G,Lm}}{\partial T_G}(i^{\kappa}_{Gm}-e^{\kappa}_{G})\Bigg]$$

$$-\Delta t\sum_{m=1}^{3}a_{G,Lm}h_{G,Lm}\left[R_{Gm,Lm}\left(\frac{\partial T^{I}_{Gm,Lm}}{\partial T_G}-1\right)+\frac{\partial R_{Gm,Lm}}{\partial T_G}(T^{I}_{Gm,Lm}-T^{\kappa}_{G})\right]$$

$$-\Delta t a_{G,L2}h_{G,L2}\left[R_{G1,L2}\left(\frac{\partial T^{I}_{G1,L2}}{\partial T_G}-1\right)+\frac{\partial R_{G1,L2}}{\partial T_G}(T^{I}_{G1,L2}-T^{\kappa}_{G})\right]$$

$$-\Delta t\sum_{m=1}^{4}\sum_{k=1}^{6}a_{G,K(k)}h_{G,K(k)}\left[R_{Gm,K(k)}\left(\frac{\partial T^{I}_{Gm,K(k)}}{\partial T_G}-1\right)\right.$$

$$\left.+\frac{\partial R_{Gm,K(k)}}{\partial T_G}(T^{I}_{Gm,K(k)}-T^{\kappa}_{G})\right],$$

$l = 1$, 2 and 3, and (5-60)

$$C(5)=\tilde{\rho}^{n}_{G}(\tilde{e}^{n}_{G}-e^{\kappa}_{G})+\Delta t\sum_{m=1}^{3}\left[\Gamma^{NE}_{Lm,G}(i^{*}_{Vap,Gm}-e^{\kappa}_{G})-\Gamma^{NE}_{G,Lm}(i^{\kappa}_{Gm}-e^{\kappa}_{G})\right]$$

$$+\Delta t\sum_{m=1}^{3}R_{Gm,Lm}a_{G,Lm}h_{G,Lm}(T^{I}_{Gm,Lm}-T^{\kappa}_{G})$$

$$+\Delta t R_{G1,L2}a_{G,L2}h_{G,L2}(T^{I}_{G1,L2}-T^{\kappa}_{G})$$

$$+\Delta t\sum_{m=1}^{2}R_{Gm,L3}a_{G,L3}h_{G,L3}(T^{I}_{Gm,L3}-T^{\kappa}_{G})$$

$$+\Delta t\sum_{k=1}^{6}\sum_{m=1}^{4}R_{Gm,K(k)}a_{G,K(k)}h_{G,K(k)}(T^{I}_{Gm,K(k)}-T^{\kappa}_{G}).$$ (5-61)

The linearized equations (5-48) – (5-61) can be further expanded using the definition of derivatives and mass-transfer rates. The detailed equations are described in Appendix B.

5.3.2. Numerical treatments in V/C iteration

To obtain the solution of linearized matrix Eq. (5-47), some special numerical treatments are required not only to avoid numerical difficulties, but also to get physically appropriate quantities. Some of the treatments used in the AFDM code are extended to SIMMER-III. The following three operations are performed before judging the convergence.

First, to mitigate excessive predictions by Eq. (5-47), $C(\mathrm{m})$ are multiplied by relaxation coefficients on the first three iterations. The coefficients are specified by the input FUND in

the Namelist /XHMT/. This operation is repeated every seven iterations if convergence has not occurred.

Second, all changes in sensitive variables are reduced by the same or a proportionate factor to avoid excessive predictions by Eq. (5-47). In particular, although all the liquid can vaporize, convergence should be achieved with some positive finite vapor density. The reduction factors are determined so as to satisfy the following conditions:

$$-f_{RG}\overline{\rho}_{Gm} \le \Delta\overline{\rho}_{Gm} \le \overline{\rho}_{Lm}, \text{ m = 1, 2 and 3,} \tag{5-62}$$

$$-f_{EL}e_{L3} \le \Delta e_{L3} \le f_{EL}e_{L3}, \text{ and} \tag{5-63}$$

$$-f_{TG}T_G \le \Delta T_G \le f_{TG}T_G, \tag{5-64}$$

where f_{RG} is the maximum fraction of vapor mass that can condense in one iteration, and f_{EL} and f_{TG} are the maximum fractional changes of coolant energy and vapor temperature allowed in one iteration, respectively. The inputs for these fractions are FRG, FEL and FTG in the Namelist /XHMT/. A minimum value in the three factors obtained by Eq. (5-62) is used commonly for changes in vapor densities.

Third, the five sensitive variables updated by iteration are adjusted by Steffensen's acceleration method whenever oscillations are detected. If $\Delta\overline{\rho}_{G1}$, $\Delta\overline{\rho}_{G2}$, $\Delta\overline{\rho}_{G3}$, Δe_{L3} and ΔT_G obtained by iteration κ are represented by Δf^{κ}, the formula is given by

$$\Delta f^{\kappa} = -\frac{\Delta f^{\kappa} - \Delta f^{\kappa-1}}{\Delta f^{\kappa}\Delta f^{\kappa-1}}. \tag{5-65}$$

The oscillation is detected when the following condition is satisfied:

$$\frac{\Delta f^{\kappa} - \Delta f^{\kappa-1}}{\Delta f^{\kappa-1}} > 10^{-6} \text{ and } \Delta f^{\kappa}\Delta f^{\kappa-1} < 0. \tag{5-66}$$

This approach appears to be successful in limiting problems that can result from the several "on-off" decisions existing in the current modeling.

Once the new densities, coolant energy, and vapor temperature are obtained, iteration with matrix Eq. (5-47) continued until convergence is obtained. There are three sets of convergence criteria. First is the absolute convergence criterion for the residual error in mass and energy conservation:

$$|C(\text{m})| \le \Delta_{VC,RG}, \text{ m = 1, 2 and 3, } |C(4)| \le \Delta_{VC,E3}, \text{ and } |C(5)| \le \Delta_{VC,TG}, \tag{5-67}$$

where $\Delta_{VC,RG}$, $\Delta_{VC,E3}$ and $\Delta_{VC,TG}$ are specified by the inputs DVCRG, DVCE3 and DVCTG

in the Namelist /XHMT/, respectively. Second is the relative convergence criterion for the residual error in mass or energy conservation:

$$\left|\frac{C(m)}{\tilde{\bar{\rho}}^{n}_{Gm}}\right| \le \varepsilon_{VC,RG},\ m = 1, 2 \text{ and } 3,\ \left|\frac{C(4)}{\tilde{e}^{n}_{L3}}\right| \le \varepsilon_{VC,E3},\ \text{and}\ \left|\frac{C(5)}{\tilde{T}^{n}_{G}}\right| \le \varepsilon_{VC,TG}, \tag{5-68}$$

where $\varepsilon_{VC,RG}$, $\varepsilon_{VC,E3}$ and $\varepsilon_{VC,TG}$ are specified by the inputs EVCRG, EVCE3 and EVCTG in the Namelist /XHMT/, respectively. Third is the relative convergence criterion for the change of sensitive variables:

$$\left|\frac{\Delta\bar{\rho}_{Gm}}{\tilde{\bar{\rho}}^{n}_{Gm}}\right| \le f_{VC,RG},\ m = 1, 2 \text{ and } 3,\ \left|\frac{\Delta e_{L3}}{\tilde{e}^{n}_{L3}}\right| \le f_{VC,E3},\ \text{and}\ \left|\frac{\Delta T_{G}}{\tilde{T}^{n}_{G}}\right| \le f_{VC,TG}, \tag{5-69}$$

where $f_{VC,RG}$, $f_{VC,E3}$ and $f_{VC,TG}$ are specified by the inputs FVCRG, FVCE3 and FVCTG in the Namelist /XHMT/, respectively. Although Eq. (5-69) is not a necessary mathematical condition for the convergence in the Newton-Raphson method, the achievement of convergence is judged if at least one of the above three sets is satisfied. If the V/C convergence is obtained without excessive change of vapor temperature, the liquid fuel, liquid steel, particle and structure energies are calculated explicitly from the finite difference representation of Eqs. (5-23) – (5-25) using the converged variables.

5.4. Treatment of supersaturated vapor

Vapor that is supersaturated below its equilibrium saturation temperature may exist in a non-equilibrium condition, which is referred to a metastable state. In this metastable state, generally, supersaturated vapor immediately undergoes phase transition (homogeneous condensation) and then its thermodynamic state becomes stable. In the non-equilibrium heat-transfer-limited model, supersaturated vapor can be transferred into liquid phase only if vapor contact areas are available for condensation and the vapor satisfies the phase-transition condition at these contact areas. However, for example, extremely supersaturated vapor could be produced if other liquids cool vapor far removed from condensation sites such as a structure surface. Even if condensation is possible on the condensation sites, its rate may be too small to achieve a stable state immediately because only heat transfer controls the phase transition. In SIMMER-III, the following mass-transfer operation is adapted to compensate the shortcoming in the non-equilibrium heat-transfer-limited model. This operation is performed after the convergence of V/C iteration.

If a vapor component satisfies the condition of $p_{Gm} > p_{Sat,Gm}$, a part of its vapor is

transferred into the liquid phase so as to get rid of the metastable state. The new vapor temperature is evaluated by solving the following equations:

$$\tilde{\bar{\rho}}_G^n \tilde{e}_G^n = \sum_{\text{stable}} \tilde{\bar{\rho}}_{Gm}^n \tilde{e}_{Gm}^{n+1}(\tilde{T}_G^{n+1}, \tilde{v}_{Gm}^n) + \sum_{\text{metastable}} \left[\bar{\rho}_{Sat,Gm}(\tilde{T}_G^{n+1}) e_{Sat,Gm}(\tilde{T}_G^{n+1}) + \delta\bar{\rho}_{Lm} e_{Sat,Lm}(\tilde{T}_G^{n+1})\right], \text{ and} \quad (5\text{-}70)$$

$$\delta\bar{\rho}_{Lm} = \tilde{\bar{\rho}}_{Gm}^n - \bar{\rho}_{Sat,Gm}(\tilde{T}_G^{n+1}), \text{ m} = 1, 2 \text{ and } 3, \quad (5\text{-}71)$$

where ~ n and ~ n+1 mean the values after the convergence of V/C iteration and the updated value in this operation, respectively, and $\sum_{\text{stable}}$ and $\sum_{\text{metastable}}$ are the summations for the stable and supersaturated vapors after the convergence of V/C iteration, respectively. Equation (5-70) is implicitly solved with respect to $\tilde{T}_G^{n+1}$ using the Newton-Raphson method. After obtaining $\tilde{T}_G^{n+1}$, the new vapor and liquid densities, and liquid energy for the initially supersaturated components are updated by

$$\tilde{\bar{\rho}}_{Gm}^{n+1} = \bar{\rho}_{Sat,Gm}(\tilde{T}_G^{n+1}), \quad (5\text{-}72)$$

$$\tilde{\bar{\rho}}_{Lm}^{n+1} = \tilde{\bar{\rho}}_{Lm}^n + \delta\bar{\rho}_{Lm}, \text{ and} \quad (5\text{-}73)$$

$$\tilde{e}_{Lm}^{n+1} = \frac{1}{\tilde{\bar{\rho}}_{Lm}^{n+1}} \left[\tilde{\bar{\rho}}_{Lm}^n \tilde{e}_{Lm}^n + \delta\bar{\rho}_{Lm} e_{Sat,Gm}(\tilde{T}_G^{n+1})\right], \quad (5\text{-}74)$$

where m = 1, 2 and 3. The updated values are the final quantities in the V/C calculation. The above operation can be controlled by the input HMTOPT(9) in the Namelist /XCNTL/.

5.5. Treatment of single-phase V/C

In the two-phase V/C treatment, the mass transfer is obtained from the heat-flux balance at an interface. Heat-transfer calculations are performed simultaneously. For single-phase cells, the initialization of the so-called α_0 volume is performed consistently with the two-phase V/C treatment. This is done by calculating the interfacial areas based on the effective vapor volume fraction, $\alpha_{ge} = \max[\alpha_0(1-\alpha_S), 1-\alpha_S-(1-\alpha_0)\alpha_L]$, and then providing reasonable liquid/vapor interfacial area even for a single-phase cell. It seems that the effect of this treatment for low-void-fraction flow is negligible as far as the minimum vapor volume fraction α_0 is small enough, e.g. $\alpha_0 < 0.01$, where α_0 can be specified by the input ALPHA0 in the Namelist /XEOS/.

The single-phase V/C calculations are performed using the same procedure as two-phase

cells only for the mass and energy transfers between the same material vapor and liquid component. Therefore, at liquid/vapor interfaces, the interface temperature is defined as the saturation temperature. At the other interfaces, the interface temperature is defined as no mass-transfer temperature defined by Eq. (2-8). For example, in two-phase cells vaporization can occur at the liquid/liquid interface such as fuel/sodium contact, and hence the interfacial temperature is defined as the saturation temperature of vaporized material. On the other hand, in single-phase cells the interface temperature of liquid/liquid contact should be independent of the vapor state. Therefore, no vaporization due to the energy transfer between the liquids is allowed in a single-phase cell. In addition, the incipient boiling superheat can be treated in single-phase cells. The superheating at liquid/vapor interfaces is considered by simply assuming the vapor superheat temperature $T_{Sup,M}$ such that the interface temperature is $T_{Sat,Gm} + T_{Sup,M(Gm)}$. The value of $T_{Sup,M}$ is specified by the input TSUP in the Namelist /XHMT/.

The interfacial areas are calculated based on the effective vapor volume fraction α_{ge} if the input IFAOPT(1) = 1 in the Namelist /XCNTL/. This should be used when the V/C phase transition is calculated. If IFAOPT(1) = 0, the real vapor volume fraction is used for the calculation of interfacial areas. This latter choice is recommended only for the calculation with no phase transition.

5.6. Special case treatments

5.6.1. Initial vapor and liquid states

Before starting the V/C iteration, the initial vapor and liquid sates are adjusted to reduce numerical difficulties in the V/C iteration. There are three initial operations. First, if a vapor component is missing although the same material component of liquid exits in a cell, a part of the liquid is transferred into the vapor field. The amount of the liquid transferred is evaluated from the saturated vapor density at the liquidus temperature. Second, supercritical liquid, of which internal energy exceeds the critical energy, is transferred into the vapor field. Finally, liquid components with a negligibly small mass are transferred into vapor field to avoid ineffective numerical calculations. The criterion for "negligibly small" mass is defined by $\tilde{\bar{\rho}}^{n}_{Lm} < f_{mt,lg}\tilde{\bar{\rho}}^{n}_{G}$, where $f_{mt,lg}$ is specified by the inputs FMTLG in the Namelist /XHMT/. After these adjustments, new vapor temperature is evaluated implicitly as the initial value of the V/C calculation, using the updated vapor energy and densities.

5.6.2. Heat-transfer coefficients and interfacial areas

To achieve numerical stability in the explicit solution, some limiters for heat-transfer coefficients are defined based on the thermal capacity. The limits are

$$h_{G,Lm} \le c_{G,Lm} \frac{\overline{\rho}_G \left(\frac{\partial e_G}{\partial T_G} \right)_{v_G}}{\Delta t a_{G,Lm}}, \text{ m = 1, 2 and 3,} \tag{5-75}$$

$$h_{G,K(k)} \le c_{G,K(k)} \frac{\overline{\rho}_G \left(\frac{\partial e_G}{\partial T_G} \right)_{v_G}}{\Delta t a_{G,K(k)}}, \text{ k = 1, 2, 3, 4, 5 and 6,} \tag{5-76}$$

$$h_{Lm,G} \le c_{Lm,G} \frac{\overline{\rho}_{Lm} \left(\frac{dT^+_{Lm}}{de_{Lm}} \right)^{-1}}{\Delta t a_{G,Lm}}, \text{ m = 1, 2 and 3,} \tag{5-77}$$

$$h_{K(k)} \le c_{K(k)} \frac{\overline{\rho}_{K(k)} \left(\frac{dT^+_{K(k)}}{de_{K(k)}} \right)^{-1}}{\Delta t a_{G,K(k)}}, \text{ k = 1, 2, 3, 4, 5 and 6, and} \tag{5-78}$$

$$h_{Lm,Lm'} \le c_{Lm,Lm'} \frac{\overline{\rho}_{Lm} \left(\frac{dT^+_{Lm}}{de_{Lm}} \right)^{-1}}{\Delta t a_{Lm,Lm'}}, \text{ m = 1, 2 and 3, and m' = 1, 2 and 3 (m' } \ne \text{ m),} \tag{5-79}$$

where $c_{G,Lm}$, $c_{G,K(k)}$, $c_{Lm,G}$, $c_{K(k)}$ and $c_{Lm,Lm'}$ are the multipliers of limiters for heat-transfer coefficients. The inputs for these multipliers are CHGL, CHGK, CHLG, CHK and CHLL in the Namelist /XHMT/, respectively.

If the V/C convergence is not obtained after a specified number of iterations, the heat-transfer coefficients only for the explicitly updated component are reduced to satisfy the above conditions, and then the V/C calculation is repeated. The criterion for the number of iterations is specified by the input HMTOPT(5) in the Namelist /XCNTL/. Optionally, the limiters can be applied to both implicitly and explicitly updated components, or interfacial areas can be reduced based on the following conditions:

$$a_{G,Lm} \le \min\left[c_{G,Lm} \frac{\overline{\rho}_G}{\Delta t h_{G,Lm}} \left(\frac{\partial e_G}{\partial T_G} \right)_{v_G}, c_{Lm,G} \frac{\overline{\rho}_{Lm}}{\Delta t h_{Lm,G}} \left(\frac{dT^+_{Lm}}{de_{Lm}} \right)^{-1} \right], \text{ m = 1, 2 and 3,} \tag{5-80}$$

$$a_{G,K(k)} \le \min\left[c_{G,K(k)} \frac{\bar{\rho}_G}{\Delta th_{G,K(k)}} \left(\frac{\partial e_G}{\partial T_G} \right)_{v_G}, c_{K(k)} \frac{\bar{\rho}_{K(k)}}{\Delta th_{K(k)}} \left(\frac{dT^+_{K(k)}}{de_{K(k)}} \right)^{-1} \right],$$

$$k = 1, 2, 3, 4, 5 \text{ and } 6, \text{ and} \tag{5-81}$$

$$a_{Lm,Lm'} \le \min\left[c_{Lm,Lm'} \frac{\bar{\rho}_{Lm}}{\Delta th_{Lm,Lm'}} \left(\frac{dT^+_{Lm}}{de_{Lm}} \right)^{-1}, c_{Lm',Lm} \frac{\bar{\rho}_{Lm'}}{\Delta th_{Lm',Lm}} \left(\frac{dT^+_{Lm'}}{de_{Lm'}} \right)^{-1} \right],$$

$$m = 1, 2 \text{ and } 3, \text{ and } m' = 1, 2 \text{ and } 3 \ (m' \ne m). \tag{5-82}$$

In general, the vapor side heat-transfer coefficients are smaller than the liquid and solid sides, and hence Eqs. (5-75) and (5-76), and the first terms in the parentheses of Eqs. (5-80) and (5-81) would be unlikely to contribute to the limits. The above two options are controlled by the input HMTOPT(6) in the Namelist /XCNTL/.

5.6.3. Effective latent heats

The effective latent heats are defined by

$$h_{Vap,Gm} = i_{Vap,Gm} - e_{Lm}, \text{ and} \tag{5-83}$$

$$h_{Con,Gm} = i_{Gm} - i_{Con,Gm}, \tag{5-84}$$

where m = 1, 2 and 3. These cannot be negative during the V/C iteration. The minimum values allowed over the first four iterations are 10^6, 10^5, 10^4 and 10^3 J/kg, respectively. The minimum beyond the fourth iteration is 10^2 J/kg. The initial high values are to lower excessive mass-transfer predictions. The value of 10^2 J/kg is to prevent oscillation. In addition, if the number of iteration exceeds a criterion, which is specified by the input IVCHLG in the Namelist /XHMT/, a larger value, 10^8 J/kg, is applied to the minimum value of effective latent heats. To realize these limit the following variables are used instead of $i_{Vap,Gm}$ and $i_{Con,Gm}$:

$$i^*_{Vap,Gm} = e_{Lm} + \max[h_{Vap,Gm}, h_{lg,min}], \text{ and} \tag{5-85}$$

$$i^*_{Con,Gm} = i_{Gm} - \max[h_{Con,Gm}, h_{lg,min}], \tag{5-86}$$

where m = 1, 2 and 3, $h_{lg,min}$ is the minimum values of the effective latent heats, and can be specified by the input HLGMIN in the Namelist /XHMT/.

5.6.4. Saturation temperature

The saturation vapor pressure and the saturation properties such as density and energy are generally defined between the liquidus and critical temperatures. However, when the vapor partial pressure becomes extremely low or high during V/C iteration, the corresponding saturation temperature could be beyond the temperature range of saturated liquid. To perform the V/C calculation reasonably even below the liquidus temperature, the EOS function $T_{\mathrm{Sat,Gm}}(p_{\mathrm{Gm}})$ is normally fitted over the temperature range above $0.5T_{\mathrm{Liq,M}}$ by extrapolating the saturation vapor pressure curve below the liquidus temperature. In addition, during V/C iteration the saturation temperature is limited to the following range:

$$f_{\mathrm{st,l}}T_{\mathrm{Liq,M}} \le T_{\mathrm{Sat,Gm}}(p_{\mathrm{Gm}}^{\kappa}) \le f_{\mathrm{st,h}}T_{\mathrm{Crt,M}}, \tag{5-87}$$

where m = 1, 2 and 3, $f_{\mathrm{st,l}}$ and $f_{\mathrm{st,h}}$ are the lower and higher multipliers for saturation temperature, respectively. The values of $f_{\mathrm{st,l}}$ and $f_{\mathrm{st,h}}$ are specified by the inputs FTSTTL and FTSTH in the Namelist /XHMT/, respectively.

During the V/C iteration, the saturation temperature could oscillate due to successive "on-off" of phase transition. Therefore, whenever the oscillation is detected after 20 V/C iterations, no mass transfer is imposed for the component concerned to avoid no-convergence in the V/C iteration.

5.6.5. Missing component

In a cell where a liquid component exists, the same material vapor component must exist. When the vapor density becomes extremely low, further condensation must not be allowed in order to avoid no-convergence of V/C iteration due to a missing vapor component. In addition, if the vapor pressure is very low or the vapor density is very small, the value of the derivative of saturation temperature with respect to density becomes very large. This affects the off-diagonal terms of $[B]$ in Eq. (5-47), resulting poor estimation of ΔT_{G}, and leads to the convergence difficulty of V/C iteration. To avoid these numerical difficulties, if $\overline{\rho}_{\mathrm{Gm}}^{\kappa} < \hat{\overline{\rho}}_{\mathrm{Gm}}^{n}$ and $\overline{\rho}_{\mathrm{Gm}}^{\kappa} < \overline{\rho}_{\mathrm{Gm,min}}$, no mass transfer is allowed for the component m at the iteration step κ. The criteria $\overline{\rho}_{\mathrm{Gm,min}}$ is specified by the input RBGMIN in the Namelist /XHMT/.

If a liquid component is completely missing and no condensation is predicted, the heat- and mass-transfer operation is excluded for this component at the iteration step concerned. This is done by setting the diagonal elements to one, the off-diagonals to zero and the

respective $\{C\}$ to zero to negate the appropriate density and energy equations contributing to matrix Eq. (5-47).

5.6.6. Overshooting in explicit solution

Using Eqs. (5-23) and (5-24), the internal energies of liquid fuel and steel, and structure components are explicitly updated after the convergence of the V/C iteration. However, the explicit solution sometimes causes overshooting of updated liquid energies. The probable cause of the overshooting is the condensation of vapor with low enthalpy. The sum of the heat-transfer terms in Eq. (5-23) or (5-24) also tends to be negative especially in the case of $\tilde{i}^{n+1}_{Con,Gm} < \tilde{e}^{n}_{Lm}$, and hence the unphysically low liquid energy could be predicted. To avoid this problem, the following equations to update the liquid energy are used instead of Eqs. (5-23) and (5-24) when the overshooting is predicted:

$$\tilde{\bar{\rho}}^{n}_{L1}\frac{\tilde{e}^{n+1}_{L1}-\tilde{e}^{n}_{L1}}{\Delta t}=\Gamma^{NE}_{G,L1}(\tilde{i}^{n+1}_{Con,G1}-\tilde{e}^{n+1}_{L1})$$
$$+\sum_{m=2}^{3}a_{L1,Lm}h_{L1,Lm}(T^{I}_{L1,Lm}-\tilde{T}^{n}_{L1})$$
$$+R_{G1,L1}a_{G,L1}h_{L1,G}(T^{I}_{G1,L1}-\tilde{T}^{n}_{L1})+R_{G4,L1}a_{G,L1}h_{L1,G}(T^{I}_{G4,L1}-\tilde{T}^{n}_{L1}),\ \text{and} \qquad (5\text{-}88)$$

$$\tilde{\bar{\rho}}^{n}_{L2}\frac{\tilde{e}^{n+1}_{L2}-\tilde{e}^{n}_{L2}}{\Delta t}=\Gamma^{NE}_{G,L2}(\tilde{i}^{n+1}_{Con,G2}-\tilde{e}^{n+1}_{L2})$$
$$+a_{L2,L1}h_{L2,L1}(T^{I}_{L2,L1}-\tilde{T}^{n}_{L2})+a_{L2,L3}h_{L2,L3}(T^{I}_{L2,L3}-\tilde{T}^{n}_{L2})$$
$$+\sum_{m=1}^{2}R_{Gm,L2}a_{G,L2}h_{L2,G}(T^{I}_{Gm,L2}-\tilde{T}^{n}_{L2})+R_{G4,L2}a_{G,L2}h_{L2,G}(T^{I}_{G4,L2}-\tilde{T}^{n}_{L2}). \qquad (5\text{-}89)$$

These can be arranged as

$$\tilde{e}^{n+1}_{L1}=\frac{\Delta t}{\tilde{\bar{\rho}}^{n}_{L1}+\Delta t\Gamma^{NE}_{G,L1}}\left\{\Gamma^{NE}_{G,L1}\tilde{i}^{n+1}_{Con,G1}+\frac{1}{\Delta t}\tilde{\bar{\rho}}^{n}_{L1}\tilde{e}^{n}_{L1}\right.$$
$$+\sum_{m=2}^{3}a_{L1,Lm}h_{L1,Lm}(T^{I}_{L1,Lm}-\tilde{T}^{n}_{L1})$$
$$+R_{G1,L1}a_{G,L1}h_{L1,G}(T^{I}_{G1,L1}-\tilde{T}^{n}_{L1})$$
$$\left.+R_{G4,L1}a_{G,L1}h_{L1,G}(T^{I}_{G4,L1}-\tilde{T}^{n}_{L1})\right\},\ \text{and} \qquad (5\text{-}90)$$

$$\tilde{e}_{L2}^{n+1} = \frac{\Delta t}{\tilde{\bar{\rho}}_{L2}^{n} + \Delta t \Gamma_{G,L2}^{NE}} \left\{ \Gamma_{G,L2}^{NE} \tilde{i}_{Con,G2}^{n+1} + \frac{1}{\Delta t} \tilde{\bar{\rho}}_{L2}^{n} \tilde{e}_{L2}^{n} \right.$$

$$+ a_{L2,L1} h_{L2,L1} (T_{L2,L1}^{I} - \tilde{T}_{L2}^{n}) + a_{L2,L3} h_{L2,L3} (T_{L2,L3}^{I} - \tilde{T}_{L2}^{n})$$

$$+ \sum_{m=1}^{2} R_{Gm,L2} a_{G,L2} h_{L2,G} (T_{Gm,L2}^{I} - \tilde{T}_{L2}^{n})$$

$$\left. + R_{G4,L2} a_{G,L2} h_{L2,G} (T_{G4,L2}^{I} - \tilde{T}_{L2}^{n}) \right\}. \qquad (5\text{-}91)$$

Equations (5-90) and (5-91) do not fully-implicitly update the liquid energy because the ~n values of the liquid temperature are used in the heat-transfer terms. In addition, the use of the above equations is not consistent with the energy conservation in the V/C operation. Nevertheless, Eqs. (5-90) and (5-91) could be useful to avoid the overshooting of updated liquid energies. The updated liquid energies are recognized to be overshot when the change of liquid temperature in one V/C operation exceeds the input DTLMAX in the Namelist /XHMT/.

5.6.7. Time step control

If convergence is not obtained after the specified number of iterations, the time-step size is halved for the next cycle. The criterion is specified by the input HMTOPT(10) in the Namelist /XCNTL/. If the number of iterations exceeds a maximum value, and hence no convergence occurs, the same cycle is recalculated with a halved time-step size. The maximum is specified by the input MIVC in the Namelist /XHMT/. On the other hand, the user can optionally select an operation to skip the V/C calculation for cells with no convergence. This option becomes active by the input HMTOPT(8) in the Namelist /XCNTL/. In this case, the next cycle should be calculated with a halved time-step size according to the input HMTOPT(10).

The code recalculates the same cycle with a halved time-step size if excessive change of vapor temperature is predicted after convergence. This is useful to avoid the prediction of unphysical vapor temperature. The fractional change of vapor temperature allowed in one time step due to V/C calculation is defined by

$$\frac{\left| \tilde{T}_{G}^{n+1} - \tilde{T}_{G}^{n} \right|}{\tilde{T}_{G}^{n}} \le f_{DTG,max}, \qquad (5\text{-}92)$$

where $f_{DTG,max}$ is specified by the input FDTGMX in the Namelist /XHMT/.

Chapter 6. Equilibrium M/F transfers

6.1. Mass- and energy-conservation equations

The equilibrium M/F operation calculates equilibrium processes resulting from the non-equilibrium heat and mass transfer. The equilibrium transfers for fuel-pin structure and can-wall interiors are treated by the structure breakup model. The mass- and energy-conservation equations to be solved are written for can-wall surfaces, fuel crusts, fuel and steel liquids, and fuel and steel particles.

The mass and energy conservation for fuel crusts are

$$\frac{\partial \overline{\rho}_{Sm}}{\partial t} = -\Gamma^{EQ}_{Sm,L1}, \text{ and} \tag{6-1}$$

$$\frac{\partial \overline{\rho}_{Sm} e_{Sm}}{\partial t} = -\Gamma^{EQ}_{Sm,L1} e_{Sol,M(Sm)}, \tag{6-2}$$

where m = 2 and 3 are for left and right fuel crusts, respectively.

The mass and energy equations for can-wall surfaces are

$$\frac{\partial \overline{\rho}_{Sm}}{\partial t} = -\Gamma^{EQ}_{Sm,L2}, \text{ and} \tag{6-3}$$

$$\frac{\partial \overline{\rho}_{Sm} e_{Sm}}{\partial t} = -\Gamma^{EQ}_{Sm,L2} e_{Sol,M(Sm)}, \tag{6-4}$$

where m = 5 and 7 are for left and right can-wall surfaces, respectively.

The mass and energy conservation for fuel particles are

$$\frac{\partial \overline{\rho}_{L4}}{\partial t} = \Gamma^{EQ}_{L1,L4} - \Gamma^{EQ}_{L4,L1}, \text{ and} \tag{6-5}$$

$$\frac{\partial \overline{\rho}_{L4} e_{L4}}{\partial t} = \Gamma^{EQ}_{L1,L4} e_{Sol,M(L4)} - \Gamma^{EQ}_{L4,L1} e_{Liq,M(L4)}. \tag{6-6}$$

The mass and energy conservation for steel particles are

$$\frac{\partial \overline{\rho}_{L5}}{\partial t} = \Gamma^{EQ}_{L2,L5} - \Gamma^{EQ}_{L5,L2}, \text{ and} \tag{6-7}$$

$$\frac{\partial \overline{\rho}_{L5} e_{L5}}{\partial t} = \Gamma^{EQ}_{L2,L5} e_{Sol,M(L5)} - \Gamma^{EQ}_{L5,L2} e_{Liq,M(L5)}. \tag{6-8}$$

The mass and energy conservation for fuel liquid are

$$\frac{\partial \overline{\rho}_{L1}}{\partial t} = \Gamma^{EQ}_{S2,L1} + \Gamma^{EQ}_{S3,L1} + \Gamma^{EQ}_{L4,L1} - \Gamma^{EQ}_{L1,L4}, \text{ and} \tag{6-9}$$

$$\frac{\partial \overline{\rho}_{L1} e_{L1}}{\partial t} = \left(\Gamma^{EQ}_{S2,L1} + \Gamma^{EQ}_{S3,L1} + \Gamma^{EQ}_{L4,L1}\right) e_{Sol,M(L1)} - \Gamma^{EQ}_{L1,L4} e_{Liq,M(L1)}. \tag{6-10}$$

The mass and energy equations for steel liquid are

$$\frac{\partial \overline{\rho}_{L2}}{\partial t} = \Gamma^{EQ}_{S5,L2} + \Gamma^{EQ}_{S7,L2} + \Gamma^{EQ}_{L5,L2} - \Gamma^{EQ}_{L2,L5}, \text{ and} \tag{6-11}$$

$$\frac{\partial \overline{\rho}_{L2} e_{L2}}{\partial t} = \left(\Gamma^{EQ}_{S5,L2} + \Gamma^{EQ}_{S7,L2} + \Gamma^{EQ}_{L5,L2}\right) e_{Sol,M(L2)} - \Gamma^{EQ}_{L2,L5} e_{Liq,M(L2)}. \tag{6-12}$$

In the case of liquid steel film freezing into structures, the mass and energy equations for solid steel are

$$\frac{\partial \overline{\rho}_{Sm}}{\partial t} = \Gamma^{EQ}_{L2,L5} X_B \frac{a_{L2,Sm}}{a_{Lf}}, \tag{6-13}$$

$$\frac{\partial \overline{\rho}_{L5}}{\partial t} = \Gamma^{EQ}_{L2,L5} (1 - X_B), \tag{6-14}$$

$$\frac{\partial \overline{\rho}_{Sm} e_{Sm}}{\partial t} = \Gamma^{EQ}_{L2,L5} e_{Sol,M(Sm)} X_B \frac{a_{L2,Sm}}{a_{Lf}}, \text{ and} \tag{6-15}$$

$$\frac{\partial \overline{\rho}_{L5} e_{L5}}{\partial t} = \Gamma^{EQ}_{L2,L5} e_{Sol,M(L5)} (1 - X_B), \tag{6-16}$$

where m = 4, 5 and 7 are for cladding, and left and right can-wall surfaces, respectively. Here, X_B represents the fraction of liquid steel component in the film, and a_{Lf} ($= \sum_m a_{L2,Sm}$) is defined as the total contact area between the liquid steel film and the structure components. It is noted that the steel film mass transferred is partitioned among the three structure components based on their fractional surface areas.

6.2. Solution procedure

In the equilibrium M/F operation, the mass- and energy-conservation equations are solved explicitly using macroscopic densities and energies following non-equilibrium transfer updates. Here, a multi-step approach is used to update the mass- and energy-conservation equations. First, the equilibrium melting of fuel crusts and fuel particles, and can-wall surfaces and steel particles are evaluated. Second, the equilibrium freezing of liquid fuel and liquid steel are evaluated.

The finite-difference representations of the mass and energy conservation for equilibrium melting of fuel crusts and fuel particles are

$$\frac{\tilde{\bar{\rho}}_{Sm}^{n+1} - \tilde{\bar{\rho}}_{Sm}^{n}}{\Delta t} = -\Gamma_{Sm,L1}^{EQ}, \text{ m = 2 and 3,} \tag{6-17}$$

$$\frac{\tilde{\bar{\rho}}_{L4}^{n+1} - \tilde{\bar{\rho}}_{L4}^{n}}{\Delta t} = -\Gamma_{L4,L1}^{EQ}, \tag{6-18}$$

$$\frac{\tilde{\bar{\rho}}_{Sm}^{n+1}\tilde{e}_{Sm}^{n+1} - \tilde{\bar{\rho}}_{Sm}^{n}\tilde{e}_{Sm}^{n}}{\Delta t} = -\Gamma_{Sm,L1}^{EQ} e_{Sol,M(Sm)}, \text{ m = 2 and 3, and} \tag{6-19}$$

$$\frac{\tilde{e}_{L4}^{n+1}\tilde{\bar{\rho}}_{L4}^{n+1} - \tilde{\bar{\rho}}_{L4}^{n}\tilde{e}_{L4}^{n}}{\Delta t} = -\Gamma_{L4,L1}^{EQ} e_{Sol,M(L4)}, \tag{6-20}$$

where $\tilde{\bar{\rho}}^{n}$ and $\tilde{e}^{n}$ are the values following non-equilibrium transfers. The positive equilibrium-melting rates are determined form

$$\Gamma_{Sm,L1}^{EQ} = \frac{1}{\Delta t}\frac{\tilde{e}_{Sm}^{n} - e_{Sol,M(Sm)}}{e_{Liq,M(Sm)} - e_{Sol,M(Sm)}}\tilde{\bar{\rho}}_{Sm}^{n}, \qquad \tilde{e}_{Sm}^{n} > e_{Sol,M(Sm)}, \text{ m = 2 and 3, and} \tag{6-21}$$

$$\Gamma_{L4,L1}^{EQ} = \frac{1}{\Delta t}\frac{\tilde{e}_{L4}^{n} - e_{Sol,M(L4)}}{e_{Liq,M(L4)} - e_{Sol,M(L4)}}\tilde{\bar{\rho}}_{L4}^{n}, \qquad \tilde{e}_{L4}^{n} > e_{Sol,M(L4)}. \tag{6-22}$$

The resulting mass and energy-conservation equations to be solved for liquid fuel are represented by

$$\frac{\tilde{\bar{\rho}}_{L1}^{n+1} - \tilde{\bar{\rho}}_{L1}^{n}}{\Delta t} = \Gamma_{S2,L1}^{EQ} + \Gamma_{S3,L1}^{EQ} + \Gamma_{L4,L1}^{EQ}, \text{ and} \tag{6-23}$$

$$\frac{\tilde{\bar{\rho}}_{L1}^{n+1}\tilde{e}_{L1}^{n+1} - \tilde{\bar{\rho}}_{L1}^{n}\tilde{e}_{L1}^{n}}{\Delta t} = \left(\Gamma_{S2,L1}^{EQ} + \Gamma_{S3,L1}^{EQ} + \Gamma_{L4,L1}^{EQ}\right) e_{Sol,M(L1)}. \tag{6-24}$$

The finite-difference representation of the mass and energy conservation for equilibrium melting of can-wall surfaces is

$$\frac{\tilde{\bar{\rho}}_{Sm}^{n+1} - \tilde{\bar{\rho}}_{Sm}^{n}}{\Delta t} = -\Gamma_{Sm,L2}^{EQ}, \text{ and} \tag{6-25}$$

$$\frac{\tilde{\bar{\rho}}_{Sm}^{n+1}\tilde{e}_{Sm}^{n+1} - \tilde{\bar{\rho}}_{Sm}^{n}\tilde{e}_{Sm}^{n}}{\Delta t} = -\Gamma_{Sm,L2}^{EQ} e_{Sol,M(Sm)}, \tag{6-26}$$

where m = 5 and 7, and for equilibrium melting of steel particles is

$$\frac{\tilde{\bar{\rho}}_{L5}^{n+1} - \tilde{\bar{\rho}}_{L5}^{n}}{\Delta t} = -\Gamma_{L5,L2}^{EQ}, \text{ and} \tag{6-27}$$

$$\frac{\tilde{e}_{L5}^{n+1}\tilde{\tilde{\rho}}_{L5}^{n+1}-\tilde{\tilde{\rho}}_{L5}^{n}\tilde{e}_{L5}^{n}}{\Delta t}=-\Gamma_{L5,L2}^{EQ}e_{Sol,M(L5)}. \tag{6-28}$$

In Eqs. (6-25) – (6-28), $\tilde{\tilde{\rho}}^{n}$ and $\tilde{e}^{n}$ are the values following non-equilibrium transfers. The positive equilibrium-melting rates are determined form

$$\Gamma_{Sm,L2}^{EQ}=\frac{1}{\Delta t}\frac{\tilde{e}_{Sm}^{n}-e_{Sol,M(Sm)}}{e_{Liq,M(Sm)}-e_{Sol,M(Sm)}}\tilde{\tilde{\rho}}_{Sm}^{n}, \qquad \tilde{e}_{Sm}^{n}>e_{Sol,M(Sm)}, \text{ m = 5 and 7, and} \tag{6-29}$$

$$\Gamma_{L5,L2}^{EQ}=\frac{1}{\Delta t}\frac{\tilde{e}_{L5}^{n}-e_{Sol.M(L5)}}{e_{Liq,M(L5)}-e_{Sol,M(L5)}}\tilde{\tilde{\rho}}_{L5}^{n}, \qquad \tilde{e}_{L5}^{n}>e_{Sol,M(L5)}. \tag{6-30}$$

The resulting mass and energy-conservation equations to be solved for liquid steel are represented by

$$\frac{\tilde{\tilde{\rho}}_{L2}^{n+1}-\tilde{\tilde{\rho}}_{L2}^{n}}{\Delta t}=\Gamma_{S5,L2}^{EQ}+\Gamma_{S7,L2}^{EQ}+\Gamma_{L5,L2}^{EQ}, \text{ and} \tag{6-31}$$

$$\frac{\tilde{\tilde{\rho}}_{L2}^{n+1}\tilde{e}_{L2}^{n+1}-\tilde{\tilde{\rho}}_{L2}^{n}\tilde{e}_{L2}^{n}}{\Delta t}=\left(\Gamma_{S5,L2}^{EQ}+\Gamma_{S7,L2}^{EQ}+\Gamma_{L5,L2}^{EQ}\right)e_{Sol,M(L2)}. \tag{6-32}$$

The above finite-difference representations, Eqs. (6-17), (6-18), (6-23), (6-25), (6-27) and (6-31), of mass conservation for equilibrium melting are solved with respect to $\tilde{\tilde{\rho}}^{n+1}$, and then the representations, Eqs. (6-19), (6-20), (6-24), (6-26), (6-28) and (6-32), of energy conservation are solved explicitly with respect to $\tilde{e}^{n+1}$ using the updated densities $\tilde{\tilde{\rho}}^{n+1}$. The updated macroscopic densities and energies are called ~n values in the following finite-difference representations for equilibrium freezing of liquid fuel and steel.

The finite-difference representations of the mass and energy conservation for equilibrium freezing of liquid fuel are

$$\frac{\tilde{\tilde{\rho}}_{L1}^{n+1}-\tilde{\tilde{\rho}}_{L1}^{n}}{\Delta t}=-\Gamma_{L1,L4}^{EQ}, \text{ and} \tag{6-33}$$

$$\frac{\tilde{\tilde{\rho}}_{L1}^{n+1}\tilde{e}_{L1}^{n+1}-\tilde{\tilde{\rho}}_{L1}^{n}\tilde{e}_{L1}^{n}}{\Delta t}=-\Gamma_{L1,L4}^{EQ}e_{Liq,M(L1)}, \tag{6-34}$$

where $\tilde{\tilde{\rho}}^{n}$ and $\tilde{e}^{n}$ are the values following equilibrium transfers of fuel-crust and fuel particle melting. The positive equilibrium-freezing rate is determined form

$$\Gamma_{L1,L4}^{EQ}=\frac{1}{\Delta t}\frac{e_{Liq,M(L1)}-\tilde{e}_{L1}^{n}}{e_{Liq,M(L1)}-e_{Sol,M(L1)}}\tilde{\tilde{\rho}}_{L1}^{n}, \qquad \tilde{e}_{L1}^{n}<e_{Liq,M(L1)}. \tag{6-35}$$

The resulting mass and energy-conservation equations to be solved for fuel particles are represented by

$$\frac{\tilde{\bar{\rho}}_{L4}^{n+1} - \tilde{\bar{\rho}}_{L4}^{n}}{\Delta t} = \Gamma_{L1,L4}^{EQ}, \text{ and} \tag{6-36}$$

$$\frac{\tilde{e}_{L4}^{n+1}\tilde{\bar{\rho}}_{L4}^{n+1} - \tilde{\bar{\rho}}_{L4}^{n}\tilde{e}_{L4}^{n}}{\Delta t} = \Gamma_{L1,L4}^{EQ} e_{Sol,M(L4)}. \tag{6-37}$$

The finite-difference representations of the mass and energy conservation for equilibrium freezing of liquid steel are

$$\frac{\tilde{\bar{\rho}}_{L2}^{n+1} - \tilde{\bar{\rho}}_{L2}^{n}}{\Delta t} = -\Gamma_{L2,L5}^{EQ}, \text{ and} \tag{6-38}$$

$$\frac{\tilde{\bar{\rho}}_{L2}^{n+1}\tilde{e}_{L2}^{n+1} - \tilde{\bar{\rho}}_{L2}^{n}\tilde{e}_{L2}^{n}}{\Delta t} = -\Gamma_{L2,L5}^{EQ} e_{Liq,M(L2)}, \tag{6-39}$$

where $\tilde{\bar{\rho}}^{n}$ and $\tilde{e}^{n}$ are the values following equilibrium transfers of can-wall surface and steel particle melting. The positive equilibrium-freezing rate is determined form

$$\Gamma_{L2,L5}^{EQ} = \frac{1}{\Delta t}\frac{e_{Liq,M(L2)} - \tilde{e}_{L2}^{n}}{e_{Liq,M(L2)} - e_{Sol,M(L2)}}\tilde{\bar{\rho}}_{L2}^{n}, \qquad \tilde{e}_{L2}^{n} < e_{Liq,M(L2)}. \tag{6-40}$$

The resulting mass and energy-conservation equations to be solved for steel particles are represented by

$$\frac{\tilde{\bar{\rho}}_{L5}^{n+1} - \tilde{\bar{\rho}}_{L5}^{n}}{\Delta t} = \Gamma_{L2,L5}^{EQ}, \text{ and} \tag{6-41}$$

$$\frac{\tilde{e}_{L5}^{n+1}\tilde{\bar{\rho}}_{L5}^{n+1} - \tilde{\bar{\rho}}_{L5}^{n}\tilde{e}_{L5}^{n}}{\Delta t} = \Gamma_{L2,L5}^{EQ} e_{Sol,M(L5)}. \tag{6-42}$$

In the case of the liquid steel film freezing into structures, the finite-difference representations of the mass and energy conservation for equilibrium freezing of solid steel are

$$\frac{\tilde{\bar{\rho}}_{Sm}^{n+1} - \tilde{\bar{\rho}}_{Sm}^{n}}{\Delta t} = \Gamma_{L2,L5}^{EQ} X_B \frac{a_{L2,Sm}}{a_{Lf}}, \tag{6-43}$$

$$\frac{\tilde{\bar{\rho}}_{L5}^{n+1} - \tilde{\bar{\rho}}_{L5}^{n}}{\Delta t} = \Gamma_{L2,L5}^{EQ}(1 - X_B), \tag{6-44}$$

$$\frac{\tilde{e}_{Sm}^{n+1}\tilde{\bar{\rho}}_{Sm}^{n+1} - \tilde{\bar{\rho}}_{Sm}^{n}\tilde{e}_{Sm}^{n}}{\Delta t} = \Gamma_{L2,L5}^{EQ} e_{Sol,M(Sm)} X_B \frac{a_{L2,Sm}}{a_{Lf}}, \text{ and} \tag{6-45}$$

$$\frac{\tilde{e}_{L5}^{n+1}\tilde{\tilde{\rho}}_{L5}^{n+1}-\tilde{\tilde{\rho}}_{L5}^{n}\tilde{e}_{L5}^{n}}{\Delta t}=\Gamma_{L2,L5}^{EQ}e_{Sol,M(L5)}(1-X_B)\cdot \tag{6-46}$$

The above finite-difference representations, Eqs. (6-33), (6-36), (6-38), (6-41), (6-43) and (6-44), of mass conservation for equilibrium freezing are solved with respect to $\tilde{\tilde{\rho}}^{n+1}$, and then the representations, Eqs. (6-34), (6-37), (6-39), (6-42), (6-45) and (6-46), of energy conservation are solved explicitly with respect to $\tilde{e}^{n+1}$ using the updated densities $\tilde{\tilde{\rho}}^{n+1}$. The updated macroscopic densities and energies are the final values in the equilibrium M/F operation.

Chapter 7. Discussion on model and method

The assessment study of the developed model integrated into the SIMMER-III code has demonstrated that the generalized heat- and mass-transfer model provides a sufficiently flexible, and often indispensable, framework to simulate transient multiphase phenomena [10, 11, 12]. The experience and knowledge from the assessment study were applied extensively to analyses of key phenomena of CDAs in LMFR [13]. These applications have also revealed potential applicability of the present model to integral multiphase, multicomponent thermal-hydraulic problems. The developed model advances satisfactorily the analytical technologies and understanding of the physical phenomena of multiphase, multicomponent flows involved in the LMFR safety analysis. Beside, the assessment study and the applications to the key phenomena of CDAs were valuable in highlighting the problem areas, as discussed below, which will guide our future model improvement and validation:

- The treatment of condensation processes of fuel or steel vapor on other colder liquids has less physical evidence in its modeling. In addition, the effect of non-condensable gas on condensation might be underestimated in principle. These modeling limitations could be improved by introducing the concept of diffusion-limited process.
- The present non-equilibrium model does not allow both melting and vaporization or freezing and condensation at an interface. For example, at the liquid fuel/coolant interface, fuel particle formation relies on the equilibrium process because only coolant vaporization is treated at this interface. To solve this problem, additional information must be utilized, such as the relationship of the vapor saturation temperature to the (liquidus/solidus) temperature, to determine which non-equilibrium process is preferred.
- The SIMMER-III non-equilibrium M/F model can represent an important sequence of fuel relocation and freezing processes: the crust formation on a can wall that furnishes thermal resistance, and steel ablation and particle formation that contribute to fluid quenching and bulk freezing. However, a more sophisticated treatment is required for general modeling of molten fuel/structure interactions. The status of the improved fuel-freezing model is described in another document.
- The film-boiling process can be treated through a reduced heat-transfer coefficient considering a vapor film surrounding a hot droplet or particle. However, the vapor film cannot be differentiated from bulk vapor. This limitation is the same with condensate films. Although additional components improve these phenomenological treatments,

the flow regime modeling could be more complicated.

Chapter 8. Concluding remarks

A closed set of the heat- and mass-transfer modeling for SIMMER-III were described in the present report. The generalized modeling of heat- and mass-transfer phenomena for more reliable analysis of CDAs was developed on the basis of phenomenological consideration of heat- and mass-transfer processes in a multiphase, multicomponent system. The numerical simulation of complex multiphase, multicomponent flow situations in a reactor core is essential to investigate CDAs in LMFRs. The present model alleviates some of the limitations in the previous SIMMER-II code and thereby provides a generalized modeling of heat- and mass-transfer phenomena in a multiphase, multicomponent system for more reliable analysis of CDAs. It is believed, therefore, that the future research with SIMMER-III will improve significantly the reliability and accuracy of LMFR safety analyses.

Acknowledgements

The initial stage of this study was jointly performed under the agreement between the United States Nuclear Regulatory Commission and the Power Reactor and Nuclear Fuel Development Corporation, presently called the Japan Nuclear Cycle Development Institute (JNC). The authors are grateful to W. R. Bohl of the Los Alamos National Laboratory for his significant contribution to forming the basis of SIMMER-III. The present study has been completed in collaboration with FZK and CEA under the SIMMER-III code development program at JNC.

Appendix A. Definition of derivatives used in V/C iteration

A.1. Mass-transfer rates

The derivatives of mass-transfer rates with respect to the sensitive variables $\overline{\rho}_{G1}$, $\overline{\rho}_{G2}$, $\overline{\rho}_{G3}$, e_{L3} and T_G are expressed by

$$\frac{\partial \Gamma^{NE}_{G,L1}}{\partial x_l} = \Lambda x^{I1}_{GL1,l} + \Lambda x^{I2}_{GL1,l} + \Lambda x^{I3}_{GL1,l} + \sum_{k=1}^{6} \Lambda x^{I(k)}_{GL1,l}, \tag{A-1}$$

$$\frac{\partial \Gamma^{NE}_{G,L2}}{\partial x_l} = \Lambda x^{I2}_{GL2,l} + \Lambda x^{I3}_{GL2,l} + \sum_{k=1}^{6} \Lambda x^{I(k)}_{GL2,l}, \tag{A-2}$$

$$\frac{\partial \Gamma^{NE}_{G,L3}}{\partial x_l} = \Lambda x^{I3}_{GL3,l} + \sum_{k=1}^{6} \Lambda x^{I(k)}_{GL3,l}, \tag{A-3}$$

$$\frac{\partial \Gamma^{NE}_{L1,G}}{\partial x_l} = \Lambda x^{I1}_{L1G,l}, \tag{A-4}$$

$$\frac{\partial \Gamma^{NE}_{L2,G}}{\partial x_l} = \Lambda x^{I2}_{L2G,l} + \Lambda x^{I7}_{L2G,l}, \text{ and} \tag{A-5}$$

$$\frac{\partial \Gamma^{NE}_{L3,G}}{\partial x_l} = \Lambda x^{I3}_{L3G,l} + \Lambda x^{I8}_{L3G,l} + \Lambda x^{I12}_{L3G,l}, \tag{A-6}$$

where x_l for l = 1, 2, 3, 4 and 5 means $\overline{\rho}_{G1}$, $\overline{\rho}_{G2}$, $\overline{\rho}_{G3}$, e_{L3} and T_G, respectively. The variables, $\Lambda x^{Im}_{GLm,l}$ (m = 1, 2 and 3), $\Lambda x^{I2}_{GL1,l}$, $\Lambda x^{I3}_{GL1,l}$, $\Lambda x^{I(k)}_{GLm,l}$ (m = 1, 2 and 3), $\Lambda x^{I3}_{GL2,l}$, $\Lambda x^{Im}_{LmG,l}$ (m = 1, 2 and 3), $\Lambda x^{I7}_{L2G,l}$, $\Lambda x^{I8}_{L3G,l}$ and $\Lambda x^{I12}_{L3G,l}$ are the derivatives of each mass-transfer rate, and they are given as a function of the intermediate variable set.

Vapor/Liquid-fuel interface: The mass-transfer rates are calculated by

$$\Gamma^{I1}_{G,L1} = \frac{q^{I}_{G1,L1}}{h_{Con,G1}}, \qquad q^{I}_{G1,L1} > 0, \text{ and} \tag{A-7}$$

$$\Gamma^{I1}_{L1,G} = -\frac{q^{I}_{G1,L1}}{h_{Vap,G1}}, \qquad q^{I}_{G1,L1} < 0, \tag{A-8}$$

where

$$q^{I}_{G1,L1} = R_{G1,L1} a_{G,L1} [h_{L1,G}(T^{I}_{G1,L1} - \tilde{T}^{n}_{L1}) + h_{G,L1}(T^{I}_{G1,L1} - \tilde{T}^{n+1}_{G})]. \tag{A-9}$$

The derivative of mass-transfer rate, Eq. (A-7), is given by

$$\Delta\Gamma^{II}_{G,L1} = \sum_{l=1}^{3} \Lambda x^{II}_{GL1,l}\Delta\overline{\rho}_{Gl} + \Lambda x^{II}_{GL1,4}\Delta e_{L3} + \Lambda x^{II}_{GL1,5}\Delta T_G, \tag{A-10}$$

where

$$\Lambda x^{II}_{GL1,l} = \Lambda R_{G1,L1}\frac{\partial R_{G1,L1}}{\partial\overline{\rho}_{Gl}} + (\Lambda T^{I}_{G1,L1}\frac{\partial T^{I}_{G1,L1}}{\partial\overline{\rho}_{Gl}} + \Lambda h_{Con,G1}\frac{\partial h_{Con,G1}}{\partial\overline{\rho}_{Gl}})\delta(l,1),$$

$$l = 1, 2 \text{ and } 3, \tag{A-11}$$

$$\Lambda x^{II}_{GL1,4} = 0, \text{ and} \tag{A-12}$$

$$\Lambda x^{II}_{GL1,5} = \Lambda R_{G1,L1}\frac{\partial R_{G1,L1}}{\partial T_G} + \Lambda T^{I}_{G1,L1}\frac{\partial T^{I}_{G1,L1}}{\partial T_G} + \Lambda T_G + \Lambda h_{Con,G1}\frac{\partial h_{Con,G1}}{\partial T_G}. \tag{A-13}$$

The expressions for intermediate variables, $\Lambda R_{G1,L1}$, $\Lambda T^{I}_{G1,L1}$, ΛT_G and $\Lambda h_{Con,G1}$, in Eqs. (A-11) and (A-13) are given by

$$\Lambda R_{G1,L1} = -\frac{a_{G,L1}[h_{L1,G}(T^{I}_{G1,L1} - T_{L1}) + h_{G,L1}(T^{I}_{G1,L1} - T_G)]}{h_{Con,G1}}H(\Gamma^{II}_{G,L1}), \tag{A-14}$$

$$\Lambda T^{I}_{G1,L1} = \frac{a_{G,L1}(h_{L1,G} + h_{G,L1})}{h_{Con,G1}}H(\Gamma^{II}_{G,L1}), \tag{A-15}$$

$$\Lambda T_G = -\frac{a_{G,L1}h_{L1,G}}{h_{Con,G1}}H(\Gamma^{II}_{G,L1}), \text{ and} \tag{A-16}$$

$$\Lambda h_{Con,G1} = -\frac{\Gamma^{II}_{G,L1}}{h_{Con,G1}}. \tag{A-17}$$

The derivative of mass-transfer rate, Eq. (A-8), is given by

$$\Delta\Gamma^{II}_{L1,G} = \sum_{l=1}^{3} \Lambda x^{II}_{L1G,l}\Delta\overline{\rho}_{Gl} + \Lambda x^{II}_{L1G,4}\Delta e_{L3} + \Lambda x^{II}_{L1G,5}\Delta T_G, \tag{A-18}$$

where

$$\Lambda x^{II}_{L1G,l} = \Lambda R_{G1,L1}\frac{\partial R_{G1,L1}}{\partial\overline{\rho}_{Gl}} + (\Lambda T^{I}_{G1,L1}\frac{\partial T^{I}_{G1,L1}}{\partial\overline{\rho}_{Gl}} + \Lambda h_{Vap,G1}\frac{\partial h_{Vap,G1}}{\partial\overline{\rho}_{Gl}})\delta(l,1),$$

$$l = 1, 2 \text{ and } 3, \tag{A-19}$$

$$\Lambda x^{II}_{L1G,4} = 0, \text{ and} \tag{A-20}$$

$$\Lambda x^{II}_{L1G,5} = \Lambda R_{G1,L1}\frac{\partial R_{G1,L1}}{\partial T_G} + \Lambda T^{I}_{G1,L1}\frac{\partial T^{I}_{G1,L1}}{\partial T_G} + \Lambda T_G + \Lambda h_{Vap,G1}\frac{\partial h_{Vap,G1}}{\partial T_G}. \tag{A-21}$$

The expressions for intermediate variables, $\Lambda R_{G1,L1}$, $\Lambda T^{I}_{G1,L1}$, ΛT_G and $\Lambda h_{Vap,G1}$, in Eqs. (A-19) and (A-21) are given by

$$\Lambda R_{G1,L1} = -\frac{a_{G,L1}[h_{L1,G}(T^{I}_{G1,L1} - T_{L1}) + h_{G,L1}(T^{I}_{G1,L1} - T_G)]}{h_{Vap,G1}} H(\Gamma^{II}_{L1,G}), \tag{A-22}$$

$$\Lambda T^{I}_{G1,L1} = -\frac{R_{G1,L1} a_{G,L1}(h_{L1,G} + h_{G,L1})}{h_{Vap,G1}} H(\Gamma^{II}_{L1,G}), \tag{A-23}$$

$$\Lambda T_G = \frac{R_{G1,L1} a_{G,L1} h_{L1,G}}{h_{Vap,G1}} H(\Gamma^{II}_{L1,G}), \text{ and} \tag{A-24}$$

$$\Lambda h_{Vap,G1} = \frac{\Gamma^{II}_{L1,G}}{h_{Vap,G1}}. \tag{A-25}$$

Vapor/Liquid-steel interface: The mass-transfer rates are calculated by

$$\Gamma^{I2}_{G,L2} = \frac{q^{I}_{G2,L2}}{h_{Con,G2}}, q^{I}_{G2,L2} > 0, \text{ and} \tag{A-26}$$

$$\Gamma^{I2}_{L2,G} = -\frac{q^{I}_{G2,L2}}{h_{Vap,G2}}, \quad q^{I}_{G2,L2} < 0, \tag{A-27}$$

where

$$q^{I}_{G2,L2} = R_{G2,L2} a_{G,L2}[h_{L2,G}(T^{I}_{G2,L2} - \tilde{T}^{n}_{L2}) + h_{G,L2}(T^{I}_{G2,L2} - \tilde{T}^{n+1}_{G})]. \tag{A-28}$$

The derivative of mass-transfer rate, Eq. (A-26), is given by

$$\Delta\Gamma^{I2}_{G,L2} = \sum_{l=1}^{3} \Lambda x^{I2}_{GL2,l} \Delta\bar{\rho}_{Gl} + \Lambda x^{I2}_{GL2,4} \Delta e_{L3} + \Lambda x^{I2}_{GL2,5} \Delta T_G, \tag{A-29}$$

where

$$\Lambda x^{I2}_{GL2,l} = \Lambda R_{G2,L2} \frac{\partial R_{G2,L2}}{\partial \bar{\rho}_{Gl}} + (\Lambda T^{I}_{G2,L2} \frac{\partial T^{I}_{G2,L2}}{\partial \bar{\rho}_{Gl}} + \Lambda h_{Con,G2} \frac{\partial h_{Con,G2}}{\partial \bar{\rho}_{Gl}}) \delta(l,2),$$

$$l = 1, 2 \text{ and } 3, \tag{A-30}$$

$$\Lambda x^{I1}_{GL2,4} = 0, \text{ and} \tag{A-31}$$

$$\Lambda x^{I2}_{GL2,5} = \Lambda R_{G2,L2} \frac{\partial R_{G2,L2}}{\partial T_G} + \Lambda T^{I}_{G2,L2} \frac{\partial T^{I}_{G2,L2}}{\partial T_G} + \Lambda T_G + \Lambda h_{Con,G2} \frac{\partial h_{Con,G2}}{\partial T_G}. \tag{A-32}$$

The expressions for intermediate variables, $\Lambda R_{G2,L2}$, $\Lambda T^{I}_{G2,L2}$, ΛT_G and $\Lambda h_{Con,G2}$, in Eqs. (A-

30) and (A-32) are given by

$$\Delta R_{G2,L2} = \frac{a_{G,L2}[h_{L2,G}(T^{I}_{G2,L2} - \tilde{T}^{n}_{L2}) + h_{G,L2}(T^{I}_{G2,L2} - \tilde{T}^{n+1}_{G})]}{h_{Con,G2}} H(\Gamma^{I2}_{G,L2}), \quad \text{(A-33)}$$

$$\Delta T^{I}_{G2,L2} = \frac{R_{G2,L2} a_{G,L2}(h_{L2,G} + h_{G,L2})}{h_{Con,G2}} H(\Gamma^{I2}_{G,L2}), \quad \text{(A-34)}$$

$$\Delta T_{G} = -\frac{R_{G2,L2} a_{G,L2} h_{L2,G}}{h_{Con,G2}} H(\Gamma^{I2}_{G,L2}), \text{ and} \quad \text{(A-35)}$$

$$\Delta h_{Con,G2} = -\frac{\Gamma^{I2}_{G,L2}}{h_{Con,G2}}. \quad \text{(A-36)}$$

The derivative of mass-transfer rate, Eq. (A-27), is given by

$$\Delta \Gamma^{I2}_{L2,G} = \sum_{l=1}^{3} \Delta x^{I2}_{L2G,l} \Delta \bar{\rho}_{Gl} + \Delta x^{I2}_{L2G,4} \Delta e_{L3} + \Delta x^{I2}_{L2G,5} \Delta T_{G}, \quad \text{(A-37)}$$

where

$$\Delta x^{I2}_{L2G,l} = \Delta R_{G2,L2} \frac{\partial R_{G2,L2}}{\partial \bar{\rho}_{Gl}} + (\Delta T^{I}_{G2,L2} \frac{\partial T^{I}_{G2,L2}}{\partial \bar{\rho}_{Gl}} + \Delta h_{Vap,G2} \frac{\partial h_{Vap,G2}}{\partial \bar{\rho}_{Gl}}) \delta(l,2),$$

$$l = 1, 2 \text{ and } 3, \quad \text{(A-38)}$$

$$\Delta x^{I2}_{L2G,4} = 0, \text{ and} \quad \text{(A-39)}$$

$$\Delta x^{I2}_{L2G,5} = \Delta R_{G2,L2} \frac{\partial R_{G2,L2}}{\partial T_{G}} + \Delta T^{I}_{G2,L2} \frac{\partial T^{I}_{G2,L2}}{\partial T_{G}} + \Delta T_{G} + \Delta h_{Vap,G2} \frac{\partial h_{Vap,G2}}{\partial T_{G}}. \quad \text{(A-40)}$$

The expressions for intermediate variables, $\Delta R_{G2,L2}$, $\Delta T^{I}_{G2,L2}$, ΔT_{G} and $\Delta h_{Vap,G2}$, in Eqs. (A-38) and (A-40) are given by

$$\Delta R_{G2,L2} = -\frac{a_{G,L2}[h_{L2,G}(T^{I}_{G2,L2} - \tilde{T}^{n}_{L2}) + h_{G,L2}(T^{I}_{G2,L2} - \tilde{T}^{n+1}_{G})]}{h_{Vap,G2}} H(\Gamma^{I2}_{G,L2}), \quad \text{(A-41)}$$

$$\Delta T^{I}_{G2,L2} = -\frac{R_{G2,L2} a_{G,L2}(h_{L2,G} + h_{G,L2})}{h_{Vap,G2}} H(\Gamma^{I2}_{L2,G}), \quad \text{(A-42)}$$

$$\Delta T_{G} = \frac{R_{G2,L2} a_{G,L2} h_{L2,G}}{h_{Vap,G2}} H(\Gamma^{I2}_{L2,G}), \text{ and} \quad \text{(A-43)}$$

$$\Delta h_{Vap,G2} = \frac{\Gamma^{I2}_{L2,G}}{h_{Vap,G2}}. \quad \text{(A-44)}$$

At this interface the condensation rate of fuel vapor is calculated by

$$\Gamma_{G,L1}^{I2} = \frac{q_{G1,L2}^{I}}{h_{Con,G1}}, \qquad q_{G1,L2}^{I} > 0, \tag{A-45}$$

where

$$q_{G1,L2}^{I} = R_{G1,L2} a_{G,L2} [h_{L2,G}(T_{G1,L2}^{I} - \tilde{T}_{L2}^{n}) + h_{G,L2}(T_{G1,L2}^{I} - \tilde{T}_{G}^{n+1})]. \tag{A-46}$$

The derivative of mass-transfer rate, Eq. (A-45), is given by

$$\Delta\Gamma_{G,L1}^{I2} = \sum_{l=1}^{3} \Lambda x_{GL1,l}^{I2} \Delta\overline{\rho}_{Gl} + \Lambda x_{GL1,4}^{I2} \Delta e_{L3} + \Lambda x_{GL1,5}^{I2} \Delta T_{G}, \tag{A-47}$$

where

$$\Lambda x_{GL1,l}^{I2} = \Lambda R_{G1,L2} \frac{\partial R_{G1,L2}}{\partial \overline{\rho}_{Gl}} + (\Lambda T_{G1,L2}^{I} \frac{\partial T_{G1,L2}^{I}}{\partial \overline{\rho}_{Gl}} + \Lambda h_{Con,G1} \frac{\partial h_{Con,G1}}{\partial \overline{\rho}_{Gl}}) \delta(l,1)$$

$$l = 1, 2 \text{ and } 3, \tag{A-48}$$

$$\Lambda x_{GL1,4}^{I2} = 0, \text{ and} \tag{A-49}$$

$$\Lambda x_{GL1,5}^{I2} = \Lambda R_{G1,L2} \frac{\partial R_{G1,L2}}{\partial T_{G}} + \Lambda T_{G1,L2}^{I} \frac{\partial T_{G1,L2}^{I}}{\partial T_{G}} + \Lambda T_{G} + \Lambda h_{Con,G1} \frac{\partial h_{Con,G1}}{\partial T_{G}}. \tag{A-50}$$

The expressions for intermediate variables, $\Lambda R_{G1,L2}$, $\Lambda T_{G1,L2}^{I}$, ΛT_{G} and $\Lambda h_{Con,G1}$, in Eqs. (A-48) and (A-50) are given by

$$\Lambda R_{G1,L2} = \frac{a_{G,L2}[h_{L2,G}(T_{G1,L2}^{I} - \tilde{T}_{L2}^{n}) + h_{G,L2}(T_{G1,L2}^{I} - \tilde{T}_{G}^{n+1})]}{h_{Con,G1}} H(\Gamma_{G,L1}^{I2}), \tag{A-51}$$

$$\Lambda T_{G1,L2}^{I} = \frac{R_{G1,L2} a_{G,L2} (h_{L2,G} + h_{G,L2})}{h_{Con,G1}} H(\Gamma_{G,L1}^{I2}), \tag{A-52}$$

$$\Lambda T_{G} = -\frac{R_{G1,L2} a_{G,L2} h_{L2,G}}{h_{Con,G1}} H(\Gamma_{G,L1}^{I2}), \text{ and} \tag{A-53}$$

$$\Lambda h_{Con,G1} = -\frac{\Gamma_{G,L1}^{I2}}{h_{Con,G1}}. \tag{A-54}$$

Vapor/Liquid-sodium interface: The mass-transfer rates are calculated by

$$\Gamma_{G,L3}^{I3} = \frac{q_{G3,L3}^{I}}{h_{Con,G3}}, q_{G3,L3}^{I} > 0, \text{ and} \tag{A-55}$$

$$\Gamma^{I3}_{L3,G} = -\frac{q^{I}_{G3,L3}}{h_{Vap,G3}}, \quad q^{I}_{G3,L3} < 0, \tag{A-56}$$

where

$$q^{I}_{G3,L3} = R_{G3,L3} a_{G,L3} [h_{L3,G}(T^{I}_{G3,L3} - \tilde{T}^{n+1}_{L3}) + h_{G,L3}(T^{I}_{G3,L3} - \tilde{T}^{n+1}_{G})]. \tag{A-57}$$

The derivative of mass-transfer rate, Eq. (A-55), is given by

$$\Delta\Gamma^{I3}_{G,L3} = \sum_{l=1}^{3} \Lambda x^{I3}_{GL3,l} \Delta\overline{\rho}_{Gl} + \Lambda x^{I3}_{GL3,4} \Delta e_{L3} + \Lambda x^{I3}_{GL3,5} \Delta T_{G}, \tag{A-58}$$

where

$$\Lambda x^{I3}_{GL3,l} = \Lambda R_{G3,L3} \frac{\partial R_{G3,L3}}{\partial \overline{\rho}_{Gl}} + (\Lambda T^{I}_{G3,L3} \frac{\partial T^{I}_{G3,L3}}{\partial \overline{\rho}_{Gl}} + \Lambda h_{Con,G3} \frac{\partial h_{Con,G3}}{\partial \overline{\rho}_{Gl}}) \delta(l,3),$$

$$l = 1, 2 \text{ and } 3, \tag{A-59}$$

$$\Lambda x^{I3}_{GL3,4} = \Lambda T_{L3} \frac{\partial T_{L3}}{\partial e_{L3}}, \text{ and} \tag{A-60}$$

$$\Lambda x^{I3}_{GL3,5} = \Lambda R_{G3,L3} \frac{\partial R_{G3,L3}}{\partial T_{G}} + \Lambda T^{I}_{G3,L3} \frac{\partial T^{I}_{G3,L3}}{\partial T_{G}} + \Lambda T_{G} + \Lambda h_{Con,G3} \frac{\partial h_{Con,G3}}{\partial T_{G}}. \tag{A-61}$$

The expressions for intermediate variables, $\Lambda R_{G3,L3}$, $\Lambda T^{I}_{G3,L3}$, ΛT_{L3}, ΛT_{G} and $\Lambda h_{Con,G3}$, in Eqs. (A-59) – (A-61) are given by

$$\Lambda R_{G3,L3} = \frac{a_{G,L3}[h_{L3,G}(T^{I}_{G3,L3} - \tilde{T}^{n}_{L3}) + h_{G,L3}(T^{I}_{G3,L3} - \tilde{T}^{n+1}_{G})]}{h_{Con,G3}} H(\Gamma^{I3}_{G,L3}), \tag{A-62}$$

$$\Lambda T^{I}_{G3,L3} = \frac{R_{G3,L3} a_{G,L3}(h_{L3,G} + h_{G,L3})}{h_{Con,G3}} H(\Gamma^{I3}_{G,L3}), \tag{A-63}$$

$$\Lambda T_{L3} = -\frac{R_{G3,L3} a_{G,L3} h_{L3,G}}{h_{Con,G3}} H(\Gamma^{I3}_{G,L3}), \tag{A-64}$$

$$\Lambda T_{G} = -\frac{R_{G3,L3} a_{G,L3} h_{L3,G}}{h_{Con,G3}} H(\Gamma^{I3}_{G,L3}), \text{ and} \tag{A-65}$$

$$\Lambda h_{Con,G3} = -\frac{\Gamma^{I3}_{G,L3}}{h_{Con,G3}}. \tag{A-66}$$

The derivative of mass-transfer rate, Eq. (A-56), is given by

$$\Delta\Gamma^{I3}_{L3,G} = \sum_{l=1}^{3} \Lambda x^{I3}_{L3G,l} \Delta\tilde{\rho}_{Gl} + \Lambda x^{I3}_{L3G,4} \Delta e_{L3} + \Lambda x^{I3}_{L3G,5} \Delta T_G , \tag{A-67}$$

where

$$\Lambda x^{I3}_{L3G,l} = \Lambda R_{G3,L3} \frac{\partial R_{G3,L3}}{\partial \bar{\rho}_{Gl}} + (\Lambda T^{I}_{G3,L3} \frac{\partial T^{I}_{G3,L3}}{\partial \bar{\rho}_{Gl}} + \Lambda h_{Vap,G3} \frac{\partial h_{Vap,G3}}{\partial \bar{\rho}_{Gl}}) \delta(l,3) ,$$

$$l = 1, 2 \text{ and } 3, \tag{A-68}$$

$$\Lambda x^{I3}_{L3G,4} = \Lambda T_{L3} \frac{\partial T_{L3}}{\partial e_{L3}} + \Lambda h_{Vap,G3} \frac{\partial h_{Vap,G3}}{\partial e_{L3}} , \text{ and} \tag{A-69}$$

$$\Lambda x^{I3}_{L3G,5} = \Lambda R_{G3,L3} \frac{\partial R_{G3,L3}}{\partial T_G} + \Lambda T^{I}_{G3,L3} \frac{\partial T^{I}_{G3,L3}}{\partial T_G} + \Lambda T_G + \Lambda h_{Vap,G3} \frac{\partial h_{Vap,G3}}{\partial T_G} . \tag{A-70}$$

The expressions for intermediate variables, $\Lambda R_{G3,L3}$, $\Lambda T^{I}_{G3,L3}$, ΛT_{L3}, ΛT_G and $\Lambda h_{Vap,G3}$, in Eqs. (A-68) – (A-70) are given by

$$\Lambda R_{G3,L3} = -\frac{a_{G,L3}[h_{L3,G}(T^{I}_{G3,L3} - \tilde{T}^{n+1}_{L3}) + h_{G,L3}(T^{I}_{G3,L3} - \tilde{T}^{n+1}_{G})]}{h_{Vap,G3}} H(\Gamma^{I3}_{L3,G}), \tag{A-71}$$

$$\Lambda T^{I}_{G3,L3} = -\frac{R_{G3,L3} a_{G,L3} (h_{L3,G} + h_{G,L3})}{h_{Vap,G3}} H(\Gamma^{I3}_{L3,G}) , \tag{A-72}$$

$$\Lambda T_{L3} = \frac{R_{G3,L3} a_{G,L3} h_{L3,G}}{h_{Vap,G3}} , \tag{A-73}$$

$$\Lambda T_G = \frac{R_{G3,L3} a_{G,L3} h_{L3,G}}{h_{Vap,G3}} H(\Gamma^{I3}_{L3,G}) , \text{ and} \tag{A-74}$$

$$\Lambda h_{Vap,G3} = \frac{\Gamma^{I3}_{L3,G}}{h_{Vap,G3}} . \tag{A-75}$$

At this interface the condensation rates of fuel and steel vapor are calculated by

$$\Gamma^{I3}_{G,Lm} = \frac{q^{I}_{Gm,L3}}{h_{Con,Gm}} , \qquad q^{I}_{Gm,L3} > 0, \text{ m} = 1 \text{ and } 2, \tag{A-76}$$

where

$$q^{I}_{Gm,L3} = R_{Gm,L3} a_{G,L3} [h_{L3,G}(T^{I}_{Gm,L3} - \tilde{T}^{n+1}_{L3}) + h_{G,L3}(T^{I}_{Gm,L3} - \tilde{T}^{n+1}_{G})] . \tag{A-77}$$

The derivative of mass-transfer rates, Eq. (A-76), are given by

$$\Delta\Gamma^{I3}_{G,Lm} = \sum_{l=1}^{3} \Lambda x^{I3}_{GLm,l}\Delta\bar{\rho}_{Gl} + \Lambda x^{I3}_{GLm,4}\Delta e_{L3} + \Lambda x^{I3}_{GLm,5}\Delta T_G, \tag{A-78}$$

where

$$\Lambda x^{I3}_{GLm,l} = \Lambda R_{Gm,L3}\frac{\partial R_{Gm,L3}}{\partial\bar{\rho}_{Gl}} + (\Lambda T^{I}_{Gm,L3}\frac{\partial T^{I}_{Gm,L3}}{\partial\bar{\rho}_{Gl}} + \Lambda h_{Con,Gm}\frac{\partial h_{Con,Gm}}{\partial\bar{\rho}_{Gl}})\delta(m,l),$$

$$l = 1, 2 \text{ and } 3, \tag{A-79}$$

$$\Lambda x^{I3}_{GLm,4} = \Lambda T_{L3}\frac{\partial T_{L3}}{\partial e_{L3}}, \text{ and} \tag{A-80}$$

$$\Lambda x^{I3}_{GLm,5} = \Lambda R_{Gm,L3}\frac{\partial R_{Gm,L3}}{\partial T_G} + \Lambda T^{I}_{Gm,L3}\frac{\partial T^{I}_{Gm,L3}}{\partial T_G} + \Lambda T_G + \Lambda h_{Con,Gm}\frac{\partial h_{Con,Gm}}{\partial T_G}. \tag{A-81}$$

The expressions for intermediate variables, $\Lambda R_{Gm,L3}$, $\Lambda T^{I}_{Gm,L3}$, ΛT_{L3}, ΛT_G and $\Lambda h_{Con,Gm}$, in Eqs. (A-79) – (A-81) are given by

$$\Lambda R_{Gm,L3} = \frac{a_{G,L3}[h_{L3,G}(T^{I}_{Gm,L3} - \tilde{T}^{n+1}_{L3}) + h_{G,L3}(T^{I}_{Gm,L3} - \tilde{T}^{n+1}_{G})]}{h_{Con,Gm}} H(\Gamma^{I3}_{G,Lm}), \tag{A-82}$$

$$\Lambda T^{I}_{Gm,L3} = \frac{R_{Gm,L3}a_{G,L3}(h_{L3,G} + h_{G,L3})}{h_{Con,Gm}} H(\Gamma^{I3}_{G,Lm}), \tag{A-83}$$

$$\Lambda T_{L3} = -\frac{R_{Gm,L3}a_{G,L3}h_{L3,G}}{h_{Con,Gm}} H(\Gamma^{I3}_{G,Lm}), \tag{A-84}$$

$$\Lambda T_G = -\frac{R_{Gm,L3}a_{G,L3}h_{L3,G}}{h_{Con,Gm}} H(\Gamma^{I3}_{G,Lm}), \text{ and} \tag{A-85}$$

$$\Lambda h_{Con,Gm} = -\frac{\Gamma^{I3}_{G,Lm}}{h_{Con,Gm}}. \tag{A-86}$$

Vapor/Particle and Vapor/Structure interfaces: The mass-transfer rates are calculated by

$$\Gamma^{I(k)}_{G,Lm} = \frac{q^{I}_{Gm,K(k)}}{h_{Con,Gm}}, \qquad q^{I}_{Gm,K(k)} > 0, \text{ m} = 1, 2 \text{ and } 3, \text{ and k} = 1-6, \tag{A-87}$$

where

$$q^{I}_{Gm,K(k)} = R_{Gm,K(k)}a_{G,K(k)}[h_{K(k)}(T^{I}_{Gm,K(k)} - \tilde{T}^{n}_{K(k)}) + h_{G,K(k)}(T^{I}_{Gm,K(k)} - \tilde{T}^{n+1}_{G})]. \tag{A-88}$$

The derivative of mass-transfer rates, Eq. (A-87), are given by

$$\Delta\Gamma^{I(k)}_{G,Lm} = \sum_{l=1}^{3} \Lambda x^{I(k)}_{GLm,l}\Delta\bar{p}_{Gl} + \Lambda x^{I(k)}_{GLm,4}\Delta e_{L3} + \Lambda x^{I(k)}_{GLm,5}\Delta T_G, \tag{A-89}$$

where

$$\Lambda x^{I(k)}_{GLm,l} = \Lambda R_{Gm,K(k)}\frac{\partial R_{Gm,K(k)}}{\partial \bar{p}_{Gl}} + (\Lambda T^{I}_{Gm,K(k)}\frac{\partial T^{I}_{Gm,K(k)}}{\partial \bar{p}_{Gl}} + \Lambda h_{Con,Gm}\frac{\partial h_{Con,Gm}}{\partial \bar{p}_{Gl}})\delta(m,l),$$

$$l = 1, 2 \text{ and } 3, \tag{A-90}$$

$$\Lambda x^{I(k)}_{GLm,4} = 0, \text{ and} \tag{A-91}$$

$$\Lambda x^{I(k)}_{GLm,5} = \Lambda R_{Gm,K(k)}\frac{\partial R_{Gm,K(k)}}{\partial T_G} + \Lambda T^{I}_{Gm,K(k)}\frac{\partial T^{I}_{Gm,K(k)}}{\partial T_G} + \Lambda T_G + \Lambda h_{Con,Gm}\frac{\partial h_{Con.Gm}}{\partial T_G}. \tag{A-92}$$

The expressions for intermediate variables, $\Lambda R_{Gm,L3}$, $\Lambda T^{I}_{Gm,L3}$, ΛT_G and $\Lambda h_{Con,Gm}$, in Eqs. (A-90) and (A-92) are given by

$$\Lambda R_{Gm,K(k)} = \frac{a_{G,K(k)}[h_{K(k)}(T^{I}_{Gm,K(k)} - \tilde{T}^{n}_{K(k)}) + h_{G,K(k)}(T^{I}_{Gm,K(k)} - \tilde{T}^{n+1}_{G})]}{h_{Con,Gm}} H(\Gamma^{I(k)}_{G,Lm}), \tag{A-93}$$

$$\Lambda T^{I}_{Gm,K(k)} = \frac{R_{Gm,K(k)}a_{G,K(k)}(h_{K(k)} + h_{G,K(k)})}{h_{Con,Gm}} H(\Gamma^{I(k)}_{G,Lm}), \tag{A-94}$$

$$\Lambda T_G = -\frac{R_{Gm,K(k)}a_{G,K(k)}h_{K(k)}}{h_{Con,Gm}} H(\Gamma^{I(k)}_{G,Lm}), \text{ and} \tag{A-95}$$

$$\Lambda h_{Con,Gm} = -\frac{\Gamma^{I(k)}_{G,Lm}}{h_{Con,Gm}}. \tag{A-96}$$

Liquid-fuel/Liquid-steel interface: The mass-transfer rate is calculated by

$$\Gamma^{I7}_{L2,G} = -\frac{q^{I}_{L1,L2}}{h_{Vap,G2}}, \quad q^{I}_{L1,L2} < 0, \tag{A-97}$$

where

$$q^{I}_{L1,L2} = a_{L1,L2}[h_{L1,L2}(T^{I}_{L1,L2} - \tilde{T}^{n}_{L1}) + h_{L2,L1}(T^{I}_{L1,L2} - \tilde{T}^{n}_{L2})]. \tag{A-98}$$

The derivative of mass-transfer rate, Eq. (A-97), is given by

$$\Delta\Gamma^{I7}_{L2,G} = \sum_{l=1}^{3} \Lambda x^{I7}_{L2G,l}\Delta\bar{p}_{Gl} + \Lambda x^{I7}_{L2G,4}\Delta e_{L3} + \Lambda x^{I7}_{L2G,5}\Delta T_G, \tag{A-99}$$

where

$$\Lambda x^{I7}_{L2G,l} = (\Lambda T^{I}_{L1,L2}\frac{\partial T^{I}_{L1,L2}}{\partial \overline{\rho}_{Gl}} + \Lambda h_{Vap,G2}\frac{\partial h_{Vap,G2}}{\partial \overline{\rho}_{Gl}})\delta(2,l),\ l = 1, 2 \text{ and } 3, \tag{A-100}$$

$$\Lambda x^{I7}_{L2G,4} = 0, \text{ and} \tag{A-101}$$

$$\Lambda x^{I7}_{L2G,5} = \Lambda T^{I}_{L1,L2}\frac{\partial T^{I}_{L1,L2}}{\partial T_G} + \Lambda h_{Vap,G2}\frac{\partial h_{Vap,G2}}{\partial T_G}. \tag{A-102}$$

The expressions for intermediate variables, $\Lambda T^{I}_{L1,L2}$ and $\Lambda h_{Vap,G2}$, in Eqs. (A-100) and (A-102) are given by

$$\Lambda T^{I}_{L1,L2} = -\frac{a_{L1,L2}(h_{L1,L2} + h_{L2,L1})}{h_{Vap,G2}} H(\Gamma^{I7}_{L2,G}), \text{ and} \tag{A-103}$$

$$\Lambda h_{Vap,G2} = \frac{\Gamma^{I7}_{L2,G}}{h_{Vap,G2}}. \tag{A-104}$$

Liquid-fuel/Liquid-sodium interface: The mass-transfer rate is calculated by

$$\Gamma^{I8}_{L3,G} = -\frac{q^{I}_{L1,L3}}{h_{Vap,G3}}, \quad q^{I}_{L1,L3} < 0, \tag{A-105}$$

where

$$q^{I}_{L1,L3} = a_{L1,L3}[h_{L1,L3}(T^{I}_{L1,L3} - \tilde{T}^{n}_{L1}) + h_{L3,L1}(T^{I}_{L1,L3} - \tilde{T}^{n+1}_{L3})]. \tag{A-106}$$

The derivative of mass-transfer rate, Eq. (A-105), is given by

$$\Delta\Gamma^{I8}_{L3,G} = \sum_{l=1}^{3}\Lambda x^{I8}_{L3G,l}\Delta\overline{\rho}_{Gl} + \Lambda x^{I8}_{L3G,4}\Delta e_{L3} + \Lambda x^{I8}_{L3G,5}\Delta T_G, \tag{A-107}$$

where

$$\Lambda x^{I8}_{L3G,l} = (\Lambda T^{I}_{L1,L3}\frac{\partial T^{I}_{L1,L3}}{\partial \overline{\rho}_{Gl}} + \Lambda h_{Vap,G3}\frac{\partial h_{Vap,G3}}{\partial \overline{\rho}_{Gl}})\delta(l,3),\ l = 1, 2 \text{ and } 3, \tag{A-108}$$

$$\Lambda x^{I8}_{L3G,4} = \Lambda T_{L3}\frac{\partial T_{L3}}{\partial e_{L3}} + \Lambda h_{Vap,G3}\frac{\partial h_{Vap,G3}}{\partial e_{L3}}, \text{ and} \tag{A-109}$$

$$\Lambda x^{I8}_{L3G,5} = \Lambda T^{I}_{L1,L3}\frac{\partial T^{I}_{L1,L3}}{\partial T_G} + \Lambda h_{Vap,G3}\frac{\partial h_{Vap,G3}}{\partial T_G}. \tag{A-110}$$

The expressions for intermediate variables, $\Lambda T^{I}_{L1,L3}$, ΛT_{L3} and $\Lambda h_{Vap,G3}$, in Eqs. (A-108) – (A-110) are given by

$$\Lambda T^{\mathrm{I}}_{\mathrm{L1,L3}} = -\frac{a_{\mathrm{L1,L3}}(h_{\mathrm{L1,L3}} + h_{\mathrm{L3,L1}})}{h_{\mathrm{Vap,G3}}} H(\Gamma^{\mathrm{I8}}_{\mathrm{L3,G}}), \tag{A-111}$$

$$\Lambda T_{\mathrm{L3}} = \frac{a_{\mathrm{L1,L3}} h_{\mathrm{L3,L1}}}{h_{\mathrm{Vap,G3}}} H(\Gamma^{\mathrm{I8}}_{\mathrm{L3,G}}), \text{ and} \tag{A-112}$$

$$\Lambda h_{\mathrm{Vap,G3}} = \frac{\Gamma^{\mathrm{I8}}_{\mathrm{L3,G}}}{h_{\mathrm{Vap,G3}}}. \tag{A-113}$$

Liquid-steel/Liquid-sodium interface: The mass-transfer rate is calculated by

$$\Gamma^{\mathrm{I12}}_{\mathrm{L3,G}} = -\frac{q^{\mathrm{I}}_{\mathrm{L2,L3}}}{h_{\mathrm{Vap,G3}}}, \quad q^{\mathrm{I}}_{\mathrm{L2,L3}} < 0, \tag{A-114}$$

where

$$q^{\mathrm{I}}_{\mathrm{L2,L3}} = a_{\mathrm{L2,L3}}[h_{\mathrm{L2,L3}}(T^{\mathrm{I}}_{\mathrm{L2,L3}} - \tilde{T}^{\mathrm{n}}_{\mathrm{L2}}) + h_{\mathrm{L3,L2}}(T^{\mathrm{I}}_{\mathrm{L2,L3}} - \tilde{T}^{\mathrm{n+1}}_{\mathrm{L3}})]. \tag{A-115}$$

The derivative of mass-transfer rate, Eq. (A-114), is given by

$$\Delta\Gamma^{\mathrm{I12}}_{\mathrm{L3,G}} = \sum_{l=1}^{3} \Lambda x^{\mathrm{I12}}_{\mathrm{L3G},l} \Delta\bar{\rho}_{\mathrm{G}l} + \Lambda x^{\mathrm{I12}}_{\mathrm{L3G},4} \Delta e_{\mathrm{L3}} + \Lambda x^{\mathrm{I12}}_{\mathrm{L3G},5} \Delta T_{\mathrm{G}}, \tag{A-116}$$

where

$$\Lambda x^{\mathrm{I12}}_{\mathrm{L3G},l} = (\Lambda T^{\mathrm{I}}_{\mathrm{L2,L3}} \frac{\partial T^{\mathrm{I}}_{\mathrm{L2,L3}}}{\partial \bar{\rho}_{\mathrm{G}l}} + \Lambda h_{\mathrm{Vap,G3}} \frac{\partial h_{\mathrm{Vap,G3}}}{\partial \bar{\rho}_{\mathrm{G}l}}) \delta(l,3), \; l = 1, 2 \text{ and } 3, \tag{A-117}$$

$$\Lambda x^{\mathrm{I12}}_{\mathrm{L3G},4} = \Lambda T_{\mathrm{L3}} \frac{\partial T_{\mathrm{L3}}}{\partial e_{\mathrm{L3}}} + \Lambda h_{\mathrm{Vap,G3}} \frac{\partial h_{\mathrm{Vap,G3}}}{\partial e_{\mathrm{L3}}}, \text{ and} \tag{A-118}$$

$$\Lambda x^{\mathrm{I12}}_{\mathrm{L3G},5} = \Lambda T^{\mathrm{I}}_{\mathrm{L2,L3}} \frac{\partial T^{\mathrm{I}}_{\mathrm{L2,L3}}}{\partial T_{\mathrm{G}}} + \Lambda h_{\mathrm{Vap,G3}} \frac{\partial h_{\mathrm{Vap,G3}}}{\partial T_{\mathrm{G}}}. \tag{A-119}$$

The expressions for intermediate variables, $\Lambda T^{\mathrm{I}}_{\mathrm{L2,L3}}$, ΛT_{L3} and $\Lambda h_{\mathrm{Vap,G3}}$, in Eqs. (A-117) – (A-119) are given by

$$\Lambda T^{\mathrm{I}}_{\mathrm{L2,L3}} = -\frac{a_{\mathrm{L2,L3}}(h_{\mathrm{L2,L3}} + h_{\mathrm{L3,L2}})}{h_{\mathrm{Vap,G3}}} H(\Gamma^{\mathrm{I12}}_{\mathrm{L3,G}}), \tag{A-120}$$

$$\Lambda T_{\mathrm{L3}} = \frac{a_{\mathrm{L2,L3}} h_{\mathrm{L2,L3}}}{h_{\mathrm{Vap,G3}}} H(\Gamma^{\mathrm{I12}}_{\mathrm{L3,G}}), \text{ and} \tag{A-121}$$

$$\Lambda h_{\mathrm{Vap,G3}} = \frac{\Gamma^{\mathrm{I12}}_{\mathrm{L3,G}}}{h_{\mathrm{Vap,G3}}}. \tag{A-122}$$

A.2. Interface temperatures

Vapor/Liquid-fuel interface: The interface temperatures are calculated by

$$T^{I}_{G1,L1} = \tilde{T}^{n+1}_{Sat,G1}, \text{ and} \tag{A-123}$$

$$T^{I}_{G4,L1} = \frac{h_{L1,G}\tilde{T}^{n}_{L1} + h_{G,L1}\tilde{T}^{n+1}_{G}}{h_{L1,G} + h_{G,L1}}. \tag{A-124}$$

The derivatives of Eqs. (A-123) and (A-124) are given by

$$\frac{\partial T^{I}_{G1,L1}}{\partial \bar{\rho}_l} = \frac{\partial T_{Sat,G1}}{\partial \bar{\rho}_l}\delta(l,1),\ l = 1, 2 \text{ and } 3, \tag{A-125}$$

$$\frac{\partial T^{I}_{G1,L1}}{\partial T_G} = \frac{\partial T_{Sat,G1}}{\partial T_G}, \tag{A-126}$$

$$\frac{\partial T^{I}_{G4,L1}}{\partial \bar{\rho}_l} = 0,\ l = 1, 2 \text{ and } 3, \text{ and} \tag{A-127}$$

$$\frac{\partial T^{I}_{G4,L1}}{\partial T_G} = \frac{h_{G,L1}}{h_{L1,G} + h_{G,L1}}. \tag{A-128}$$

Vapor/Liquid-steel interface: The interface temperatures are calculated by

$$T^{I}_{G2,L2} = \tilde{T}^{n+1}_{Sat,G2}, \text{ and} \tag{A-129}$$

$$T^{I}_{G1,L2} = \max[\tilde{T}^{n+1}_{Sat,G1}, T_{GL2}], \tag{A-130}$$

where T_{GL2} is calculated by

$$T_{GL2} = \frac{h_{L2,G}\tilde{T}^{n}_{L2} + h_{G,L2}\tilde{T}^{n+1}_{G}}{h_{L2,G} + h_{G,L2}}. \tag{A-131}$$

The derivatives of Eqs. (A-129) and (A-130) are given by

$$\frac{\partial T^{I}_{G2,L2}}{\partial \bar{\rho}_l} = \frac{\partial T_{Sat,G2}}{\partial \bar{\rho}_l}\delta(l,2),\ l = 1, 2 \text{ and } 3, \tag{A-132}$$

$$\frac{\partial T^{I}_{G2,L2}}{\partial T_G} = \frac{\partial T_{Sat,G2}}{\partial T_G}, \tag{A-133}$$

$$\frac{\partial T^{I}_{G1,L2}}{\partial \bar{\rho}_l} = \frac{\partial T_{Sat,G1}}{\partial \bar{\rho}_l}\delta(l,1)H(\xi_{G1,L2}),\ l = 1, 2 \text{ and } 3, \tag{A-134}$$

$$\frac{\partial T^{I}_{G1,L2}}{\partial T_G} = \frac{\partial T_{Sat,G1}}{\partial T_G} H(\xi_{G1,L2}) + \frac{h_{G,L2}}{h_{L2,G} + h_{G,L2}} H(-\xi_{G1,L2}), \tag{A-135}$$

where $\xi_{G1,L2}$ is

$$\xi_{G1,L2} = \tilde{T}^{n+1}_{Sat,G1} - T_{GL2}. \tag{A-136}$$

Vapor/Liquid-sodium interface: The interface temperatures are calculated by

$$T^{I}_{G3,L3} = \tilde{T}^{n+1}_{Sat,G3}, \text{ and} \tag{A-137}$$

$$T^{I}_{Gm,L3} = \max[\tilde{T}^{n+1}_{Sat,Gm}, T_{GL3}], \text{ m} = 1 \text{ and } 2, \tag{A-138}$$

where T_{GL3} is calculated by

$$T_{GL3} = \frac{h_{L3,G}\tilde{T}^{n+1}_{L3} + h_{G,L3}\tilde{T}^{n+1}_{G}}{h_{L3,G} + h_{G,L3}}. \tag{A-139}$$

The derivatives of Eqs. (A-137) and (A-138) are given by

$$\frac{\partial T^{I}_{G3,L3}}{\partial \overline{\rho}_l} = \frac{\partial T_{Sat,G3}}{\partial \overline{\rho}_l} \delta(l,3), \; l = 1, 2 \text{ and } 3, \tag{A-140}$$

$$\frac{\partial T^{I}_{G3,L3}}{\partial e_{L3}} = 0, \tag{A-141}$$

$$\frac{\partial T^{I}_{G3,L3}}{\partial T_G} = \frac{\partial T_{Sat,G3}}{\partial T_G}, \tag{A-142}$$

$$\frac{\partial T^{I}_{Gm,L3}}{\partial \overline{\rho}_l} = \frac{\partial T_{Sat,Gm}}{\partial \overline{\rho}_l} \delta(l,\text{m}) H(\xi_{Gm,L3}), \; l = 1, 2 \text{ and } 3, \tag{A-143}$$

$$\frac{\partial T^{I}_{Gm,L3}}{\partial e_{L3}} = \frac{h_{L3,G}}{h_{L3,G} + h_{G,L3}} \frac{\partial T_{L3}}{\partial e_{L3}} H(-\xi_{Gm,L3}), \text{ and} \tag{A-144}$$

$$\frac{\partial T^{I}_{Gm,L3}}{\partial T_G} = \frac{\partial T_{Sat,Gm}}{\partial T_G} H(\xi_{Gm,L3}) + \frac{h_{G,L3}}{h_{L3,G} + h_{G,L3}} H(-\xi_{Gm,L3}), \tag{A-145}$$

where $\xi_{Gm,L3}$ is

$$\xi_{Gm,L3} = \tilde{T}^{n+1}_{Sat,Gm} - T_{GL3}. \tag{A-146}$$

Vapor/Particle and Vapor/Structure interfaces: The interface temperatures are calculated by

$$T^{I}_{Gm,K(k)} = \max[\tilde{T}^{n+1}_{Sat,Gm}, T_{GK(k)}], \text{ and} \tag{A-147}$$

$$T^{I}_{G4,K(k)} = T_{GK(k)}, \tag{A-148}$$

where k = 1 – 6 and $T_{GK(k)}$ is calculated by

$$T_{GK(k)} = \frac{h_{K(k)}\tilde{T}^{n}_{K(k)} + h_{G,K(k)}\tilde{T}^{n+1}_{G}}{h_{K(k)} + h_{G,K(k)}}. \tag{A-149}$$

The derivatives of Eqs. (A-147) and (A-148) are given by

$$\frac{\partial T^{I}_{Gm,K(k)}}{\partial \overline{\rho}_l} = \frac{\partial T_{Sat,Gm}}{\partial \overline{\rho}_l}\delta(l,\mathrm{m})H(\xi_{Gm,K(k)}),\ l = 1, 2 \text{ and } 3, \tag{A-150}$$

$$\frac{\partial T^{I}_{Gm,K(k)}}{\partial T_G} = \frac{\partial T_{Sat,Gm}}{\partial T_G}H(\xi_{Gm,K(k)}) + \frac{h_{G,K(k)}}{h_{K(k)} + h_{G,K(k)}}H(-\xi_{Gm,K(k)}), \tag{A-151}$$

$$\frac{\partial T^{I}_{G4,K(k)}}{\partial \overline{\rho}_l} = 0, \text{ and} \tag{A-152}$$

$$\frac{\partial T^{I}_{G4,K(k)}}{\partial T_G} = \frac{h_{G,K(k)}}{h_{K(k)} + h_{G,K(k)}}, \tag{A-153}$$

where $\xi_{Gm,K(k)}$ is

$$\xi_{Gm,K(k)} = \tilde{T}^{n+1}_{Sat,Gm} - T_{GK(k)}. \tag{A-154}$$

Liquid-fuel/Liquid-steel interface: The interface temperature is calculated by

$$T^{I}_{L1,L2} = \max[\tilde{T}^{n+1}_{Sat,G2}, T_{L1L2}], \tag{A-155}$$

where T_{L1L2} is calculated by

$$T_{L1L2} = \frac{h_{L1,L2}\tilde{T}^{n}_{L1} + h_{L2,L1}\tilde{T}^{n}_{L2}}{h_{L1,L2} + h_{L2,L1}}. \tag{A-156}$$

The derivative of Eq. (A-155) is given by

$$\frac{\partial T^{I}_{L1,L2}}{\partial \overline{\rho}_l} = \frac{\partial T_{Sat,G2}}{\partial \overline{\rho}_l}\delta(l,2)H(\xi_{L1,L2}),\ l = 1, 2 \text{ and } 3, \text{ and} \tag{A-157}$$

$$\frac{\partial T^{I}_{L1,L2}}{\partial T_G} = \frac{\partial T_{Sat,G2}}{\partial T_G}H(\xi_{L1,L2}), \tag{A-158}$$

where $\xi_{L1,L2}$ is

$$\xi_{L1,L2} = \tilde{T}^{n+1}_{Sat,G2} - T_{L1L2}. \tag{A-159}$$

Liquid-fuel/Liquid-sodium interface: The interface temperature is calculated by

$$T^{I}_{L1,L3} = \max[\tilde{T}^{n+1}_{Sat,G3}, T_{L1L3}], \tag{A-160}$$

where T_{L1L3} is calculated by

$$T_{L1L3} = \frac{h_{L1,L3}\tilde{T}^{n}_{L1} + h_{L3,L1}\tilde{T}^{n+1}_{L3}}{h_{L1,L3} + h_{L3,L1}}. \tag{A-161}$$

The derivative of Eq. (A-160) is given by

$$\frac{\partial T^{I}_{L1,L3}}{\partial \overline{\rho}_l} = \frac{\partial T_{Sat,G3}}{\partial \overline{\rho}_l}\delta(l,3)H(\xi_{L1,L3}),\ l = 1, 2 \text{ and } 3, \tag{A-162}$$

$$\frac{\partial T^{I}_{L1,L3}}{\partial e_{L3}} = \frac{h_{L3,L1}}{h_{L1,L3} + h_{L3,L1}}\frac{\partial T_{L3}}{\partial e_{L3}}H(-\xi_{L1,L3}), \text{ and} \tag{A-163}$$

$$\frac{\partial T^{I}_{L1,L3}}{\partial T_G} = \frac{\partial T_{Sat,G3}}{\partial T_G}H(\xi_{L1,L3}), \tag{A-164}$$

where $\xi_{L1,L3}$ is

$$\xi_{L1,L3} = \tilde{T}^{n+1}_{Sat,G3} - T_{L1L3}. \tag{A-165}$$

Liquid-steel/Liquid-sodium interface: The interface temperature is calculated by

$$T^{I}_{L2,L3} = \max[\tilde{T}^{n+1}_{Sat,G3}, T_{L2L3}], \tag{A-166}$$

where T_{L2L3} is calculated by

$$T_{L2L3} = \frac{h_{L2,L3}\tilde{T}^{n}_{L2} + h_{L3,L2}\tilde{T}^{n+1}_{L3}}{h_{L2,L3} + h_{L3,L2}}. \tag{A-167}$$

The derivative of Eq. (A-166) is given by

$$\frac{\partial T^{I}_{L2,L3}}{\partial \overline{\rho}_l} = \frac{\partial T_{Sat,G3}}{\partial \overline{\rho}_l}\delta(l,3)H(\xi_{L2,L3}), \tag{A-168}$$

$$\frac{\partial T^{I}_{L2,L3}}{\partial e_{L3}} = \frac{h_{L3,L2}}{h_{L2,L3} + h_{L3,L2}}\frac{\partial T_{L3}}{\partial e_{L3}}H(-\xi_{L2,L3}), \text{ and} \tag{A-169}$$

$$\frac{\partial T^{I}_{L2,L3}}{\partial T_G} = \frac{\partial T_{Sat,G3}}{\partial T_G}H(\xi_{L2,L3}), \tag{A-170}$$

where $\xi_{L2,L3}$ is

$$\xi_{L2,L3} = \tilde{T}^{n+1}_{Sat,G3} - T_{L2L3}. \tag{A-171}$$

A.3. Interface fractions

The following quantities are defined:

$$R_{Gm} = \frac{\tilde{p}_{Gm}^{n+1}}{p_G^*}, \text{ m = 1, 2 and 3, and} \tag{A-172}$$

$$R_{G4} = \frac{p_{G4}^*}{p_G^*}, \tag{A-173}$$

where p_{G4}^* and p_G^* are calculated by

$$p_{G4}^* = f_{G4,L}\tilde{p}_{G4}^{n+1}, \text{ and} \tag{A-174}$$

$$p_G^* = \sum_{m=1}^{3}\tilde{p}_{Gm}^{n+1} + p_{G4}^*. \tag{A-175}$$

The derivatives of Eqs. (A-172) and (A-173) are given by

$$\frac{\partial R_{Gm}}{\partial \bar{\rho}_l} = \frac{1}{(p_G^*)^2}\frac{\partial p_{GL}}{\partial \bar{\rho}_l}\left[p_G^*\delta(m,l) - \tilde{p}_{Gm}^{n+1}\right], \; l = 1, 2 \text{ and } 3, \tag{A-176}$$

$$\frac{\partial R_{G4}}{\partial \bar{\rho}_l} = -\frac{p_{G4}^*}{(p_G^*)^2}\frac{\partial p_{GL}}{\partial \bar{\rho}_l}, \; l = 1, 2 \text{ and } 3, \tag{A-177}$$

$$\frac{\partial R_{Gm}}{\partial T_G} = \frac{1}{(p_G^*)^2}\left(p_G^*\frac{\partial p_{Gm}}{\partial T_G} - \tilde{p}_{Gm}^{n+1}\frac{\partial p_G^*}{\partial T_G}\right), \text{ and} \tag{A-178}$$

$$\frac{\partial R_{G4}}{\partial T_G} = \frac{1}{(p_G^*)^2}\left(p_G^*\frac{\partial p_{G4}^*}{\partial T_G} - p_{G4}^*\frac{\partial p_G^*}{\partial T_G}\right), \tag{A-179}$$

where

$$\frac{\partial p_{G4}^*}{\partial T_G} = f_{G4,L}\frac{\partial p_{G4}}{\partial T_G}, \text{ and} \tag{A-180}$$

$$\frac{\partial p_G^*}{\partial T_G} = \sum_{m=1}^{3}\frac{\partial p_{Gm}}{\partial T_G} + \frac{\partial p_{G4}^*}{\partial T_G}. \tag{A-181}$$

Vapor/Liquid-fuel interface: The interface fractions are calculated by

$$R_{G4,L1} = \min\left[\frac{p_{G4}^*}{p_G^*}, R_{GL,\max}\right], \text{ and} \tag{A-182}$$

$$R_{Gl,L1} = 1 - R_{G4,L1}. \tag{A-183}$$

The derivatives of Eqs. (A-182) and (A-183) are given by

$$\frac{\partial R_{G4,L1}}{\partial \overline{\rho}_l} = H(\xi_{G4,L1})\frac{\partial R_{G4}}{\partial \overline{\rho}_l},\ l = 1,\ 2 \text{ and } 3, \tag{A-184}$$

$$\frac{\partial R_{G4,L1}}{\partial T_G} = H(\xi_{G4,L1})\frac{\partial R_{G4}}{\partial T_G}, \tag{A-185}$$

$$\frac{\partial R_{G1,L1}}{\partial \overline{\rho}_l} = -\frac{\partial R_{G4,L1}}{\partial \overline{\rho}_l},\ l = 1,\ 2 \text{ and } 3, \text{ and} \tag{A-186}$$

$$\frac{\partial R_{G1,L1}}{\partial T_G} = -\frac{\partial R_{G4,L1}}{\partial T_G}, \tag{A-187}$$

where $\xi_{G4,L1}$ is

$$\xi_{G4,L1} = R_{GL,max} - \frac{p^*_{G4}}{p^*_G}. \tag{A-188}$$

Vapor/Liquid-steel interface: The interface fractions are calculated by

$$R_{G1,L2} = \min\left[\frac{\tilde{p}^{n+1}_{G1}}{p^*_G}, R_{GL,max}\frac{\tilde{p}^{n+1}_{G1}}{\tilde{p}^{n+1}_{G1} + p^*_{G4}}\right], \tag{A-189}$$

$$R_{G4,L2} = \min\left[\frac{p^*_{G4}}{p^*_G}, R_{GL,max}\frac{p^*_{G4}}{\tilde{p}^{n+1}_{G1} + p^*_{G4}}\right], \text{ and} \tag{A-190}$$

$$R_{G2,L2} = 1 - R_{G1,L2} - R_{G4,L2}. \tag{A-191}$$

The derivatives of Eqs. (A-189) – (A-191) are given by

$$\frac{\partial R_{G1,L2}}{\partial \overline{\rho}_{Gl}} = H(\xi_{G1,L2})\frac{\partial R_{G1}}{\partial \overline{\rho}_{Gl}}$$

$$+H(-\xi_{G1,L2})R_{GL,max}\frac{p^*_{G4}}{(\tilde{p}^{n+1}_{G1} + p^*_{G4})^2}\frac{\partial p_{G1}}{\partial \overline{\rho}_{Gl}}\delta(l,1),\ l = 1,\ 2 \text{ and } 3, \tag{A-192}$$

$$\frac{\partial R_{G1,L2}}{\partial T_G} = H(\xi_{G1,L2})\frac{\partial R_{G1}}{\partial T_G}$$

$$+H(-\xi_{G1,L2})R_{GL,max}\frac{1}{(\tilde{p}^{n+1}_{G1} + p^*_{G4})^2}\left(p^*_{G4}\frac{\partial p_{G1}}{\partial T_G} - \tilde{p}^{n+1}_{G1}\frac{\partial p^*_{G4}}{\partial T_G}\right), \tag{A-193}$$

$$\frac{\partial R_{G4,L2}}{\partial \overline{\rho}_{Gl}} = H(\xi_{G4,L2})\frac{\partial R_{G4}}{\partial \overline{\rho}_{Gl}}$$

$$+H(-\xi_{G4,L2})R_{GL,max}\frac{p^*_{G4}}{(\tilde{p}^{n+1}_{G1} + p^*_{G4})^2}\frac{\partial p_{G1}}{\partial \overline{\rho}_{Gl}}\delta(l,1),\ l = 1,\ 2 \text{ and } 3, \tag{A-194}$$

$$\frac{\partial R_{G4,L2}}{\partial T_G} = H(\xi_{G4,L2})\frac{\partial R_{G4}}{\partial T_G}$$

$$+H(-\xi_{G4,L2})R_{GL,max}\frac{1}{(\tilde{p}_{G1}^{n+1}+p_{G4}^{*})^2}\left(\frac{\partial p_{G4}^{*}}{\partial T_G}-p_{G4}^{*}\frac{\partial p_{G1}}{\partial T_G}\right), \quad \text{(A-195)}$$

$$\frac{\partial R_{G2,L2}}{\partial \bar{\rho}_{Gl}} = -\frac{\partial R_{G1,L2}}{\partial \bar{\rho}_{Gl}} - \frac{\partial R_{G4,L2}}{\partial \bar{\rho}_{Gl}}, \; l = 1, 2 \text{ and } 3, \text{ and} \quad \text{(A-196)}$$

$$\frac{\partial R_{G2,L2}}{\partial T_G} = -\frac{\partial R_{G1,L2}}{\partial T_G} - \frac{\partial R_{G4,L2}}{\partial T_G}, \quad \text{(A-197)}$$

where $\xi_{G1,L2}$ and $\xi_{G4,L2}$ are

$$\xi_{G1,L2} = R_{GL,max}\frac{\tilde{p}_{G1}^{n+1}}{\tilde{p}_{G1}^{n+1}+p_{G4}^{*}} - R_{G1}, \text{ and} \quad \text{(A-198)}$$

$$\xi_{G4,L2} = R_{GL,max}\frac{p_{G4}^{*}}{\tilde{p}_{G1}^{n+1}+p_{G4}^{*}} - R_{G4}. \quad \text{(A-199)}$$

Vapor/Liquid-sodium interface: The interface fractions are calculated by

$$R_{G1,L3} = \min\left[\frac{\tilde{p}_{G1}^{n+1}}{p_G^{*}}, R_{GL,max}\frac{\tilde{p}_{G1}^{n+1}}{\tilde{p}_{G1}^{n+1}+\tilde{p}_{G2}^{n+1}+p_{G4}^{*}}\right], \quad \text{(A-200)}$$

$$R_{G2,L3} = \min\left[\frac{\tilde{p}_{G2}^{n+1}}{p_G^{*}}, R_{GL,max}\frac{\tilde{p}_{G2}^{n+1}}{\tilde{p}_{G1}^{n+1}+\tilde{p}_{G2}^{n+1}+p_{G4}^{*}}\right], \quad \text{(A-201)}$$

$$R_{G4,L3} = \min\left[\frac{p_{G4}^{*}}{p_G^{*}}, R_{GL,max}\frac{p_{G4}^{*}}{\tilde{p}_{G1}^{n+1}+\tilde{p}_{G2}^{n+1}+p_{G4}^{*}}\right], \text{ and} \quad \text{(A-202)}$$

$$R_{G3,L3} = 1 - R_{G1,L3} - R_{G2,L3} - R_{G4,L3}. \quad \text{(A-203)}$$

The derivatives of Eqs. (A-200) – (A-203) are given by

$$\frac{\partial R_{G1,L3}}{\partial \bar{\rho}_{G1}} = H(\xi_{G1,L3})\frac{\partial R_{G1}}{\partial \bar{\rho}_{G1}} + H(-\xi_{G1,L3})R_{GL,max}\frac{\tilde{p}_{G2}^{n+1}+p_{G4}^{*}}{(\tilde{p}_{G1}^{n+1}+\tilde{p}_{G2}^{n+1}+p_{G4}^{*})^2}\frac{\partial p_{G1}}{\partial \bar{\rho}_{G1}}, \quad \text{(A-204)}$$

$$\frac{\partial R_{G1,L3}}{\partial \bar{\rho}_{G2}} = H(\xi_{G1,L3})\frac{\partial R_{G1}}{\partial \bar{\rho}_{G2}} - H(-\xi_{G1,L3})R_{GL,max}\frac{\tilde{p}_{G1}^{n+1}}{(\tilde{p}_{G1}^{n+1}+\tilde{p}_{G2}^{n+1}+p_{G4}^{*})^2}\frac{\partial p_{G2}}{\partial \bar{\rho}_{G2}}, \quad \text{(A-205)}$$

$$\frac{\partial R_{G1,L3}}{\partial \bar{\rho}_{G3}} = H(\xi_{G1,L3})\frac{\partial R_{G1}}{\partial \bar{\rho}_{G3}}, \quad \text{(A-206)}$$

$$\frac{\partial R_{G1,L3}}{\partial T_G} = H(\xi_{G1,L3})\frac{\partial R_{G1}}{\partial T_G} + H(-\xi_{G1,L3})R_{GL,max}\frac{1}{(\tilde{p}_{G1}^{n+1}+\tilde{p}_{G2}^{n+1}+p_{G4}^{*})^2}$$

$$\left[(\tilde{p}_{G2}^{n+1}+p_{G4}^{*})\frac{\partial p_{G1}}{\partial T_G}-\tilde{p}_{G1}^{n+1}\left(\frac{\partial p_{G2}}{\partial T_G}+\frac{\partial p_{G4}^{*}}{\partial T_G}\right)\right], \tag{A-207}$$

$$\frac{\partial R_{G2,L3}}{\partial \overline{\rho}_{G1}}=H(\xi_{G2,L3})\frac{\partial R_{G2}}{\partial \overline{\rho}_{G1}}+H(-\xi_{G2,L3})R_{GL,max}\frac{\tilde{p}_{G2}^{n+1}}{(\tilde{p}_{G1}^{n+1}+\tilde{p}_{G2}^{n+1}+p_{G4}^{*})^2}\frac{\partial p_{G1}}{\partial \overline{\rho}_{G1}}, \tag{A-208}$$

$$\frac{\partial R_{G2,L3}}{\partial \overline{\rho}_{G2}}=H(\xi_{G2,L3})\frac{\partial R_{G2}}{\partial \overline{\rho}_{G2}}+H(-\xi_{G2,L3})R_{GL,max}\frac{\tilde{p}_{G1}^{n+1}+p_{G4}^{*}}{(\tilde{p}_{G1}^{n+1}+\tilde{p}_{G2}^{n+1}+p_{G4}^{*})^2}\frac{\partial p_{G2}}{\partial \overline{\rho}_{G2}}, \tag{A-209}$$

$$\frac{\partial R_{G2,L3}}{\partial \overline{\rho}_{G3}}=H(\xi_{G2,L3})\frac{\partial R_{G2}}{\partial \overline{\rho}_{G3}}, \tag{A-210}$$

$$\frac{\partial R_{G2,L3}}{\partial T_G}=H(\xi_{G2,L3})\frac{\partial R_{G2}}{\partial T_G}+H(-\xi_{G2,L3})R_{GL,max}\frac{1}{(\tilde{p}_{G1}^{n+1}+\tilde{p}_{G2}^{n+1}+p_{G4}^{*})^2}$$

$$\left[(\tilde{p}_{G1}^{n+1}+p_{G4}^{*})\frac{\partial p_{G2}}{\partial T_G}-\tilde{p}_{G2}^{n+1}\left(\frac{\partial p_{G1}}{\partial T_G}+\frac{\partial p_{G4}^{*}}{\partial T_G}\right)\right], \tag{A-211}$$

$$\frac{\partial R_{G3,L3}}{\partial \overline{\rho}_l}=-\frac{\partial R_{G1,L3}}{\partial \overline{\rho}_l}-\frac{\partial R_{G2,L3}}{\partial \overline{\rho}_l}-\frac{\partial R_{G4,L3}}{\partial \overline{\rho}_l},\ l=1,\ 2\ \text{and}\ 3,\ \text{and} \tag{A-212}$$

$$\frac{\partial R_{G3,L3}}{\partial T_G}=-\frac{\partial R_{G1,L3}}{\partial T_G}-\frac{\partial R_{G2,L3}}{\partial T_G}-\frac{\partial R_{G4,L3}}{\partial T_G}, \tag{A-213}$$

where $\xi_{G1,L3}$, $\xi_{G2,L3}$ and $\xi_{G4,L3}$ are

$$\xi_{G1,L3}=R_{GL,max}\frac{\tilde{p}_{G1}^{n+1}}{\tilde{p}_{G1}^{n+1}+\tilde{p}_{G2}^{n+1}+p_{G4}^{*}}-R_{G1}, \tag{A-214}$$

$$\xi_{G2,L3}=R_{GL,max}\frac{\tilde{p}_{G2}^{n+1}}{\tilde{p}_{G1}^{n+1}+\tilde{p}_{G2}^{n+1}+p_{G4}^{*}}-R_{G2},\ \text{and} \tag{A-215}$$

$$\xi_{G4,L3}=R_{GL,max}\frac{p_{G4}^{*}}{\tilde{p}_{G1}^{n+1}+\tilde{p}_{G2}^{n+1}+p_{G4}^{*}}-R_{G4}. \tag{A-216}$$

Vapor/Particle and Vapor/Structure interfaces: The interface fractions are calculated by

$$R_{Gm,K(k)}=R_{Gm},\ \text{m}=1,\ 2,\ 3\ \text{and}\ 4,\ \text{and}\ \text{k}=1-6. \tag{A-217}$$

The derivative of Eq. (A-217) are given by

$$\frac{\partial R_{Gm,K(k)}}{\partial \overline{\rho}_l}=\frac{\partial R_{Gm}}{\partial \overline{\rho}_l},\ l=1,\ 2\ \text{and}\ 3,\ \text{and} \tag{A-218}$$

$$\frac{\partial R_{Gm,K(k)}}{\partial T_G}=\frac{\partial R_{Gm}}{\partial T_G}. \tag{A-219}$$

A.4. Effective latent heats

The effective heats of vaporization, $h_{Vap,Gm}$, are calculated by

$$h_{Vap,Gm} = i^*_{Vap,Gm} - \tilde{e}^n_{Lm}, \text{ m = 1 and 2, and} \quad \text{(A-220)}$$

$$h_{Vap,G3} = i^*_{Vap,G3} - \tilde{e}^{n+1}_{L3}, \quad \text{(A-221)}$$

where $i^*_{Vap,Gm}$ is given by

$$i^*_{Vap,Gm} = \tilde{e}^n_{Lm} + \max[\tilde{i}^{n+1}_{Vap,Gm} - \tilde{e}^n_{Lm}, h_{lg,min}], \text{ m = 1 and 2, and} \quad \text{(A-222)}$$

$$i^*_{Vap,G3} = \tilde{e}^{n+1}_{L3} + \max[\tilde{i}^{n+1}_{Vap,G3} - \tilde{e}^{n+1}_{L3}, h_{lg,min}]. \quad \text{(A-223)}$$

The derivatives of Eqs. (A-220) and (A-221) are expressed by

$$\frac{\partial h_{Vap,Gm}}{\partial \overline{\rho}_l} = \frac{\partial i^*_{Vap,Gm}}{\partial \overline{\rho}_l} \delta(m,l), \text{ m = 1, 2 and 3, and } l \text{ = 1, 2 and 3,} \quad \text{(A-224)}$$

$$\frac{\partial h_{Vap,G3}}{\partial e_{L3}} = \frac{\partial i^*_{Vap,G3}}{\partial e_{L3}} + 1, \text{ and} \quad \text{(A-225)}$$

$$\frac{\partial h_{Vap,Gm}}{\partial T_G} = \frac{\partial i^*_{Vap,Gm}}{\partial T_G}, \text{ m = 1, 2 and 3.} \quad \text{(A-226)}$$

The derivatives of $i^*_{Vap,Gm}$ are given by

$$\frac{\partial i^*_{Vap,Gm}}{\partial \overline{\rho}_{Gm}} = \frac{\partial i_{Vap,Gm}}{\partial \overline{\rho}_{Gm}} H(\xi_{Vap,Gm}), \text{ m = 1, 2 and 3,} \quad \text{(A-227)}$$

$$\frac{\partial i^*_{Vap,G3}}{\partial e_{L3}} = H(-\xi_{Vap,G3}), \text{ and} \quad \text{(A-228)}$$

$$\frac{\partial i^*_{Vap,Gm}}{\partial T_G} = \frac{\partial i_{Vap,Gm}}{\partial T_G} H(\xi_{Vap,Gm}), \text{ m = 1, 2 and 3,} \quad \text{(A-229)}$$

where $\xi_{Vap,Gm}$ is

$$\xi_{Vap,Gm} = (\tilde{i}^{n+1}_{Vap,Gm} - \tilde{e}^{n+1}_{Lm}) - h_{lg,min}. \quad \text{(A-230)}$$

The effective heats of condensation, $h_{Con,Gm}$, are calculated by

$$h_{Con,Gm} = \tilde{i}^{n+1}_{Gm} - i^*_{Con,Gm}, \text{ m = 1, 2 and 3,} \quad \text{(A-231)}$$

where $i^*_{Con,Gm}$ is

$$i^{*}_{\mathrm{Con,Gm}} = \tilde{i}^{\,n+1}_{\mathrm{Gm}} - \max[\tilde{i}^{\,n+1}_{\mathrm{Gm}} - \tilde{i}^{\,n+1}_{\mathrm{Con,Gm}}, h_{\mathrm{lg,min}}]. \quad \text{(A-232)}$$

The derivatives of Eq. (A-231) are expressed by

$$\frac{\partial h_{\mathrm{Con,Gm}}}{\partial \overline{\rho}_l} = \left(\frac{\partial i_{\mathrm{Gm}}}{\partial \overline{\rho}_l} - \frac{\partial i^{*}_{\mathrm{Con,Gm}}}{\partial \overline{\rho}_l} \right) \delta(\mathrm{m},l)\text{, m = 1, 2 and 3, and } l = 1, 2 \text{ and } 3, \text{ and} \quad \text{(A-233)}$$

$$\frac{\partial h_{\mathrm{Con,Gm}}}{\partial T_{\mathrm{G}}} = \frac{\partial i_{\mathrm{Gm}}}{\partial T_{\mathrm{G}}} - \frac{\partial i^{*}_{\mathrm{Con,Gm}}}{\partial T_{\mathrm{G}}}. \quad \text{(A-234)}$$

The derivatives of $i^{*}_{\mathrm{Con,Gm}}$ are given by

$$\frac{\partial i^{*}_{\mathrm{Con,Gm}}}{\partial \overline{\rho}_{\mathrm{Gm}}} = \frac{\partial i_{\mathrm{Con,Gm}}}{\partial \overline{\rho}_{\mathrm{Gm}}} H(\xi_{\mathrm{Con,Gm}}) + \frac{\partial i_{\mathrm{Gm}}}{\partial \overline{\rho}_{\mathrm{Gm}}} H(-\xi_{\mathrm{Con,Gm}}), \text{ and} \quad \text{(A-235)}$$

$$\frac{\partial i^{*}_{\mathrm{Con,Gm}}}{\partial T_{\mathrm{G}}} = \frac{\partial i_{\mathrm{Con,Gm}}}{\partial T_{\mathrm{G}}} H(\xi_{\mathrm{Con,Gm}}) + \frac{\partial i_{\mathrm{Gm}}}{\partial T_{\mathrm{G}}} H(-\xi_{\mathrm{Con,Gm}}), \quad \text{(A-236)}$$

where $\xi_{\mathrm{Con,Gm}}$ is

$$\xi_{\mathrm{Con,Gm}} = (i_{\mathrm{Gm}} - i_{\mathrm{Con,Gm}}) - h_{\mathrm{lg,min}}. \quad \text{(A-237)}$$

A.5. EOS variables

The saturation temperature is defined as a function of the vapor partial pressure. Its derivatives are

$$\frac{\partial T_{\mathrm{Sat,Gm}}}{\partial \overline{\rho}_{\mathrm{Gm}}} = \frac{\partial p_{\mathrm{Gm}}}{\partial \overline{\rho}_{\mathrm{Gm}}} \frac{\partial T_{\mathrm{Sat,Gm}}}{\partial p_{\mathrm{Gm}}}, \text{ and} \quad \text{(A-238)}$$

$$\frac{\partial T_{\mathrm{Sat,Gm}}}{\partial T_{\mathrm{G}}} = \frac{\partial p_{\mathrm{Gm}}}{\partial T_{\mathrm{G}}} \frac{\partial T_{\mathrm{Sat,Gm}}}{\partial p_{\mathrm{Gm}}}, \quad \text{(A-239)}$$

where m = 1, 2 and 3.

The condensate enthalpies are defined by

$$i_{\mathrm{Con,Gm}} = e_{\mathrm{Con,Gm}} + p_{\mathrm{Gm}} v_{\mathrm{Con,Gm}}\text{, m = 1, 2 and 3} \quad \text{(A-240)}$$

where $e_{\mathrm{Con,Gm}}$ and $v_{\mathrm{Con,Gm}}$ are defined as a function of saturation temperature. The derivatives of $i_{\mathrm{Con,Gm}}$ are

$$\frac{\partial i_{\mathrm{Con,Gm}}}{\partial \overline{\rho}_{\mathrm{Gm}}} = \frac{\partial T_{\mathrm{Sat,Gm}}}{\partial \overline{\rho}_{\mathrm{Gm}}} \frac{\partial e_{\mathrm{Con,Gm}}}{\partial T_{\mathrm{Sat,Gm}}} + v_{\mathrm{Con,Gm}} \frac{\partial p_{\mathrm{Gm}}}{\partial \overline{\rho}_{\mathrm{Gm}}} + p_{\mathrm{Gm}} \frac{\partial T_{\mathrm{Sat,Gm}}}{\partial \overline{\rho}_{\mathrm{Gm}}} \frac{\partial v_{\mathrm{Con,Gm}}}{\partial T_{\mathrm{Sat,Gm}}}, \text{ and} \quad \text{(A-241)}$$

$$\frac{\partial i_{\mathrm{Con,Gm}}}{\partial T_{\mathrm{G}}} = \frac{\partial T_{\mathrm{Sat,Gm}}}{\partial T_{\mathrm{G}}} \frac{\partial e_{\mathrm{Con,Gm}}}{\partial T_{\mathrm{Sat,Gm}}} + \upsilon_{\mathrm{Con,Gm}} \frac{\partial p_{\mathrm{Gm}}}{\partial T_{\mathrm{G}}} + p_{\mathrm{Gm}} \frac{\partial T_{\mathrm{Sat,Gm}}}{\partial T_{\mathrm{G}}} \frac{\partial \upsilon_{\mathrm{Con,Gm}}}{\partial T_{\mathrm{Sat,Gm}}}. \tag{A-242}$$

The vaporization enthalpies are defined by

$$i_{\mathrm{Vap,Gm}} = e_{\mathrm{Vap,Gm}} + p_{\mathrm{Gm}} \upsilon_{\mathrm{Vap,Gm}}, \ \mathrm{m} = 1, 2 \text{ and } 3, \tag{A-243}$$

where $e_{\mathrm{Vap,Gm}}$ and $\upsilon_{\mathrm{Vap,Gm}}$ are defined as a function of saturation temperature. The derivatives of $i_{\mathrm{Vap,Gm}}$ are

$$\frac{\partial i_{\mathrm{Vap,Gm}}}{\partial \overline{\rho}_{\mathrm{Gm}}} = \frac{\partial T_{\mathrm{Sat,Gm}}}{\partial \overline{\rho}_{\mathrm{Gm}}} \frac{\partial e_{\mathrm{Vap,Gm}}}{\partial T_{\mathrm{Sat,Gm}}} + \upsilon_{\mathrm{Vap,Gm}} \frac{\partial p_{\mathrm{Gm}}}{\partial \overline{\rho}_{\mathrm{Gm}}} + p_{\mathrm{Gm}} \frac{\partial T_{\mathrm{Sat,Gm}}}{\partial \overline{\rho}_{\mathrm{Gm}}} \frac{\partial \upsilon_{\mathrm{Vap,Gm}}}{\partial T_{\mathrm{Sat,Gm}}}, \text{ and} \tag{A-244}$$

$$\frac{\partial i_{\mathrm{Vap,Gm}}}{\partial T_{\mathrm{G}}} = \frac{\partial T_{\mathrm{Sat,Gm}}}{\partial T_{\mathrm{G}}} \frac{\partial e_{\mathrm{Vap,Gm}}}{\partial T_{\mathrm{Sat,Gm}}} + \upsilon_{\mathrm{Vap,Gm}} \frac{\partial p_{\mathrm{Gm}}}{\partial T_{\mathrm{G}}} + p_{\mathrm{Gm}} \frac{\partial T_{\mathrm{Sat,Gm}}}{\partial T_{\mathrm{G}}} \frac{\partial \upsilon_{\mathrm{Vap,Gm}}}{\partial T_{\mathrm{Sat,Gm}}}. \tag{A-245}$$

The vapor enthalpies are defined by

$$i_{\mathrm{Gm}} = e_{\mathrm{Gm}} + p_{\mathrm{Gm}} \upsilon_{\mathrm{Gm}}, \ \mathrm{m} = 1, 2 \text{ and } 3. \tag{A-246}$$

The derivatives of i_{Gm} are

$$\frac{\partial i_{\mathrm{Gm}}}{\partial \overline{\rho}_{\mathrm{Gm}}} = \frac{\partial e_{\mathrm{Gm}}}{\partial \overline{\rho}_{\mathrm{Gm}}} + \upsilon_{\mathrm{Gm}} \frac{\partial p_{\mathrm{Gm}}}{\partial \overline{\rho}_{\mathrm{Gm}}} - p_{\mathrm{Gm}} \frac{\alpha_{\mathrm{ge}}}{(\overline{\rho}_{\mathrm{Gm}})^2}, \text{ and} \tag{A-247}$$

$$\frac{\partial i_{\mathrm{Gm}}}{\partial T_{\mathrm{G}}} = \frac{\partial e_{\mathrm{Gm}}}{\partial T_{\mathrm{G}}} + \upsilon_{\mathrm{Gm}} \frac{\partial p_{\mathrm{Gm}}}{\partial T_{\mathrm{G}}}. \tag{A-248}$$

During the V/C operations, the vapor volume in a cell is assumed constant, and hence the derivatives of e_{Gm} and p_{Gm} with respect to the macroscopic density of vapor component are calculated by

$$\frac{\partial p_{\mathrm{Gm}}}{\partial \overline{\rho}_{\mathrm{Gm}}} = \frac{1}{\alpha_{\mathrm{ge}}} \frac{\partial p_{\mathrm{Gm}}}{\partial \rho_{\mathrm{Gm}}}, \text{ and} \tag{A-249}$$

$$\frac{\partial e_{\mathrm{Gm}}}{\partial \overline{\rho}_{\mathrm{Gm}}} = \frac{1}{\alpha_{\mathrm{ge}}} \frac{\partial e_{\mathrm{Gm}}}{\partial \rho_{\mathrm{Gm}}}, \tag{A-250}$$

where m = 1, 2, 3 and 4.

Appendix B. Matrix equations to be solved in V/C operation

The final matrix equations to be solved in V/C operation are expressed in this appendix. All the definition of derivatives are shown in Appendix A.

The elements of $[B]$ matrix are

$$B(\mathrm{m},1)=\delta(\mathrm{m},1)+\Delta t\Big\{\Lambda x^{\mathrm{Im}}_{\mathrm{GLm},1}+\sum_{k=1}^{6}\Lambda x^{\mathrm{I(k)}}_{\mathrm{GLm},1}-\Lambda x^{\mathrm{Im}}_{\mathrm{LmG},1}+(\Lambda x^{\mathrm{I2}}_{\mathrm{GL1},1}+\Lambda x^{\mathrm{I3}}_{\mathrm{GL1},1})\delta(\mathrm{m},1)+\Lambda x^{\mathrm{I3}}_{\mathrm{GL2},1}\delta(\mathrm{m},2)\Big\},\ \mathrm{m}=1,\ 2\ \text{and}\ 3, \tag{B-1}$$

$$B(\mathrm{m},2)=\delta(\mathrm{m},2)+\Delta t\Big\{\Lambda x^{\mathrm{Im}}_{\mathrm{GLm},2}+\sum_{k=1}^{6}\Lambda x^{\mathrm{I(k)}}_{\mathrm{GLm},2}-\Lambda x^{\mathrm{Im}}_{\mathrm{LmG},2}+(\Lambda x^{\mathrm{I2}}_{\mathrm{GL1},2}+\Lambda x^{\mathrm{I3}}_{\mathrm{GL1},2})\delta(\mathrm{m},1)+(\Lambda x^{\mathrm{I3}}_{\mathrm{GL2},2}-\Lambda x^{\mathrm{I7}}_{L2G,2})\delta(\mathrm{m},2)\Big\},\ \mathrm{m}=1,\ 2\ \text{and}\ 3, \tag{B-2}$$

$$B(\mathrm{m},3)=\delta(\mathrm{m},3)+\Delta t\Big\{\Lambda x^{\mathrm{Im}}_{\mathrm{GLm},3}+\sum_{k=1}^{6}\Lambda x^{\mathrm{I(k)}}_{\mathrm{GLm},3}-\Lambda x^{\mathrm{Im}}_{\mathrm{LmG},3}+(\Lambda x^{\mathrm{I2}}_{\mathrm{GL1},3}+\Lambda x^{\mathrm{I3}}_{\mathrm{GL1},3})\delta(\mathrm{m},1)+\Lambda x^{\mathrm{I3}}_{\mathrm{GL2},3}\delta(\mathrm{m},2)-(\Lambda x^{\mathrm{I8}}_{\mathrm{L3G},3}+\Lambda x^{\mathrm{I12}}_{\mathrm{L3G},3})\delta(\mathrm{m},3)\Big\},\ \mathrm{m}=1,\ 2\ \text{and}\ 3, \tag{B-3}$$

$$B(\mathrm{m},4)=\Delta t\Big\{\Lambda x^{\mathrm{I3}}_{\mathrm{GL1},4}\delta(\mathrm{m},1)+\Lambda x^{\mathrm{I3}}_{\mathrm{GL2},4}\delta(\mathrm{m},2)+(\Lambda x^{\mathrm{Im}}_{\mathrm{GLm},4}-\Lambda x^{\mathrm{Im}}_{\mathrm{LmG},4}-\Lambda x^{\mathrm{I8}}_{\mathrm{L3G},4}-\Lambda x^{\mathrm{I12}}_{\mathrm{L3G},4})\delta(\mathrm{m},3)\Big\}, \tag{B-4}$$

$$B(\mathrm{m},5)=\Delta t\Big\{\Lambda x^{\mathrm{Im}}_{\mathrm{GLm},5}+\sum_{k=1}^{6}\Lambda x^{\mathrm{I(k)}}_{\mathrm{GLm},5}-\Lambda x^{\mathrm{Im}}_{\mathrm{LmG},5}+(\Lambda x^{\mathrm{I2}}_{\mathrm{GL1},5}+\Lambda x^{\mathrm{I3}}_{\mathrm{GL1},5})\delta(\mathrm{m},1)+(\Lambda x^{\mathrm{I3}}_{\mathrm{GL2},5}-\Lambda x^{\mathrm{I7}}_{\mathrm{L2G},5})\delta(\mathrm{m},2)-(\Lambda x^{\mathrm{I8}}_{\mathrm{L3G},5}+\Lambda x^{\mathrm{I12}}_{\mathrm{L3G},5})\delta(\mathrm{m},3)\Big\},\ \mathrm{m}=1,\ 2\ \text{and}\ 3, \tag{B-5}$$

$$B(4,l)=-\Delta t\Big\{\Big(\Lambda x^{\mathrm{I3}}_{\mathrm{GL3},l}+\sum_{k=1}^{6}\Lambda x^{\mathrm{I(k)}}_{\mathrm{GL3},l}\Big)(i^{*}_{\mathrm{Con,G3}}-e^{\kappa}_{\mathrm{L3}})+\Big(\Gamma^{\mathrm{I3}}_{\mathrm{G,L3}}+\sum_{k=1}^{6}\Gamma^{\mathrm{I(k)}}_{\mathrm{G,L3}}\Big)\frac{\partial i^{*}_{\mathrm{Con,G3}}}{\partial\overline{\rho}_{\mathrm{G3}}}\delta(l,3)+\sum_{m=1}^{2}a_{\mathrm{L3,Lm}}h_{\mathrm{L3,Lm}}\frac{\partial T^{\mathrm{I}}_{\mathrm{L3,Lm}}}{\partial\overline{\rho}_{\mathrm{G}l}}\delta(l,3)$$

$$+\sum_{m=1}^{4}\left[\frac{\partial R_{Gm,L3}}{\partial \overline{\rho}_{Gl}} a_{G,L3} h_{L3,G}(T^{I}_{Gm,L3} - T^{\kappa}_{L3}) \right.$$

$$\left. + R_{Gm,L3} a_{G,L3} h_{L3,G} \frac{\partial T^{I}_{Gm,L3}}{\partial \overline{\rho}_{Gl}} \delta(m,l)\right]\Bigg\}, \quad l = 1 \text{ and } 2, \tag{B-6}$$

$$B(4,4) = \tilde{\overline{\rho}}^{n}_{L3} - \Delta t\Bigg\{\Lambda x^{I3}_{GL3,4}(i^{*}_{Con,G3} - e^{\kappa}_{L3}) - \left(\Gamma^{I3}_{G,L3} + \sum_{k=1}^{6}\Gamma^{I(k)}_{G,L3}\right)$$

$$+\sum_{m=1}^{2} a_{L3,Lm} h_{L3,Lm}\left(\frac{\partial T^{I}_{L3,Lm}}{\partial e_{L3}} - \frac{\partial T_{L3}}{\partial e_{L3}}\right)$$

$$+\sum_{m=1}^{4} R_{Gm,L3} a_{G,L3} h_{L3,G}\left(\frac{\partial T^{I}_{Gm,L3}}{\partial e_{L3}} - \frac{\partial T_{L3}}{\partial e_{L3}}\right)\Bigg\}, \tag{B-7}$$

$$B(4,5) = -\Delta t\Bigg\{\left(\Lambda x^{I3}_{GL3,5} + \sum_{k=1}^{6}\Lambda x^{I(k)}_{GL3,5}\right)(i^{*}_{Con,G3} - e^{\kappa}_{L3})$$

$$+\left(\Gamma^{I3}_{G,L3} + \sum_{k=1}^{6}\Gamma^{I(k)}_{G,L3}\right)\frac{\partial i^{*}_{Con,G3}}{\partial T_{G}} + \sum_{m=1}^{2} a_{L3,Lm} h_{L3,Lm} \frac{\partial T^{I}_{L3,Lm}}{\partial T_{G}}$$

$$+\sum_{m=1}^{4}\left[\frac{\partial R_{Gm,L3}}{\partial T_{G}} a_{G,L3} h_{L3,G}(T^{I}_{Gm,L3} - T^{\kappa}_{L3}) + R_{Gm,L3} a_{G,L3} h_{L3,G} \frac{\partial T^{I}_{Gm,L3}}{\partial T_{G}}\right]\Bigg\}, \tag{B-8}$$

$$B(5,1) = \tilde{H}_{1} - \Delta t\left\{-(\Gamma^{I2}_{G,L1} + \Gamma^{I3}_{G,L1})\frac{\partial i_{G1}}{\partial \overline{\rho}_{G1}} + \sum_{m=2}^{3} a_{G,Lm} h_{G,Lm} R_{G1,Lm} \frac{\partial T^{I}_{G1,Lm}}{\partial \overline{\rho}_{G1}}\right\}, \tag{B-9}$$

$$B(5,2) = \tilde{H}_{2} - \Delta t\Bigg\{\Lambda x^{I7}_{L2G,2}(i^{*}_{Vap,G2} - e^{\kappa}_{G}) + \Gamma^{I7}_{L2,G}\frac{\partial i^{*}_{Vap,G2}}{\partial \overline{\rho}_{G2}}$$

$$\left. - \Gamma^{I3}_{G,L2}\frac{\partial i_{G2}}{\partial \overline{\rho}_{G2}} + a_{G,L3} h_{G,L3} R_{G2,L3} \frac{\partial T^{I}_{G2,L3}}{\partial \overline{\rho}_{G2}}\right\}, \tag{B-10}$$

$$B(5,3) = \tilde{H}_{3} - \Delta t\left\{(\Lambda x^{I8}_{L3G,3} + \Lambda x^{I8}_{L3G,3})(i^{*}_{Vap,G3} - e^{\kappa}_{G}) + (\Gamma^{I8}_{L3,G} + \Gamma^{I12}_{L3,G})\frac{\partial i^{*}_{Vap,G3}}{\partial \overline{\rho}_{G3}}\right\}, \tag{B-11}$$

$$B(5,4) = -\Delta t\Big\{(\Lambda x^{I3}_{L3G,4} + \Lambda x^{I8}_{L3G,4} + \Lambda x^{I12}_{L3G,4})(i^{*}_{Vap,G3} - e^{\kappa}_{G})$$

$$+(\Gamma^{I3}_{L3,G} + \Gamma^{I8}_{L3,G} + \Gamma^{I12}_{L3,G})\frac{\partial i^{*}_{Vap,G3}}{\partial e_{L3}}$$

$$-\sum_{m=1}^{3}\Lambda x^{I3}_{GLm,4}(i^{\kappa}_{Gm}-e^{\kappa}_{G})+\sum_{m=1}^{4}a_{G,L3}h_{G,L3}R_{Gm,L3}\frac{\partial T^{I}_{Gm,L3}}{\partial e_{L3}}\Bigg\}, \text{ and} \qquad \text{(B-12)}$$

$$B(5,5)=\tilde{\bar{\rho}}^{n}_{G}\frac{\partial e_{G}}{\partial T_{G}}$$

$$-\Delta t\Bigg\{\sum_{m=1}^{3}\Bigg[\Lambda x^{Im}_{LmG,5}(i^{*}_{Vap,Gm}-\tilde{e}^{\kappa}_{G})+\Gamma^{Im}_{Lm,G}\left(\frac{\partial i^{*}_{Vap,Gm}}{\partial T_{G}}-\frac{\partial e_{G}}{\partial T_{G}}\right)$$

$$-\left(\Lambda x^{Im}_{GLm,5}+\sum_{k=1}^{6}\Lambda x^{I(k)}_{GLm,5}\right)(i^{\kappa}_{Gm}-e^{\kappa}_{G})-\left(\Gamma^{I3}_{G,L3}+\sum_{k=1}^{6}\Gamma^{I(k)}_{G,L3}\right)\left(\frac{\partial i_{Gm}}{\partial T_{G}}-\frac{\partial e_{G}}{\partial T_{G}}\right)\Bigg]$$

$$+\Lambda x^{I7}_{L2G,5}(i^{*}_{Vap,G2}-\tilde{e}^{\kappa}_{G})+(\Lambda x^{I8}_{L3G,5}+\Lambda x^{I12}_{L3G,5})(i^{*}_{Vap,G3}-\tilde{e}^{\kappa}_{G})$$

$$+\Gamma^{I7}_{L2,G}\left(\frac{\partial i^{*}_{Vap,G2}}{\partial T_{G}}-\frac{\partial e_{G}}{\partial T_{G}}\right)+(\Gamma^{I8}_{L3,G}+\Gamma^{I12}_{L3,G})\left(\frac{\partial i^{*}_{Vap,G3}}{\partial T_{G}}-\frac{\partial e_{G}}{\partial T_{G}}\right)$$

$$-(\Lambda x^{I2}_{GL1,5}+\Lambda x^{I3}_{GL1,5})(i^{\kappa}_{G1}-e^{\kappa}_{G})-\Lambda x^{I3}_{GL2,5}(i^{\kappa}_{G2}-e^{\kappa}_{G})$$

$$-(\Gamma^{I2}_{G,L1}+\Gamma^{I3}_{G,L1})\left(\frac{\partial i_{G1}}{\partial T_{G}}-\frac{\partial e_{G}}{\partial T_{G}}\right)-\Gamma^{I3}_{G,L2}\left(\frac{\partial i_{G2}}{\partial T_{G}}-\frac{\partial e_{G}}{\partial T_{G}}\right)$$

$$+\sum_{m=1}^{3}a_{G,Lm}h_{G,Lm}\left[\frac{\partial R_{Gm,Lm}}{\partial T_{G}}(T^{I}_{Gm,Lm}-T^{\kappa}_{G})+R_{Gm,Lm}\left(\frac{\partial T^{I}_{Gm,Lm}}{\partial T_{G}}-1\right)\right]$$

$$+\sum_{m=1}^{3}a_{G,Lm}h_{G,Lm}\left[\frac{\partial R_{G4,Lm}}{\partial T_{G}}(T^{I}_{G4,Lm}-T^{\kappa}_{G})+R_{G4,Lm}\left(\frac{\partial T^{I}_{G4,Lm}}{\partial T_{G}}-1\right)\right]$$

$$+a_{G,L2}h_{G,L2}\left[\frac{\partial R_{G1,L2}}{\partial T_{G}}(T^{I}_{G1,L2}-T^{\kappa}_{G})+R_{G1,L2}\left(\frac{\partial T^{I}_{G1,L2}}{\partial T_{G}}-1\right)\right]$$

$$+\sum_{m=1}^{2}a_{G,L3}h_{G,L3}\left[\frac{\partial R_{Gm,L3}}{\partial T_{G}}(T^{I}_{Gm,L3}-T^{\kappa}_{G})+R_{Gm,L3}\left(\frac{\partial T^{I}_{Gm,L3}}{\partial T_{G}}-1\right)\right]$$

$$+\sum_{k=1}^{6}\sum_{m=1}^{4}a_{G,K(k)}h_{G,K(k)}\left[\frac{\partial R_{Gm,K(k)}}{\partial T_{G}}(T^{I}_{Gm,K(k)}-T^{\kappa}_{G})+R_{Gm,K(k)}\left(\frac{\partial T^{I}_{Gm,K(k)}}{\partial T_{G}}-1\right)\right]\Bigg]\Bigg\}. \qquad \text{(B-13)}$$

The quantities $\tilde{H}_{l}$ in Eqs. (B-9) – (B-11) are expressed by

$$\tilde{H}_{l}=\tilde{\bar{\rho}}^{n}_{G}\frac{\partial e_{G}}{\partial \bar{\rho}_{Gl}}$$

$$-\Delta t\Bigg\{\sum_{m=1}^{3}\Bigg[\Gamma^{Im}_{Lm,G}\left(\frac{\partial i^{*}_{Vap,Gm}}{\partial\overline{\rho}_{Gl}}\delta(m,l)-\frac{\partial e_G}{\partial\overline{\rho}_{Gl}}\right)+\Lambda x^{Im}_{LmG,l}(i^{*}_{Vap,Gm}-e^{\kappa}_{G})$$

$$-\left(\Gamma^{Im}_{G,Lm}+\sum_{k=1}^{6}\Gamma^{I(k)}_{G,Lm}\right)\left(\frac{\partial i_{Gm}}{\partial\overline{\rho}_{Gl}}\delta(m,l)-\frac{\partial e_G}{\partial\overline{\rho}_{Gl}}\right)$$

$$-\left(\Lambda x^{Im}_{GLm,l}+\sum_{k=1}^{6}\Lambda x^{I(k)}_{GLm,l}\right)(i^{\kappa}_{Gm}-e^{\kappa}_{G})\Bigg]$$

$$-\left[(\Gamma^{I2}_{L2,G}+\Gamma^{I8}_{L3,G}+\Gamma^{I12}_{L3,G})-(\Gamma^{I2}_{G,L1}+\Gamma^{I3}_{G,L1}+\Gamma^{I3}_{G,L2})\right]\frac{\partial e_G}{\partial\overline{\rho}_{Gl}}$$

$$-\left[(\Lambda x^{I2}_{GL1,l}+\Lambda x^{I3}_{GL1,l})(i^{\kappa}_{G1}-e^{\kappa}_{G})+\Lambda x^{I3}_{GL2,l}(i^{\kappa}_{G2}-e^{\kappa}_{G})\right]$$

$$+\sum_{m=1}^{3}a_{G,Lm}h_{G,Lm}\left[\frac{\partial R_{Gm,Lm}}{\partial\overline{\rho}_{Gl}}(T^{I}_{Gm,Lm}-T^{\kappa}_{G})+R_{Gm,Lm}\frac{\partial T^{I}_{Gm,Lm}}{\partial\overline{\rho}_{Gl}}\delta(m,l)\right]$$

$$+\sum_{m=1}^{3}a_{G,Lm}h_{G,Lm}\frac{\partial R_{G4,Lm}}{\partial\overline{\rho}_{Gl}}(T^{I}_{G4,Lm}-T^{\kappa}_{G})$$

$$+a_{G,L2}h_{G,L2}\frac{\partial R_{G1,L2}}{\partial\overline{\rho}_{Gl}}(T^{I}_{G1,L2}-T^{\kappa}_{G})+\sum_{m=1}^{2}a_{G,L3}h_{G,L3}\frac{\partial R_{Gm,L3}}{\partial\overline{\rho}_{Gl}}(T^{I}_{Gm,L3}-T^{\kappa}_{G})$$

$$+\sum_{m=1}^{4}\sum_{k=1}^{6}a_{G,K(k)}h_{G,K(k)}\left[\frac{\partial R_{Gm,K(k)}}{\partial\overline{\rho}_{Gl}}(T^{I}_{Gm,K(k)}-T^{\kappa}_{G}),\right.$$

$$\left.+R_{Gm,K(k)}\frac{\partial T^{I}_{Gm,K(k)}}{\partial\overline{\rho}_{Gl}}\delta(m,l)\right]\Bigg\},\ l=1,\ 2\ \text{and}\ 3, \qquad \text{(B-14)}$$

The elements of column vector $\{C\}$ are

$$C(m)=\tilde{\overline{\rho}}^{n}_{Gm}-\overline{\rho}^{\kappa}_{Gm}$$

$$-\Delta t\Bigg\{\Gamma^{Im}_{G,Lm}+\sum_{k=1}^{6}\Gamma^{I(k)}_{G,Lm}-\Gamma^{Im}_{Lm,G}+(\Gamma^{I2}_{G,L1}+\Gamma^{I3}_{G,L1})\delta(m,1)$$

$$+(\Gamma^{I3}_{G,L2}-\Gamma^{I7}_{L2,G})\delta(m,2)-(\Gamma^{I8}_{L3,G}+\Gamma^{I12}_{L3,G})\delta(m,3)\Bigg\},\ m=1,\ 2\ \text{and}\ 3, \qquad \text{(B-15)}$$

$$C(4)=\tilde{\overline{\rho}}^{n}_{L3}(\tilde{e}^{n}_{L3}-e^{\kappa}_{L3})$$

$$+\Delta t\Bigg\{\left(\Gamma^{I3}_{G,L3}+\sum_{k=1}^{6}\Gamma^{I(k)}_{G,L3}\right)(i^{*}_{Con,G3}-e^{\kappa}_{L3})$$

$$+\sum_{m=1}^{4} R_{Gm,L3}\, a_{G,L3}\, h_{L3,G}\,(T^{I}_{Gm,L3} - T^{\kappa}_{L3}) + \sum_{m=1}^{2} a_{L3,Lm}\, h_{L3,Lm}\,(T^{I}_{L3,Lm} - T^{\kappa}_{L3})\Bigg\}, \text{ and} \quad \text{(B-16)}$$

$$C(5) = \tilde{\bar{\rho}}^{n}_{G}\,(\tilde{e}^{n}_{G} - e^{\kappa}_{G})$$

$$+\Delta t\Bigg\{\sum_{m=1}^{3}\Bigg[\Gamma^{Im}_{Lm,G}\,(i^{*}_{Vap,Gm} - e^{\kappa}_{G}) - \Bigg(\Gamma^{Im}_{G,Lm} + \sum_{k=1}^{6}\Gamma^{I(k)}_{G,Lm}\Bigg)(i^{\kappa}_{Gm} - e^{\kappa}_{G})\Bigg]$$

$$+\Gamma^{I7}_{L2,G}\,(i^{*}_{Vap,G2} - e^{\kappa}_{G}) + (\Gamma^{I8}_{L3,G} + \Gamma^{I12}_{L3,G})(i^{*}_{Vap,G3} - e^{\kappa}_{G})$$

$$-(\Gamma^{I2}_{G,L1} + \Gamma^{I3}_{G,L1})(i^{\kappa}_{G1} - e^{\kappa}_{G}) - \Gamma^{I3}_{G,L2}\,(i^{\kappa}_{G2} - e^{\kappa}_{G})$$

$$+\sum_{m=1}^{3} a_{G,Lm}\, h_{G,Lm}\,\Big[R_{Gm,Lm}\,(T^{I}_{Gm,Lm} - T^{\kappa}_{G}) + R_{G4,Lm}\,(T^{I}_{G4,Lm} - T^{\kappa}_{G})\Big]$$

$$+a_{G,L2}\, h_{G,L2}\, R_{G1,L2}\,(T^{I}_{G1,L2} - T^{\kappa}_{G})$$

$$+\sum_{m=1}^{2} R_{Gm,L3}\, a_{G,L3}\, h_{G,L3}\,(T^{I}_{Gm,L3} - T^{\kappa}_{G})$$

$$+\sum_{m=1}^{4}\sum_{k=1}^{6} R_{Gm,K(k)}\, a_{G,K(k)}\, h_{G,K(k)}\,(T^{I}_{Gm,K(k)} - T^{\kappa}_{G})\Bigg\}. \quad \text{(B-17)}$$

Nomenclature

a	binary-contact area per unit volume (m^{-1})
c	specific heat ($J\ kg^{-1}\ K^{-1}$)
e	specific internal energy ($J\ kg^{-1}$)
$H(x)$	Heaviside unit function
h	heat-transfer coefficient ($W\ m^{-2}\ K^{-1}$)
h_{Con}	effective latent heat of condensation ($J\ kg^{-1}$)
h_{Vap}	effective latent heat of vaporization ($J\ kg^{-1}$)
i	specific enthalpy ($J\ kg^{-1}$)
p	pressure (Pa)
Q_{Int}	heat transfer rate from structure interior ($W\ m^{-3}$)
Q_N	nuclear heating rate ($W\ m^{-3}$)
q	heat transfer rate ($W\ m^{-3}$)
R	fraction of interface
T	temperature (K)
t	time (s)
X_B	fraction of liquid steel component in liquid steel film

Greek letters

α_0	minimum vapor volume fraction
α_G	vapor volume fraction ($= 1-\alpha_S-\alpha_L$)
α_{ge}	effective vapor-volume fraction ($= \max[\alpha_0(1-\alpha_S), 1-\alpha_S-(1-\alpha_0)\alpha_L]$)
α_L	volume fraction of liquid field
α_S	volume fraction of structure field
Δt	time step size (s)
δ	Kronecker symbol
κ	thermal conductivity ($W\ m^{-1}\ K^{-1}$) or index of iteration step
Γ	mass-transfer rate per unit volume ($kg\ s^{-1}\ m^{-3}$)
$\bar{\rho}$	macroscopic (smeared) density ($kg\ m^{-3}$)

Subscripts

A, B, C, D	labels of energy components
Con	saturated liquid
Crt	critical point
G	vapor mixture
Gm	material component m in vapor field m = 1 : fuel, m = 2 : steel, m = 3 : sodium, and m = 4 : fission gas
K(k)	solid energy component contacting to fluid representing L4, L5, L6, k1, k2 and k3 for k = 1 - 6, respectively.
km	energy component of structure surface m = 1 : pin, m = 2 : left can wall, and m = 3 : right can wall
Liq	liquidus point
Lf	liquid steel film on structure components

Lm	energy component m in liquid field m = 1 : liquid fuel, m = 2 : liquid steel, m = 3 : liquid sodium, m = 4 : fuel particles, m = 5 : steel particles, and m = 6 : control particles
M	material component M = 1 : fuel, M = 2 : steel, M = 3 : sodium, M = 4 : control, and M = 5 : fission gas
Sat	saturation
Sm	energy component m in structure field m = 1 : pin-fuel surface node, m = 2 : left crust fuel, m = 3 : right crust fuel, m = 4 : cladding, m = 5 : left can-wall surface node, m = 6 : left can wall interior node, m = 7 : right can wall surface node, m = 8 : right can wall interior node, and m = 9 : control
Sol	solidus point
SK(k)	energy component of structure surfaces k = 1 : fuel pin (SK(1) = S1 or S4) k = 2 : left can wall (SK(2) = S2, S5 or S6) k = 3 : right can wall (SK(3) = S3, S7 or S8)
Sup	superheat
Vap	saturated vapor

Superscripts

EQ	equilibrium mass transfer
I	interfacial quantity
I(k)	interface identification of solid-fluid contact representing I4, I5, I6, I22, I29 and I30 for k = 1 - 6, respectively.
NE	non-equilibrium mass transfer
+	lack of pressure dependence
~ n	initial value
~ n+1	updated value

References

1. L.L. Smith, N.N. Sheheen, SIMMER-II: A computer program for LMFBR disrupted core analysis, LA-7515-M, Rev., Los Alamos Scientific Laboratory, June 1980.
2. W.R. Bohl, L.B. Luck, SIMMER-II: A computer program for LMFBR disrupted core analysis, LA-11415-MS, Los Alamos National Laboratory, June 1990.
3. W.R. Bohl, D. Wilhelm, F.R. Parker, J. Berthier, L. Goutagny, H. Ninokata, AFDM: An advanced fluid-dynamics model, Volume I: Scope, approach, and summary, LA-11692-MS, Vol. I, Los Alamos National Laboratory, September 1990.
4. Sa. Kondo, H. Yamano, T. Suzuki, Y. Tobita, S. Fujita, X. Cao, K. Kamiyama, K. Morita, E.A. Fischer, D.J. Brear, N. Shirakawa, M. Mizuno, S. Hosono, T. Kondo, W. Maschek, E. Kiefhaber, G. Buckel, A. Rineiski, M. Flad, P. Coste, S. Pigny, J. Louvet, T. Cadiou, SIMMER-III: A Computer Program for LMFR Core Disruptive Accident Analysis, Version 2.H Model Summary and Program Description, JNC TN9400 2001-002, Japan Nuclear Cycle Development Institute, November 2000.
5. Sa. Kondo, H. Yamano, Y. Tobita, S. Fujita, K. Morita, M. Mizuno, S. Hosono, T. Kondo, SIMMER-IV: A Three-Dimensional Computer Program for LMFR Core Disruptive Accident Analysis, Version 1.B Model Summary and Program Description, JNC TN9400 2001-003, Japan Nuclear Cycle Development Institute, November 2000.
6. Sa. Kondo, H. Yamano, Y. Tobita, S. Fujita, K. Kamiyama, W. Maschek, P. Coste, S. Pigny and J. Louvet, Phase 2 Code Assessment of SIMMER-III, A Computer Program for LMFR Core Disruptive Accident Analysis, JNC TN9400 2000-105, Japan Nuclear Cycle Development Institute, September 2000.
7. W.R. Bohl, J. Berthier, L. Goutagny, P. Schmuck, AFDM: An advanced fluid-dynamics model, Volume IV: The AFDM Heat-and Mass-Transfer Solution Algorithm, LA-11692-MS, Vol. IV, Los Alamos National Laboratory, September 1990.
8. G. Henneges, S. Kleinheins, AFDM: An advanced fluid-dynamics model, Volume VI: EOS-AFDM interface, LA-11692-MS, Vol. VI, Los Alamos National Laboratory, January 1994.
9. K. Morita, Y. Tobita, Sa. Kondo, E.A. Fischer, K. Thurnay, SIMMER-III Analytic Equation-of-Sate Model, JNC TN9400 2000-005, Japan Nuclear Cycle Development Institute, May 1999.
10. Sa. Kondo, D.J. Brear, Y. Tobita, K. Morita, W. Maschek, P. Coste, D. Wilhelm, Status and Achievement of Assessment Program for SIMMER-III, A Multiphase, Multicomponent Code for LMFR Safety Analysis, Proceedings of the Eighth International Topical Meeting on Nuclear Reactor Thermal-Hydraulics (NURETH-8), Vol. 3, pp. 1340-1348, Kyoto, Japan, September 30-October 3, 1997.
11. Sa. Kondo, Y. Tobita, K. Morita, D.J. Brear, K. Kamiyama, H. Yamano, S. Fujita, W. Maschek, E.A. Fischer, E. Kiefhaber, G. Buckel, E. Hesserschwerdt, P. Coste, S. Pigny, Current Status and Validation of the SIMMER-III LMFR Safety Analysis Code, Proceedings of the Seventh International Conference on Nuclear Engineering (ICONE-7), No. 7249, Kyoto, Japan, April 19-23, 1999.
12. Y. Tobita, Sa. Kondo, H. Yamano, S. Fujita, K. Morita, W. Maschek, J. Louvet, P. Coste, S. Pigny, Current Status and Application of SIMMER-III, An Advanced Computer Program for LMFR Safety Analysis, Proceedings of the Second Japan-Korea

Symposium on Nuclear Thermal Hydraulics and Safety (NTHAS-2), Fukuoka, Japan, October 15-18, 2000.

13. K. Morita, Y. Tobita, Sa. Kondo, N. Nonaka, SIMMER-III Applications to Key Phenomena of CDAs in LMFR, Proceedings of the Eighth International Topical Meeting on Nuclear Reactor Thermal-Hydraulics (NURETH-8), Vol. 3, pp. 1332-1339, Kyoto, Japan, September 30-October 3, 1997.